ICES COOPERATIVE RESEARCH REPORT

RAPPORT DES RECHERCHES COLLECTIVES

NO. 235

Methodology for Target Strength Measurements

(With special reference to *in situ* techniques for fish and mikro-nekton)

Prepared by the Study Group on Target Strength Methodology

Edited by

E. Ona

International Council for the Exploration of the Sea

Conseil International pour l'Exploration de la Mer

Palægade 2–4 DK-1261 Copenhagen K Denmark

August 1999

ISSN 2707-7144

ISBN 978-87-7482-433-6

ICES Cooperative Research Report No. 235

https://doi.org/10.17895/ices.pub.5367

TABLE OF CONTENTS

Acknowledgements

Thanks are expressed to the members of the study group who have written large sections of the report and also provided helpful comments to the report.

An important and experienced member of the group, Dr Jim Traynor died in May 1998. His effort on the report, and in particular on the dual beam section was of the greatest value. We all miss Jim both as a colleague and as a good friend.

Other members of the study group who participated and gave their comments during the study group meetings are also acknowledged. A special appreciation is expressed to Dr Kenneth Foote and to Dr David MacLennan for invaluable help with improving the quality of the report, and to Elen Hals for typing the manuscript.

Main contributors:

E. Ona (Chair)
Institute of Marine Research
P.O. Box 1870
N-5024 Bergen,
Norway
Tel. + 47 55 23 85 00
Fax. + 47 55 23 85 31
E-mail: egil.ona@imr.no

Dr M. Barange
Sea Fisheries Research Institute
Private bag X2
8012 Rogge Bay
South Africa
Tel. +27 21 402 3149
Fax. +27 21 25 39 30
E-mail: mbarange@sfri.sfri.ac.za

Dr I. Everson
British Antarctic Survey
High Cross, Madingley Road
Cambridge CB3 0ET
UK
Tel. +44 1223 251563
Fax. +44 1223 362616

Dr D. V. Holliday
Tracor Applied Sciences
9150 Chesapeake Drive
San Diego, CA 92123
USA
Tel. +1 619 268 9775
Fax. +1 619 268 9777
E-mail: holliday@galileo.traeor.com

R. Kloser
CSIRO
Division of Fisheries
P.O. Box 1538
Hobart, Tasmania 7001
Australia
Tel. +61 02 325222
Fax. +61 02 325000
e-mail: Rudy.Kloser@marine.csiro.au

D. Miller
Dept. of Fisheries and Ocean
Science Branch
P.O. Box 5667
St. John's, Newfoundland
Canada A1C 5X1
Tel. +1 709 772 5542
Fax. +1 709 772 4105
E-mail: miller@athena.nwafe.nf.ca

P. Reynisson
Marine Research Institute
P.O. Box 1390
Skulagata 4
IS-121 Reykjavik
Iceland
Tel. +354 1 20240
Fax. +354 1 623790
E-mail: pall@hafro.is

Dr L. Rudstam
Cornell Biological Station and Dept. of Natural Resources
Cornell University
900 Shackelton Point Road
Bridgeport NY 13030
USA
e-mail: lgr1@crnx2.cornell.edu

Dr J. Traynor
Alaska Fisheries Science Center
NMFS/NOAA
7600 Sand Point Way N.E.
Seattle, WA 98115-0070
USA

1 Introduction

This report has been produced as a result of discussions in the Fisheries Acoustics Science and Technology (FAST) Working Group of the International Council of the Exploration of the Sea (ICES). Following discussions in the FAST Working Group, it was proposed that a study group on Target Strength Methodology be formed, which was recommended by the Fish Capture Committee. This resulted in ICES Resolution C Res 1992 2:11: "A Study group on Target strength Methodology is established under the Chairship of E. Ona (Norway) and will meet in Gothenburg, Sweden on 19 April 1993 to prepare a report, with a view to publication in the ICES Cooperative Report Series on the methodology for Target Strength measurements with special reference to *in situ* techniques for fish and micro- nekton"

The content of the report was outlined at the meeting in Gothenburg, and the work divided among the members of the group. The group has had further meetings in Montpelier, France, 25–26 April 1994, and in Aberdeen, UK, 8–10 June 1995. It was decided to prepare a preliminary draft for the 1994 and 1995 FAST WG, and to present the latter draft to the Fish Capture Committee at the 1995 Statutory Meeting.

Acoustic surveys have during the last three decades become one of the most widely used methods for fish stock abundance estimation, and now form an important part of routine stock management all over the world. It is also the main method used in exploratory fishing surveys.

An acoustic stock estimate requires (a) calibrated equipment, (b) a knowledge of the acoustic scattering properties of the surveyed fish, and (c) a proper survey coverage of the stock at a time when its distribution is favourable with respect to horizontal and vertical movement within the survey period. Calibration of echo sounders and integrators for echo integration surveys have been described in detail in Foote *et al.* (1987), and will not be treated further in this report. Calibration of the equipment needed for target strength measurement, however, will be described in detail. Survey design and analysis of survey results are dealt with in Simmonds *et al.* (1992). It is the intention of this report to cover the remaining topic, and to describe in detail methods for *in situ* measurement of the scattering properties of the fish and micronecton. This includes a description of the physical limitation of the existing methods, detailed examples and also the errors involved when conducting measurements under unfavourable conditions. The report will not cover the use of target strength as a tool for size classification.

It is noted at the outset that the aims of target strength measurement have changed only slightly, if at all, over the past forty years. Such works as those by Hashimoto and Maniwa (1955), Harden Jones and Pearce (1958), Richardson *et al.* (1959), Haslett (1962), Midttun and Hoff (1962), Cushing *et al.* (1963), Shishkova (1964), Love (1969, 1971), McCartney and Stubbs (1971), and Shibata (1971), among others, have motivated the search for improvements and technique. Advances in these have benefited or facilitated especially *in situ* methods, hence acknowledgement of the mentioned authors and their colleagues.

References

Cushing, D. H., Harden Jones, F. R., Mitson, R. B., Ellis, G. H., and Pearce, G. 1963. Measurement of the target strength of fish. Journal of the British Institution of Radio Engineers, 25: 299–303.

Foote, K. G., Knudsen, H. P., Vestnes, G., MacLennan, D. N., and Simmonds, E. J. 1987. Calibration of acoustic instruments for fish density estimation: a practical guide. Cooperative Research Report, International Council for the Exploration of the Sea, 144, 57 pp.

Harden Jones, F. R., and Pearce, G. 1958. Acoustic reflexion experiments with perch (*Perca fluviatilis* Linn.) to determine the proportion of the echo returned by the swimbladder. Journal of Experimental Biology and Ecology, 35: 437–450.

Hashimoto, T., and Maniwa, Y. 1955. Study on reflection loss of ultrasonic wave on fish-body by millimeter wave. Technical Report on Fishing Boat, Tokyo, 8: 113–118.

Haslett, R. W. G. 1962. Determination of the acoustic backscattering patterns and cross sections of fish. British Journal of Applied Physics, 13: 349–357.

Love, R. H. 1969. Maximum side-aspect target strength of fish. Journal of Acoustical Society of America, 46: 746–762.

Love, R. H. 1971. Dorsal-aspect target strength of an individual fish. Journal of Acoustical Society of America, 49: 816–823.

McCartney, B. S., and Stubbs, A. R. 1971. Measurements of the acoustic target strength of fish in dorsal aspect, including swimbladder resonance. Journal of Sound and Vibration, 15: 397–420.

Midttun, L., and Hoff, I. 1962. Measurements of the reflection of sound by fish. Fiskeridirektoratet. Skrifter. Serie Havundersoekelser, 13(3): 1–18.

Richardson, I. D., Cushing, D. H., Harden Jones, F .R., Beverton, R. J. H., and Blacker, R. W. 1959. Echo sounding experiments in the Barents Sea. Fishery Investigations Series II23 August 1999, 22(9): 1–57.

Simmonds, E. J., Williamson, N. J., Gerlotto, F., and Aglen, A. 1992. Acoustic survey design and analysis procedure: a comprehensive review of current practice. ICES Cooperative Research Report, 187.

Shibata, K. 1971. Experimental measurement of target strength of fish, pp. 104–108. *In* Modern fishing gear of the world, 2. Fishing News (Books), London.

Shishkova, E. V. 1964. Study of acoustical characteristics of fish, pp. 404–409. *In* Modern fishing gear of the world, 2. Fishing News (Books), London

2 Nomenclature and definitions

2.1 List of symbols

I_r	received sound intensity (power per area)
I_t	transmitted sound intensity
I[dB]	sound intensity, expressed in decibels
g_{t0}	transmitting response of the transducer at acoustic axis
g_{r0}	receiving response of the transducer at acoustic axis
θ	target direction relative to transducer axis in alongship plane
ϕ	target direction relative to transducer axis in athwartship plane
$b(\theta, \phi)$	directivity function of the transducer at (θ, ϕ)
r	range or distance [m]
$g(r)$	range dependent gain
σ	acoustic backscattering cross section [m^2]
C	constant term
B	ratio
V	variance or volume
Φ	estimated opening angle of the transducer between the half power points
θ_0	offset angle (estimated offset between measured electrical zero degrees and transducer acoustic axis in alongship direction on split-beam transducers)
ϕ_0	offset angle (estimated offset between measured electrical zero degrees and transducer acoustic axis in athwartship direction on split beam transducers)
E	beam shape parameter for split beam transducers
c	sound speed in water [m/s]
d	distance or distance between centres of transducer quadrants [m]
δ	phase difference
t	time [s]
k	wavenumber $(2\pi/\lambda)$
λ	wavelength [m]
φ	azimuthal angle in the transducer plane [deg]
ϑ	angle from acoustic axis [deg]
w	weighting factor
ρ_A	area density [$1/m^2$] [1/n.mi.^{2}]
ρ_V	volume density [1/m3]
ρ_0	density of water [kg/m^3]
τ	pulse duration [msec]
z	depth [m]
α	absorption coefficient in dB per unit distance (note that α and β also are used, for the sake of clarity, as notation for alongship and athwartship target direction angles in split beam systems)
TS	target strength [dB]
<TS>	average target strength [dB], as defined in terms of <σ>
<σ>	average acoustic backscattering cross section [m^2]
L	length of fish [cm]
f	frequency of sound [Hz]
ψ	equivalent beam angle [sterad]
Ω	solid angle [sterad]
PDF	probability density function
u	echo amplitude [volt]
w	probability element
n.mi.	nautical mile

2.2 Terminology and definitions

When echo integration is used as the main tool for quantifying the abundance of marine fish or plankton organisms, echo integration values must, at some stage, be converted to units of biomass. If done locally, measures of numbers of scatterers per unit area or volume are determined. These are commonly referred to as area or volume densities. If done globally, an average measure of density may be determined. When integrated over the surveyed area or volume, a measure of abundance is derived.

The described measures of density or abundance may be relative or absolute. If the measuring instruments, namely echo sounders and echo integrators, are calibrated in accordance with current standards (Foote *et al.*, 1987), the results of echo integration may be expressed in absolute units (Foote and Knudsen 1994). A convenient quantity is the area backscattering coefficient, often distinguished as s_a when referring to the units [m^2/m^2] (Clay and Medwin 1977), or as s_A when referring to the units [m^2/(n.mi)2] (Knudsen 1990). The volume backscattering coefficient, abbreviated s_v, typically refers to the units [m^2/m^3], and is related to s_a through the expression:

$$s_a = \int_{z_1}^{z_2} s_V(z)\,dz \qquad (2.1)$$

where z is the range from the transducer centre, or depth when referring specifically to a vertically oriented downwards-pointing transducer, as in echo sounding. When referred to the area of one square nautical mile,

$$s_A = 4\pi(1852)^2 \int_{z_1}^{z_2} s_V(z)\,dz \qquad (2.2)$$

Attention is called to the former expression of echo integration values in terms of millimeters of pen deflection per unit of sailed distance, e.g., one nautical mile. This refers to some of the earliest analogue echo integrators, where the result of echo integration was shown graphically by a monotonically increasing line that was automatically reset at some maximum level. The rigors of custom extended use of the archaic analogue units well into the 1980s, even following introduction of digital echo integrators (Brede 1984).

Here, only the absolute measure of echo integration s_A is used. Its convenience is seen from the fundamental equation of echo integration, namely:

$$s_A = \rho_A \langle\sigma\rangle \qquad (2.3)$$

Thus the area fish density ρ_A may be expressed simply as:

$$\rho_A = \frac{s_A}{<\sigma>} \tag{2.4}$$

The volumetric measure of density applicable to a layer of thickness Δz, namely ρ_v, is expressed similarly,

$$\rho_v = \frac{s_a}{<\sigma>\Delta z} \tag{2.5}$$

Thus, in order to determine absolute measures of scatterer density, it is necessary to know the average backscattering cross section $<\sigma>$. Its determination by measurement *in situ* is the subject of this report.

Target strength TS is defined as the logarithmic measure of backscattering cross section σ in the following way:

$$TS = 10 \log \frac{\sigma}{4\pi r_o^2} \tag{2.6}$$

where r_o is the reference distance. If $r_0 = 1$ m, which is the usual reference, the definition may be simplified:

$$TS = 10 \log \frac{\sigma}{4\pi} \tag{2.7}$$

where SI units are implied.

It is noted that the units employed in the definition by Urick (1983) are different, incurring an overestimate in TS by the amount 0.4 dB. Thus TS values expressed according to Urick's convention, which is that of much earlier underwater acoustics literature, must be reduced by 0.4 dB to conform to SI units.

Throughout this report, target strength is considered to be solely a narrowband quantity. Thus its value as determined with an echo sounder is assumed to be indistinguishable from that determined in the idealized case of a perfectly harmonic source at the transducer centre frequency *f*. In this idealized case, the measured quantity of TS is strictly a property of the target organism, independent of characteristics of the measuring instruments.

Averaging

The average target strength <TS> is defined in terms of the average backscattering cross section $<\sigma>$:

$$TS = 10 \log \frac{<\sigma>}{4\pi} \tag{2.8}$$

where $<\sigma>$ is expressed in SI units. It is important to note that the averaging is performed with respect to σ or, equivalently when being measured, in terms of intensity. Averaging is not performed in the logarithmic domain.

At typical echo sounder frequencies for fish of commercial importance, TS depends on animal orientation. This dependence describes the directivity function or pattern. The average backscattering cross section thus depends on animal behaviour, as characterized by the orientation distribution. Insofar as this changes with behaviour, so do $<\sigma>$ and <TS>.

During ordinary echo integration, the transducer is oriented vertically downwards. The dorsal part of the directivity pattern is sensed. For fish in dorsal aspect, including near-dorsal angels, the dependence on roll aspect is essentially negligible. During usual survey measurements, only slight roll movement occurs. This is discussed in detail in Nakken and Olsen (1977) and Foote (1979, 1980). Consequently, the average backscattering cross section needed for conversion to biomass in equation (1.4) is derived from the dorsal part of the directivity pattern in the dorso-ventral plane of the scatterer. It is a summation or integral of σ weighted by the probability density function (PDF) of the tilt angle. This is essentially what is observed within the finite opening angle of a transduced, hence measured in a field situation when observing freely swimming fish.

Changes in $<\sigma>$ for a particular fish species and size generally reflect changes in the orientation distribution of the fish, hence in behaviour.

Where to measure TS

Target strength is defined in the farfield of the transducer and in the farfield of the target, that is, beyond the respective nearfields.

The nearfield of a transducer is defined relatively conservatively by the limiting range:

$$(R_N)_{\text{Transducer}} = d^2/\lambda, \tag{2.9}$$

where d is the maximum linear dimension of the transducer, and λ is the acoustic wavelength. For ranges greater than R_N, the transmitted acoustic pressure field decreases inversely with range.

The nearfield of a target is defined similarly,

$$(R_N)_{\text{Target}} = l^2/\lambda \tag{2.10}$$

where l is the maximum linear dimension of the target.

When making measurements with large transducers at high frequencies or measuring large fish at short ranges, it is important to compute the respective nearfield limit. Valid measurements are confined to the region beyond R_N for both transducer and target.

References

Brede, R. 1984. SIMRAD EK400 scientific echo sounder. *In* R.B. Mitson (ed.) Acoustic systems for the assessment of fisheries. FAO Fisheries Circular, 778: 44-56.

Clay, C. S., and Medwin, H. 1977. Acoustical Oceanography: Principles and Applications. Wiley, New York, 544 pp.

Foote, K. G. 1979. On representing the length dependence of acoustic target strengths of fish. Journal of Fisheries Research Board of Canada, 36: 1490–1496.

Foote, K. G. 1980. Averaging of fish target strength functions. Journal of the Acoustical Society of America, 67: 504–515.

Foote, K. G., and Knudsen, H. P. 1994. Physical measurement with modern echo integrators. Journal of Acoustic Society of Japan (English Edition), 15: 393–395.

Foote, K. G., Knudsen, H. P., Vestnes, G., MacLennan, D. N., and Simmonds, E. J. 1987. Calibration of acoustic instruments for fish density estimation: a practical guide. Cooperative Research Report, International Council for the Exploration of the Sea, 144, 57 pp.

Knudsen, H. P. 1990. The Bergen Echo Integrator: an introduction. Journal du Conseil International pour l'Exploration de la Mer, 47: 167–74.

Nakken, O. and Olsen, K. 1977. Target strength measurements of fish. Rapports et Procès-Verbaux des Réunions du Conseil International pour l' Exploration de la Mer, 170: 52–69.

Urick, R J. 1983. Principles of Underwater Sound for Engineers. 3rd edition. McGraw-Hill, New York, 384 pp.

3 The single beam analysis

L. G. Rudstam, T. Lindem and G. LaBar

3.1 Physics

The physics of sound propagation in water is well known and described in standard textbooks such as Clay and Medwin (1977) and Urick (1983). For a single scatterer with backscattering cross section σ, located at range r and angular position (θ,ϕ) in the farfield of the transducer, the intensity of the echo received at the transducer is:

$$I_e = I_t g_{to} g_{ro} \sigma r^{-4} 10^{-2\alpha r/10} b^2(\theta,\phi) , \quad (3.1)$$

where I_t is the intensity of the transmitted signal at unit distance, g_{to} and g_{ro} are gain factors associated respectively with transmitter and receiver, α is the absorption coefficient at the centre frequency of the transmitted signal, and $b^2(\theta,\phi)$ is the product of transmit and receive beam patterns evaluated in the direction (θ, ϕ). The factor $r^{-4}10^{-2\alpha r/10}$ accounts for the two-way propagation loss of the signal due to spherical spreading and attenuation.

A range dependent gain function $g(r)$ is now introduced (this is the time varied gain, or TVG):

$$g(r) = g_o r^4 10^{2\alpha r/10} . \quad (3.2)$$

When applied to the echo intensity I_e, the resulting received signal intensity is:

$$I_r = g(r) I_e = I_t g_{to} g_{ro} g_o \sigma b^2(\theta,\phi) . \quad (3.3)$$

Solving for σ,

$$\sigma = I_r \left(I_t g_{to} g_{ro} g_o b^2(\theta,\phi) \right)^{-1} \quad \text{or}$$
$$\sigma = I_r C_g C_b , \quad (3.4)$$

where $C_g = (I_t g_{to} g_{ro} g_o)^{-1}$, and $C_b = (b^2(\theta,\phi))^{-1}$.

The equation for the backscattering cross section describes a number of dependencies. Of particular importance in the context of target strength measurements is that of the beam pattern ($b^2(\theta,\phi)$). For a single-beam transducer, the location of the target, and therefore the value of b, is generally unknown for individual measurements. Given the fulfilment of certain assumptions, however, the effect of the beam pattern can be removed in a statistical sense, described below.

3.2 Statistics

In order to extract the essential statistics, it is convenient to work with a variant of equation (3.3), namely:

$$\epsilon = g\, b^2(\theta,\phi)\sigma . \quad (3.5)$$

Here, ϵ represents the received intensity, and g is a range independent scaling factor including I_t and other gain factors. The probability of observing a particular value of ϵ depends on the probabilities of occurrence of b^2 and σ. In fact, the probability density function (PDF) of ϵ, $w_E(\epsilon)$, is an integral of the PDF's of b^2 and σ.

Introducing the variables $s = g\sigma$ and $\beta = b^2$ in equation (3.5), $\epsilon = s\beta$, and:

$$w_E(\epsilon) = \int_0^1 w_S(\epsilon/\beta) w_B(\beta)\, d\beta/\beta . \quad (3.6)$$

The integration is performed over the total range of values of b^2, namely [0, 1].

An alternative expression of equation (3.5) can be made in the amplitude domain. In terms of the echo amplitude $u = \epsilon^{1/2}$,

$$w_U(u) = \int_0^1 w_F(\mu/b)\, w_T(b)\, db/b , \quad (3.7)$$

where $\mu = (g\sigma)^{1/2}$. The indices F and T refer to the fish- and transducer-parts of the equation.

Yet another expression can be obtained in the logarithmic domain. For example, equation 3.5 can be written:

$$\log \epsilon = \log (g\sigma) + \log (b^2) , \quad (3.8)$$

or $z = x + y$, where z denotes log ϵ, x denotes log $(g\sigma)$, and y denotes log (b^2). Accordingly,

$$w_Z(z) = \int_{-\infty}^{0} w_X(z-y)\, w_Y(y)\, dy , \quad (3.9)$$

where the integration is performed over the range of log (b^2).

There are numerous solutions to equations (3.6), (3.7), and (3.9). Craig and Forbes (1969) describe a basic solution, which is still in use (Lindem 1983). Physically this derives from the recognition that a large echo can only be obtained from a large target in the middle of the beam, whereas a medium-sized echo can be obtained from a large target further from the beam axis or a medium-sized target on the acoustic axis. This realization can be expressed through a set of n linear equations in n unknowns:

$$\begin{aligned} N_1 &= \rho_1 V_1 \\ N_2 &= \rho_2 V_1 + \rho_1 V_2 \\ N_3 &= \rho_3 V_1 + \rho_2 V_2 + \rho_1 V_3 \\ &\cdots\cdots \\ N_n &= \rho_n V_1 + \rho_{n-1} V_2 + \ldots + \rho_1 V_n \end{aligned} \quad (3.10)$$

where N_i is the number of echoes of size I, size 1 being the largest, ρ_i is the number density of targets of size I, V_j is the volume or solid angle increment associated with the decrease in intensity relative to the beam axis at increment j, increment 1 referring to the immediate vicinity of the beam axis itself (Figure 3.1). Sets of linear equations, such as that in equation (3.10), are readily solved by standard software available for digital computers. An example is presented in Table 3.1.

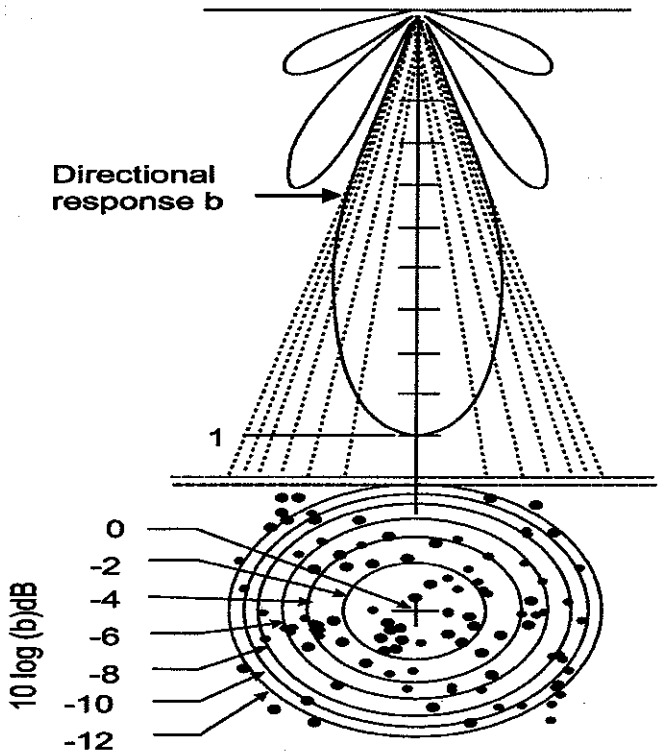

Figure 3.1. The beam pattern diagram and the diversion of the beam in areas for the Craig-Forbes algorithm.

The described solution (equation 3.10, Table 3. 1) is known to be unstable because oscillating results may occur when solving equation 3.10 if the observations of the number of echoes in each size class have a significant error component. This is the case when too few echoes are observed, when the beam pattern is not well defined, and/or when the echoes are measured with insufficient precision (as is the case for small size classes when using early analysis programs written for AT computers, see example in Table 3.1). Setting negative solutions to zero is incorrect and will cause target strength distributions to be biased. Such solutions should not be used for target strength measurements.

To overcome the innate instability in the described simple solution method, Degnbol *et al.* (1985) added a constraint to the set of linear equations in equation (3.10), namely that ρ_i be non-negative. The extended equation set is solved by means of a least-mean-squares method. This solution is applicable in all cases, hence is to be preferred to the first solution presented above.

Many other techniques have been developed to solve the equation for the PDF of σ or related variable or statistic. Some techniques, such as those already described, involve no assumptions about the characteristic form of the PDF of σ. Other techniques do assume definite forms for this PDF. Examples of the various techniques are described in Ehrenberg (1972, 1983), Robinson (1982, 1983), Clay (1983), Degnbol *et al.* (1985), Muligan and Kieser (1986), Rudstam *et al.* (1987, 1992), Jacobson *et al.* (1990), Hedgepeth (1994). A full evaluation of these techniques requires detailed comparisons of analyses on identical data sets by both single-beam and dual-beam or split-beam methods.

3.3 A fallacy concerning assignment of target strength values to fish size classes

Many authors have attempted to associate densities of different fish size classes with the solved target strength data, as by equating a particular target strength value to a definite size class. Fish are complicated scatterers, and fish target strength depends on size, orientation, swimbladder volume, and degree of activity, among other things (Huang

Table 3.1 Example of a solution to Craig and Forbes' algorithm. The data is from an October 1987 survey in a coastal area of the Baltic Sea. Vertical gill nets and midwater trawls caught primarily herring and sprat with a peak in the distribution around 7 cm (age-0 fish) and a wider distribution of fish sizes between 10 and 30 cm (older herring and sprat). The data was collected with a 70 kHz Simrad EY/M with 11.2° full half-power beam angle. Density is calculated as number of echoes registered in a given size class minus the number of echoes expected from the larger size classes (below) divided by the volume V_1 (= 277.77 10^3 m^3 for this particular measurement). For example, the number of echoes registered between -44 and -46 dB were 565. The number expected from larger fish was 128.77 + 40.72 + 8.11 + 17.19 = 194.79. The number of echoes attributable to that size class is then 565 - 194.79 = 370.21, and the density of that size class is 370.21/27770 = 1.33 f/1000 m^3. The volumes represent V_1, V_2 ... and the # of single fish echoes represent N_1, N_2 ... in equation (3.10). The negative densities in the smallest target strength bin are the result of the limited number of amplitude bins that were used with programs developed for XT and AT computers. This is no longer a limitation with newer software designed for faster computers.

		Volume (m^3)	27777	26778	25945	24913	23887	22934	21662	20810	19557	18531
				Number of echoes expected from the larger size classes								
Size class	TS bin (dB)	# single-fish echoes	Density (f/1000m3)	size class n-1	size class n-2	size class n-3	size class n-4	size class n-5	size class n-6	size class n-7	size class n-8	size class n-9
1	over -38	20	72									
2	-38 to -40	28	325	1928								
3	-40 to -42	71	157	871	1868							
4	-42 to -44	202	481	4203	844	1793						
5	-44 to -46	565	1333	12877	4072	811	1719					
6	-46 to -48	1179	2282	35687	12477	3910	7774	1651				
7	-48 to -50	1549	1482	61115	34577	11980	3749	746	1559			
8	-50 to -52	2126	2329	39689	59215	33201	11487	3599	705	1498		
9	-52 to -54	2537	1791	62373	38455	56858	31834	11029	3400	677	1408	
10	-54 to -56	2071	-1213	47958	60434	36924	54517	30564	10417	3266	636	1334
Sum		10348										

and Clay 1980, Nash *et al.*, 1987). Even for fish of constant size, the corresponding distributions of target strength may span a range exceeding 10 db (Ehrenberg *et al.*, 1981, Clay and Heist 1984, Dawson and Karp 1990). However, it may be possible to distinguish acoustically several distinct fish size classes.

Experience indicates that a relative size difference of at least a factor of 2 is necessary to separate different peaks in the target strength distribution, hence to compute densities of different size classes. If the number of clearly defined size classes is known, it may be possible to separate the contribution from each size group by means of an automatic algorithm, such as a peak identification computer program (Parkinson *et al.*, 1994), or by fitting a theoretical model for fish scattering to the target strength distribution. In this case, Clay and Heist (1984), Rudstam *et al.* (1987), and Kieser and Ehrenberg (1990) have used the Rice PDF.

3.4 Calibration

Scientific use of echo sounders in quantitative fish stock assessment requires calibration for two reasons: to ensure stability in performance and to relate the echo sounder output to an absolute physical quantity. Echo sounders need to be calibrated at regular intervals to ensure proper operation.

A range of techniques has been used to calibrate echo sounders. At one time, hydrophones were commonly used. These are secondary standards (Robinson 1984); however, themselves requiring calibration. They are additionally rather sensitive to changes in environmental conditions, for example, temperature, and often in ways that defy simple compensation.

An alternative to hydrophone calibration is that of standard-target calibration. A known target is suspended on the acoustic axis in the transducer beam and the response related to the target strength, which is known *a priori*. The method is thus primary. Given proper choice of the standard target, the method can also be robust, that is, relatively insensitive to changes in environmental conditions, for which moreover compensation is possible. Details of the ICES-recommended calibration method using standard spheres are given in Foote *et al.* (1987). Background information on the choice of standard spheres with respect to both size and material is given in Foote (1982) and Foote and MacLennan (1984).

Two matters of some practical importance in standard-target calibrations are suspending the target in the transducer beam and positioning this on the acoustic axis. Details are given in Foote *et al.* (1987) and MacLennan and Simmonds (1992). Target positioning is generally done by an exploratory procedure, where the small angular region that gives the maximum echo strength is sought. Immediate feedback is provided by observing the echo level. When the target is on the acoustic axis, $C_b = 1$ in equation (3.4) and $\sigma = C_g I_r$. Since I_r is measured, C_g is thus determined, and the calibration is complete.

It is also useful, and sometimes necessary, to know the beam pattern. This can be measured by hydrophone or,

better, by target sphere, but with hydrophone or target at known angle. In a laboratory, a transducer can be rotated or translated. When mounted on a hull or towed vehicle, the hydrophone or target may be moved.

3.5 Field examples

Field studies using analysed single-beam data are more common in freshwater than in marine systems, possibly because freshwater fisheries investigators operate with smaller budgets than their marine counterparts and are less able to afford the dual-beam or split-beam systems described in subsequent chapters. The HADAS software is the most widely used method for extracting target strength distribution from single-beam data and measuring fish abundance and spatial distributions. Examples are described in Lindem and Sandlund (1984), Jurvelius *et al.* (1988), Brabrand *et al.* (1990), Guillard and Gerdeaux (1993), Walline *et al.* (1992), Brenner *et al.* (1987), Snorrason *et al.* (1992), Rudstam *et al.* (1993), and Hansson (1993). However, other single-beam methods have also been used (Degnbol *et al.*, 1985, Muligan and Kieser 1986, Rudstam *et al.*, 1987, 1992, Jacobson *et al.*, 1990). Comparisons between dual-beam and single-beam acoustics show similar target strength distributions in both European (Dahm *et al.*, 1992) and North American lakes (Parkinson *et al.*, 1994, see also below). Here we will present two field examples of data sets obtained with single-beam sonars that exemplify (1) a situation where different fish sizes can be separated as distinct peaks in the target strength distribution, and (2) a situation where this is not possible and only average target strength of the whole fish population present can be measured.

Example 1: Amisk Lake, Alberta

Aku *et al.* (1997) studied the effect of oxygen injection on the distribution of cold-water fish in Amisk Lake, a naturally eutrophic lake in central Alberta, Canada. Two size groups of cisco *Coregonus artedi* (age-1; age-3 and older) were the dominant pelagic fish caught in multimesh vertical gill nets. Acoustic data on fish size, vertical distributions and abundances were obtained with a single-beam 70 kHz Simrad EY-M echo-sounder (half-power beam angle 5.6°, 0.6 ms pulse duration, 3 pings s^{-1}, TVG 40LogR) operated at night. The data were recorded on cassette tapes and analysed using the HADAS software. Target strength distributions show two distinct peaks which correspond to age-1 and to older cisco (Figure 3.2). In this case, two size classes could be separated with acoustics with average target strength (calculated from the backscattering cross sections) of -42.2 dB and -36.1 dB. The average length of cisco in the gill nets was 18.1 cm for age-1 and 36.2 cm for age 2 and older. We expect target strengths between -42.8 and -36.8 dB for these fish sizes (from TS=20 log L - 68, Lindem and Sandlund 1984). Note that it is not possible to separate age-2 fish from age-3 fish in the target strength distribution since the size difference between these two groups is too small (29 cm versus 36 cm).

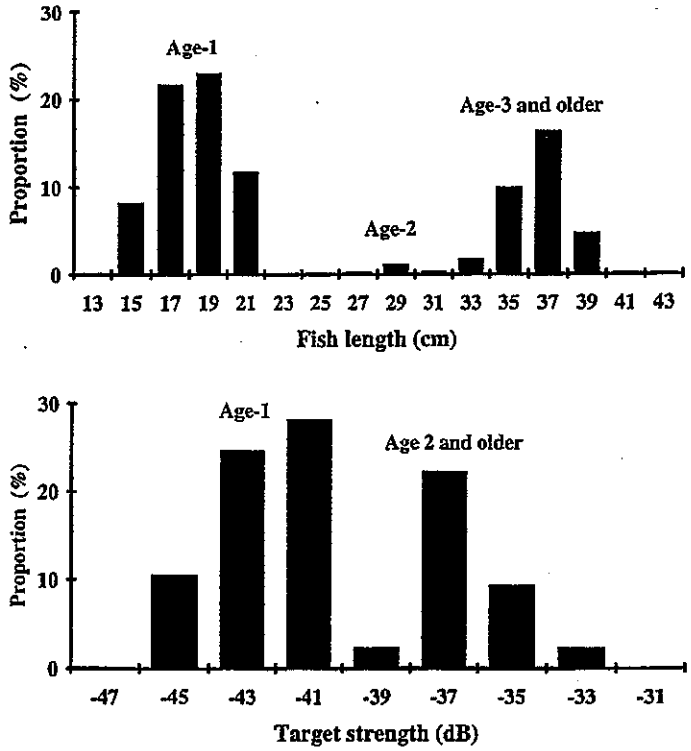

Figure 3.2. Fish sizes in vertical gill nets and target strength distributions from Amisk Lake, Alberta. These data were collected by Peter Aku, University of Alberta, during the night of July 25, 1989. The target strength distribution is based on 451 single fish echoes. Modified from Aku *et al.* (1997).

In our experience, a relative size difference of about a factor of 2 is necessary to separate two fish size classes in the target strength distribution if both size classes are approximately equally abundant (Parkinson *et al.*, 1994). Smaller targets than -48 dB were present and were likely due to age-0 cisco which were not vulnerable to the gill nets. Age-0 cisco must have been present in the lake at the time of the survey as many age-1 fish were caught the following year. Thus, it is possible that three distinct size classes can be detected in the target strength distribution under ideal conditions. Fast growing cisco populations may be close to this ideal as we can find abundant fish in three distinct size classes around 7-9 cm (age-0), 15–20 cm (age-1) and over 28 cm (age-2 and older) in July - August.

Example 2. Lake Champlain, Vermont and New York
LaBar (unpubl. data) collected acoustic data with a Biosonics model 102 dual-beam echo-sounder (200 kHz, 0.5 ms pulse duration, 6/15 degree dual-beam transducer, source level 212 dB re 1 µPa at 1 m) as part of a survey of rainbow smelt (*Osmerus mordax*) abundance in Lake Champlain in 1990. LaBar surveyed two areas of the lake with different fish densities: the Inland Sea and Malletts Bay. Acoustic signals were recorded on digital cassette tapes. Trawl samples with a 5 m x 5 m midwater trawl were collected concurrently with the acoustic data using the stepped-oblique trawling technique described by Kirn and LaBar (1991). The dual-beam analysis was done with Biosonics ESP software at Biosonics Inc., Seattle. Acceptable single fish echoes had a pulse duration of between 0.35 and 0.60 msec at -6 dB below the peak value. Maximum half-angle for processed targets was 4.0 degrees. Target tracking routines were not applied to these data. Single-beam analysis was performed on data collected with the narrow beam using the HADAS software. The trawl data and results of target strength analyses are presented in Figure 3.3.

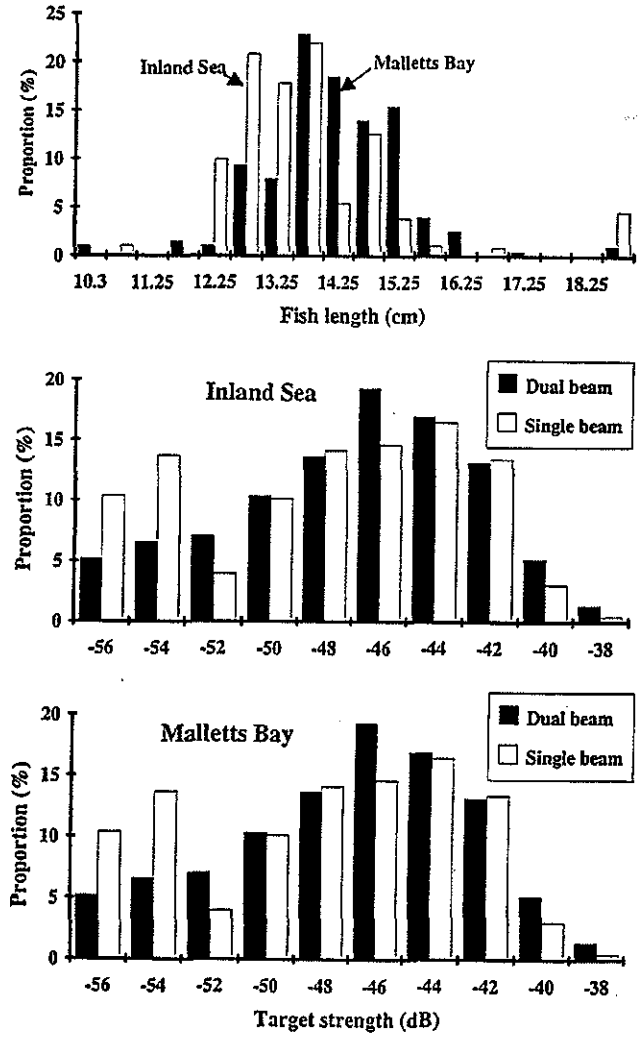

Figure 3.3. Fish sizes in trawls and target strength distributions in two areas of Lake Champlain. The acoustic target strength distributions were based on either dual-beam (filled bars) or single-beam (open bars) analysis.

Trawl catches were dominated by 9-to-24-cm-long rainbow smelt with no distinct size peaks. Average fish size was 13.8 cm in the Inland Sea and 14.2 cm in Malletts Bay. Catches were about twice as high in the Inland Sea as in Malletts Bay. Acoustic data revealed similar differences in fish size and density between the two areas. The average target strengths (calculated from the backscattering cross section of echoes larger than -57 dB) were -45.6 dB (dual beam, DB) and -46.7 dB (single beam, SB) in the Inland Sea and -45.0 dB (DB) and -45.7 dB (SB) in Malletts Bay. Corresponding fish sizes (calculated with the equation TS= 20 log L - 68) are 13.2 cm (DB) and 11.6 cm (SB) in the Inland Sea and 14.1 cm (DB) and 13.0 cm (SB) in Malletts Bay. Thus, both methods measured target strengths that were close to what we expect from trawl catches and our target strength-to-length regressions. Also, changes in size distribution with depth were similar for the two acoustic methods. Both show smaller and fewer fish towards the surface and small changes in fish size between 15 and 30 m depth. Although neither method could differentiate between different fish size groups in the target strength distribution (because of the broad overlapping length distribution of the fish present), it is encouraging that both methods are sensitive enough to detect differences in average target strength from two fish populations differing in average size by less than 1 cm.

The similarity between the target strength distributions obtained by the two methods may not be surprising since both methods used the same input data. However, the two methods are quite different and rely on either a ratio between echoes received on two different transducers (dual-beam method, see chapter 4) or on a deconvolution of data from only one of these transducers (single-beam method). Both methods discriminate single-fish echoes used for the target strength distributions from multiple-fish echoes, but the criteria are different. Therefore, the target strength distributions are based on different numbers of echoes. In some depth layers the single-beam method accepted more than eight times as many echoes as single fish than the dual-beam method. This is likely the result of the larger sampling volume in the wide beam compared to the narrow beam (the only data used by the single-beam method). A larger insonified volume results in more multiple echoes and fewer single-fish echoes if fish density is high. The single-beam method detected a higher proportion of smaller targets (-57 to -51 dB) than the dual-beam method. Unfortunately, the trawl samples cannot help us determine whether the dual-beam method is biased against small targets or whether the single-beam method is biased towards small targets since gear escapement is a problem for smaller fish in the applied trawl.

3.6 Concluding remarks

In situ target strength estimation is becoming a routine part of acoustic surveys. Although dual-beam and split-beam methods should give more accurate target strength estimates, our data and other comparisons (Dahm *et al.*, 1992, Parkinson *et al.*, 1994) indicate that single-beam methods also give reliable results that can be used in fish population estimates. Foote (1991) suggested that the relatively consistent target strengths obtained with either dual-beam, split-beam or single-beam analysis indicate that these methods give viable results. Because of lower cost and simpler equipment, single-beam analysis will continue to be used by many scientists and fisheries managers, especially for work in freshwater.

Acknowledgment

We are grateful to Peter Aku and Bill Tonn for access to data from Amisk Lake and to Egil Ona and Kenneth Foote for comments on the manuscript. Contribution # 165 from the Cornell Biological Field Station.

References

Aku, P. M. K., Rudstam, L .G., and Tonn, W. M. (1997). Impact of hypolimnetic oxygenation on the vertical distribution of cisco (*Coregonus artedi*) in Amisk Lake, Alberta. Canadian Journal of Fisheries Aquatic Science, 54(9): 2182–2195.

Brabrand, A., Faafeng, B. A., and Nilssen, J. P. M. 1990. Relative importance of phosphorus supply to phytoplankton production: fish excretion versus external loading. Canadian Journal of Fisheries Aquatic Sciences, 47: 364–372.

Brenner, T., Clasen, J., Lange, K., and Lindem, T. 1987. The whitefish (*Coregonus lavaretus* (L.)) of the Wahnbach reservoir and their assessment by hydroacoustic methods. Schweizerische Zeitschrift für Hydrologie, 49: 363–371.

Clay, C. S. 1983. Deconvolution of fish scattering PDF from echo PDF for a single transducer sonar. Journal of the Acoustical Society of America, 73: 1989–1994.

Clay, C. S., and Heist, B. G. 1984. Acoustic scattering by fish - acoustic models and a two-parameter fit. Journal of the Acoustical Society of America, 75: 1077–1083.

Clay, C. S., and Medwin, H. 1977. Acoustical oceanography: principles and application. John Wiley & Sons, London, 544 pp.

Craig, R. E., and Forbes, S. T. 1969. A sonar for fish counting. FiskDir. Skr. Ser. Havunders., 15: 210–219.

Dahm, E., Hartmann, J., Jurvelius, J., Löffler, H., and Völzke, V. 1992. Review of the European-Inland-Fisheries-Advisory-Commission (EIFAC) Experiments on Stock Assessment in Lakes. Journal of Applied Ichthyology, 8: 1–9.

Dawson, J. J., and Karp, W. A. 1990. *In situ* measures of target-strength variability of individual fish. Rapports et Procès-Verbaux des Réunions du Conseil International pour l'Exploration de la Mer, 189: 264–273.

Degnbol, P., Lassen, H., and Staehr, K.-J. 1985. *In situ* determination of target strength of herring and sprat at 38 and 120 kHz. Dana, 5: 45–54.

Dickie, L. M., and Boudreau, P. R. 1987. Comparison of aoustic reflections from spherical objects and fish using a dual-beam echosounder. Canadian Journal of Fisheries Aquatic Sciences, 44: 1915–1921.

Ehrenberg, J. E. 1972. A method for extracting the fish target strength distribution from acoustic echoes. Proceedings of International Conference on Engineering in the Ocean Environment, 1: 61–64.

Ehrenberg, J. E. 1983. New methods for indirectly measuring the mean acoustic backscattering cross section of fish. FAO Fisheries Report, 300: 91–98.

Ehrenberg, J. E., Carlson, T. J., Traynor, J. J., and Williamson, N. J. 1981. Indirect measurement of the mean acoustic backscattering cross-section of fish. Journal of the Acoustical Society of America, 69: 955–962.

Foote, K. G. 1982. Optimizing copper spheres for precision calibration of hydroacoustic equipment. Journal of the Acoustical Society of America, 71: 742–747.

Foote, K. G. 1991. Summary of methods for determining fish target strength at ultrasonic frequencies. ICES Journal of Marine Science, 48: 211–218.

Foote, K. G., and MacLennan, D. N. 1984. Comparison of copper and tungsten carbide calibration spheres. Journal of the Acoustical Society of America, 75: 612–616.

Foote, K. G., Knudsen, H. P., MacLennan, D. N., and Simmonds, E .J. 1987. Calibration of acoustic instruments for fish density estimation: a practical guide. Cooperative Research Report, International Council for the Exploration of the Sea, 144.

Guillard, J., and Gerdeaux, D. 1993. *In situ* determination of the target strength of roach (*Rutilus rutilus*) in lake Bouget with a single beam sounder. Aquatic Living Resources, 6:285–289.

Hansson, S. 1993. Variation in hydroacoustic abundance of pelagic fish. Fisheries Research, 16:203–222.

Hedgepeth, J. B. 1994. Stock assessment via tuning and smoothed EN estimation. Ph. D. thesis, University of Washington, Seattle, WA, USA.

Huang, K., and Clay, C. S. 1980. Backscattering cross sections of live fish: PDF and aspect. Journal of the Acoustical Society of America, 67:795–802.

Jacobson, P. T., Clay, C. S., and Magnuson, J. J. 1990. Size, distribution, and abundance by deconvolution of single-beam acoustic data. Rapports et Procès-Verbaux des Réunions du Conseil International pour l'Exploration de la Mer, 189: 304–311.

Jurvelius, J., Lindem, T., and Heikkinen, T. 1988. The size of a vendace, *Coregonus albula* L., stock in a deep lake basin monitored by hydroacoustic methods. Journal of Fish Biology, 32: 679–687.

Kieser, R., and Ehrenberg, J. E. 1990. An unbiased, stochastic echo counting model. Rapports et Procès-Verbaux des Réunions du Conseil International pour l'Exploration de la Mer, 189: 65–72.

Kirn, R. A., and LaBar, G. W. 1991. Stepped-oblique midwater trawling as an assessment technique for rainbow smelt. North American Journal of Fisheries Management, 11: 167–176.

Lindem, T. 1983. Successes with conventional *in situ* determination of fish target strength. FAO Fisheries Report, 300: 104–111.

Lindem, T., and Sandlund, O. T. 1984. New methods in assessment of pelagic fish stocks - coordinated use of echo-sounder, pelagic trawl and pelagic nets. Fauna, 37: 105–111.

MacLennan, D. N., and Simmonds, E. J. 1992. Fisheries Acoustics. Chapman & Hall, London.

Mulligan, T. J., and Kieser, R. 1986. Comparison of acoustic population estimates of salmon in a lake with a weir count. Canadian Journal of Fisheries and Aquatic Sciences, 43:1373–1385.

Nash, R. D. M., Sun, Y., and Clay, C. S. 1987. High resolution acoustic structure of fish. Journal du Conseil International pour l'Exploration de la Mer, 43: 23–31.

Parkinson, E. A., Reiman, B. E., and Rudstam, L. G. 1994. A comparison of acoustic and trawl methods for estimating density and age structure in kokanee. Transactions of the American Fisheries Society, 123(6): 841–854.

Robinson, B. J. 1982. An *in situ* technique to determine fish target strength with results for blue whiting (*Micromesistius poutassou* Risso). Journal du Conseil International pour l'Exploration de la Mer, 40: 153–160.

Robinson, B. J. 1983. *In situ* measurement of the target strengths of pelagic fishes. FAO Fisheries Report, 300: 99–103.

Robinson, B. J. 1984. Calibration of equipment. Subject group C. Rapports et Procès-Verbaux des Réunions du Conseil International pour l'Exploration de la Mer, 184: 62–67.

Rudstam, L. G., Clay, C. S., and Magnuson, J. J. 1987. Density and size estimates of cisco, Coregonus artedii using analysis of echo peak a single transducer sonar. Canadian Journal of Fisheries Aquatic Sciences, 44: 811–821.

Rudstam, L. G., Hansson, S. Johansson, S., and Larsson, U. 1992. Dynamics of planktivory in a coastal area of the northern Baltic Sea. Marine Ecology Progress Series, 80: 159–173.

Rudstam, L. G., Lathrop, R. C., and Carpenter, S. R. 1993. The rise and fall of a dominant planktivore: effects on zooplankton species composition and seasonal dynamics. Ecology, 74: 303–319.

Rudstam, L. G., Palmén, L.-E., Hansson, S., and Hagström, O. 1989. Acoustic fish abundance in a Baltic archipelago: comparison between results from echo integration and from analysis of echo peaks. ICES CM 1989/B:27.

Snorrason, S. S., Jonasson, P. M., Jonsson, B., Lindem, T., Malmquist, H. J., Sandlund, O. T., and Skulason, S. 1992. Population dynamics of the planktivorous arctic charr *Salvelinus alpinus* (Murta) in Thingvallavatn. Oikos, 64:352–364.

Urick, B. J. 1983. Principles of underwater sound for engineers. 3rd edition. McGraw-Hill, New York 384 pp.

Walline, P. D., Pisanty, S., and Lindem, T. 1992. Acoustic Assessment of the Number of Pelagic Fish in Lake Kinneret, Israel. Hydrobiologia, 231:153–163.

4 Dual-beam method

J. J. Traynor

4.1 Principle

The dual-beam target strength measurement technique is the simplest multi-beam procedure. A simplified block diagram for this system is presented in Figure 4.1. The transducer consists of two beams, a narrow and a wide beam, with their acoustic axes aligned. The acoustic signal is transmitted on the narrow beam, and the echo is received on the narrow and wide beams simultaneously. Typical beam pattern functions for the narrow and wide beams of a dual-beam system are provided in Figure 4.2. The echo intensity on the narrow (I_n) and wide (I_w) beams will be:

$$I_n = c_n\left(10^{2\alpha r}r^4\right)^{-1} b_n^2(\theta,\phi)\sigma, \quad \text{and} \tag{4.1}$$

$$I_w = c_w\left(10^{2\alpha r}r^4\right)^{-1} b_n(\theta,\phi)b_w(\theta,\phi)\sigma, \tag{4.2}$$

where c_n and c_w are narrow- and wide-beam constants dependent on source level and the system gain on each channel, $b_n(\theta,\phi)$ and $b_w(\theta,\phi)$ are beam pattern functions for the wide and narrow beams, $(10^{2\alpha r}r^4)^{-1}$ is the two-way transmission loss, r is range in meters and α is the attenuation coefficient.

The dual-beam technique was first proposed by Ehrenberg (1974). Early implementations of the technique are reported in Traynor (1975) and Weimer and Ehrenberg (1975). Early systems were built at 38, 105 and 120 kHz. The transducers for these systems were designed so that wide-beam directivity, $b_w(\theta,\phi)$, was essentially unity over the main lobe of the narrow beam. Under these conditions, the intensity on the wide beam becomes:

$$I_w = c_w\left(10^{2\alpha r}r^4\right)^{-1} b_n(\theta,\phi)\sigma \tag{4.3}$$

From this, it follows that:

$$\frac{I_n}{I_w} = \frac{c_n\left(10^{2\alpha r}r^4\right)^{-1} b_n^2(\theta,\phi)\sigma}{c_w\left(10^{2\alpha r}r^4\right)^{-1} b_n(\theta,\phi)\sigma} = c_{nw}b_n(\theta,\phi)\ , \tag{4.4}$$

where c_{nw} is unity if each system has the appropriate time-varied gain (TVG, to correct for two-way transmission loss) and the non-TVG gain in the two channels is equal. Ehrenberg (personal communication) examined the performance of dual-beam systems in the presence of noise and concluded that optimum performance was obtained when the wide beam was 2 to 3 times the narrow-beam angle (to -3 dB points). In this situation, $b_w(\theta,\phi)$ will not be unity over the main lobe of the narrow beam. If $b_w(\theta,\phi)$ is not unity over the main lobe of the narrow beam, the ratio of the intensity on the two beams will be:

$$\frac{I_n}{I_w} = c_{nw}\frac{b_n(\theta,\phi)}{b_w(\theta,\phi)}\ . \tag{4.5}$$

After logarithmic transformation, and, assuming c_{nw} is unity, this equation becomes:

$$B_n(\theta,\phi) - B_w(\theta,\phi) = I_n[dB] - I_w[dB]\ . \tag{4.6}$$

An approximately linear relationship was observed between $BN(\theta,\phi)$ and $(BN(\theta,\phi) - BW(\theta,\phi))$:

$$B_n(\theta,\phi) = c_r\left[(B_n(\theta,\phi) - B_w(\theta,\phi)\right], \text{ and} \tag{4.7}$$

$$B_n(\theta,\phi) = c_r(I_n[dB] - I_n[dB]) \tag{4.8}$$

where c_r is a constant equal to 1 when the wide-beam directivity is unity over the narrow beam's main lobe, and is greater than 1 for transducers with beam drop-off. This constant is typically determined empirically.

4.2 Removal of beam effect

Once the beam effect is calculated using equation 4.8, beam effect is removed using the formula relating target strength and echo strength:

$$TS = I_n[dB] + 2B_n(\theta,\phi)\ . \tag{4.9}$$

4.3 Effect of noise and thresholds involved

It is useful to discuss the impact of noise on the estimation of the beam pattern effect, $b_n(\theta,\phi)$. As discussed above, $b_n(\theta,\phi)$ is calculated as a function of intensities on the two acoustic beams:

$$b_n(\theta,\phi) = f(I_n I_w^{-1})\ . \tag{4.10}$$

The impact of noise on the narrow- and wide-beam pulses is complicated and dependent on the nature of the noise. However, the impact of noise on the estimate of $b_n(\theta,\phi)$ can be generally discussed. The dual-beam technique is especially sensitive to noise since $b_n(\theta,\phi)$ is estimated as a ratio of two intensities, particularly since the wide beam may be subject to additional noise due to increased beam width. The likely effect of noise will be to spread out the estimates of $b_n(\theta,\phi)$ derived using the dual-beam procedure. It is common for estimates of $b_n(\theta,\phi)$ to exceed unity, particularly for targets near the acoustic axis (-Traynor and Ehrenberg, 1990).

To minimize the impact of noise in the analysis, two procedures are usually employed. (1) Targets are usually only accepted at fairly short ranges (less than about 75 m for 120 kHz systems and perhaps 150 m for 38 kHz systems). The exact values for these maximum ranges will depend on the fish size and the prevailing noise conditions; however, these values are reasonable values for typical operating situations. (2) A beam pattern threshold is imposed which requires beam pattern estimates derived from a target to be greater than a beam pattern threshold

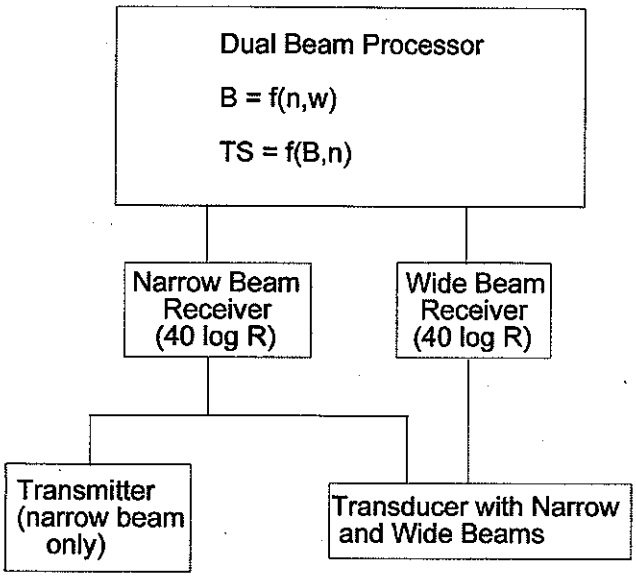

Figure 4.1. Block diagram of a dual-beam system.

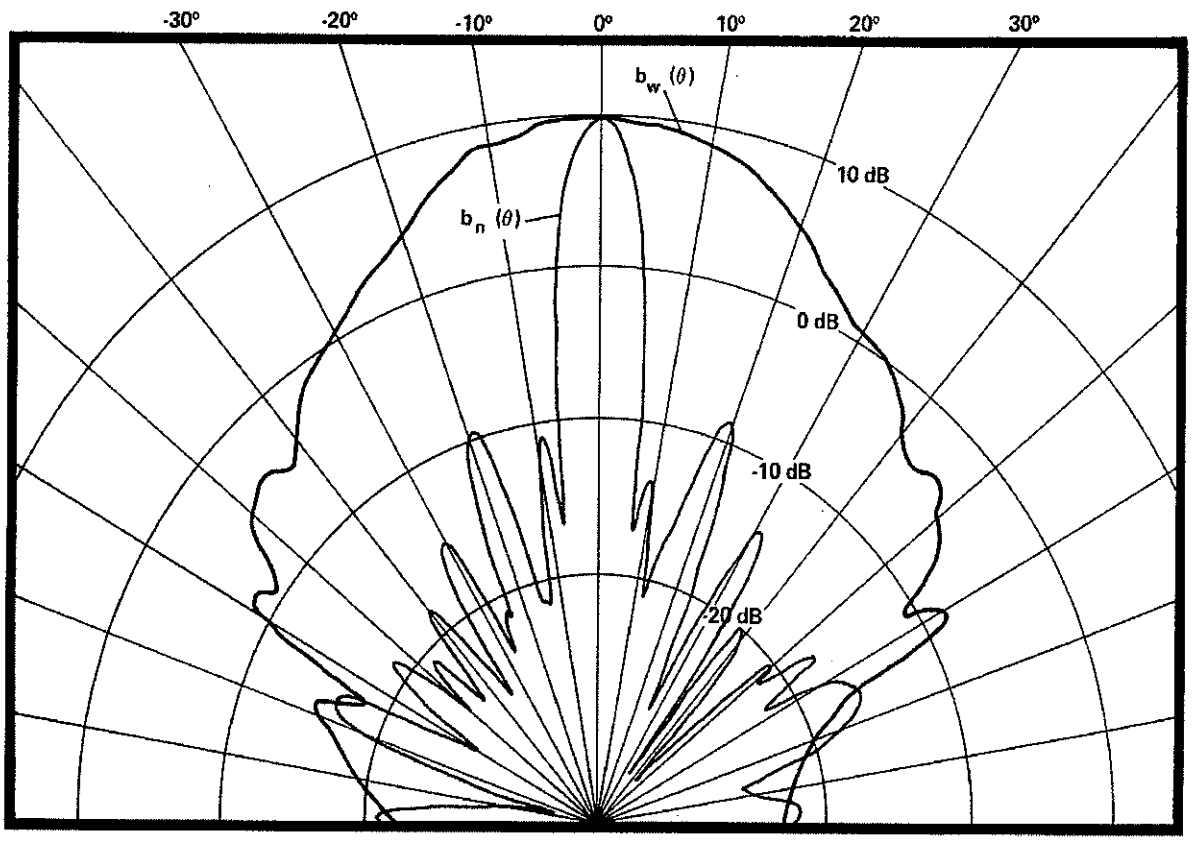

Figure 4.2. Typical beam pattern functions for the narrow and wide beams of a dual-beam system.

(only targets near the centre of the beam are accepted). Use of this threshold reduces the bias against small targets.

4.4 Calibration

Initial calibrations are conducted by comparison calibration using standard hydrophones to adjust the narrow and wide beam receivers to provide approximately equal output voltages for on-axis targets. Typically, a standard sphere is suspended beneath the dual-beam transducer and the target is moved fore and aft and side to side while monitoring the narrow-beam channel response. The standard sphere is held stationary once the maximum response on the narrow beam is obtained. Either the gain on the wide beam is adjusted to provide the same output voltage as on the narrow beam, or an adjustment factor is calculated to correct the wide beam.

In addition, the beam patterns of the wide and narrow beams need to be measured. This is usually obtained using standard hydrophone techniques although initial beam pattern measurements are often supplied by the manufacturer.

4.5 Detailed example

The following calibration procedure is provided from measurements described by Rose and Porter (1996). All acoustic measurements were made using a dual-beam acoustic system operating at 38 kHz (full angles to the -3 dB point of: narrow beam - 6°, wide beam - 16°). The transducer was bolted on a floating platform over the centre of the experimental compound. A 38 mm tungsten-carbide standard target was suspended on monofilament line approximately 7.5 m beneath the transducer and measurements were made as the target swung freely through the acoustic beam.

In an actual system, the measured variable is echo voltage (u). Echo intensity is calculated as

$$I(dB) = 20\log(u) - rS\ , \qquad (4.11)$$

where rS is receiving sensitivity. Also, source level (SL) is required to determine the constants c_n and c_w in equations 4.1 and 4.2. For the field calibration, an iterative process was used to estimate the dual-beam parameters: SL, the narrow-beam receiver sensitivity (rS_n), the wide-beam sensitivity (rS_w), and the wide-beam drop-off (c_r). To begin, best guesses of these parameters are employed (based on hydrophone measurements or previous calibrations). TS levels are calculated and plotted against the axis position and a regression generated (Figure 4.3). The parameters are adjusted in further iterations until the measured target strengths cluster around the true value and show no trend with $BN(\theta,\phi)$, at least for $BN(\theta,\phi)$ -6 dB (Figure 4.3).

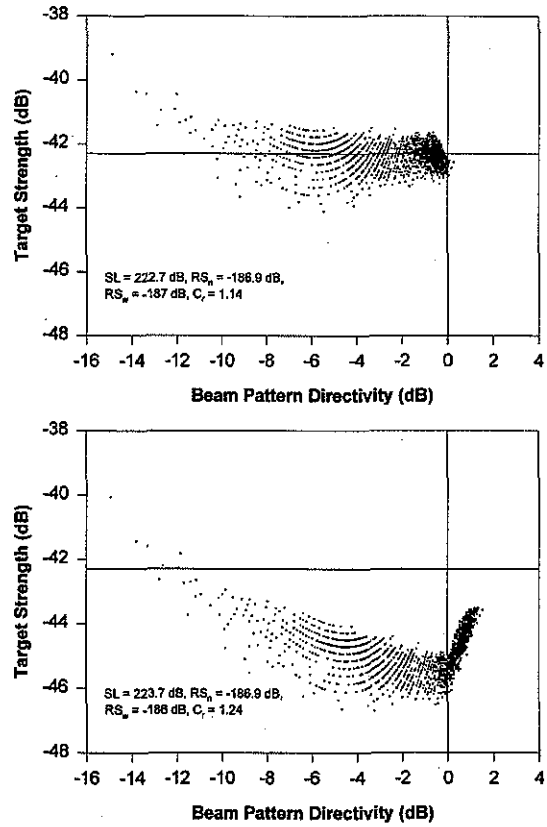

Figure 4.3. Estimated target strength of a 38 mm tungsten carbide sphere allowed to swing freely through the acoustic beam of a 38-kHz dual-beam echo sounder. Top panel shows calibrated results; bottom panel shows uncalibrated results. Parameters to obtain the calibrated results are derived using an iterative procedure. (From Rose and Porter 1996.)

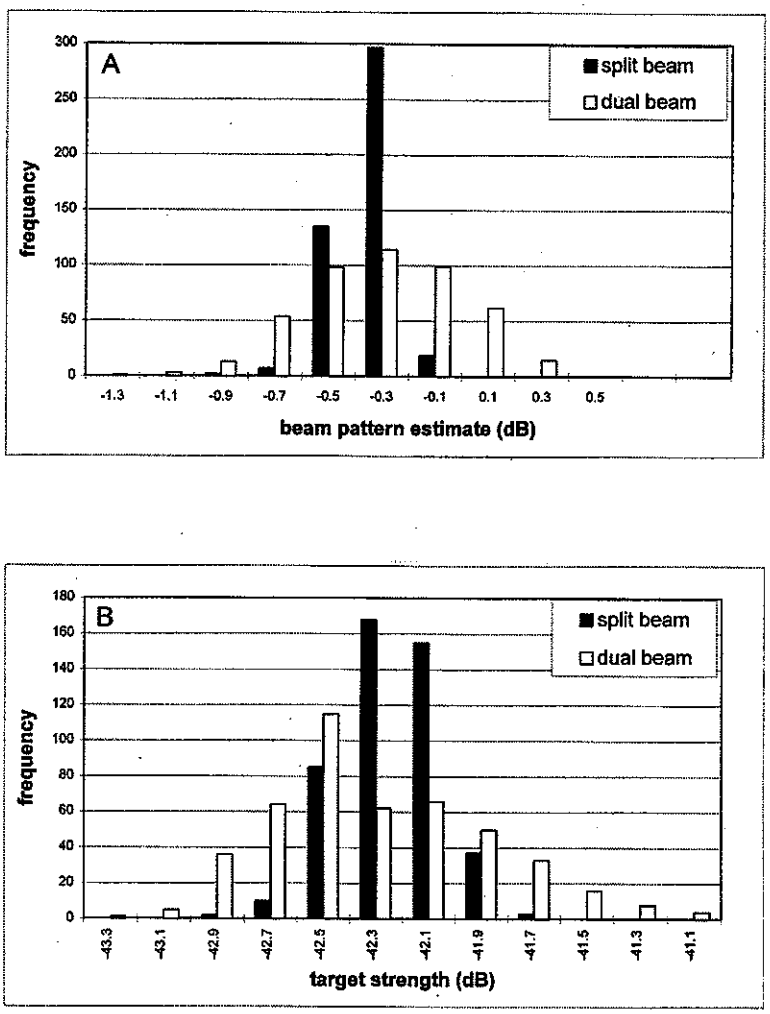

Figure 4.4. Beam pattern (A) and target strength (B) measurements of a 38.1 mm tungsten carbide sphere using the dual-beam and split-beam techniques (from Traynor and Ehrenberg, 1990).

In brief, changes in the parameters have the following effects: the relative values of rS_n and rS_w affect the individual beam pattern estimates and as a consequence the proportion of observations with estimates of $BN(\theta,\phi) > 0$ dB; the SL value changes the intercept; and, c_r influences the slope of the data. A correct calibration is achieved when TS values measured at any position in the beam are equivalent in mean (equal to theoretical value, here -42.3 dB) and variance, the slope = 0, and the proportion of positive values of the axis measure comprise less than about 5% of the total data. In practice, the TS values should be constant to about 4 dB off axis since, for most applications, returns from further off axis are rejected to reduce bias against small targets. The parameter values are then further tested in subsequent calibration runs. It is very important when using this procedure that the target passes through the acoustic axis. Shipboard calibrations (where divers and cameras are not used to centre the standard target in the beam) employed a calibration frame wherein the target is incrementally stepped through the beam using a three- or four-line cradle to be certain the beam centre has been crossed (e.g. Foote *et al.*, 1987; MacLennan and Simmonds, 1992).

The dual-beam system is inherently more sensitive to noise than the split-beam system. Figure 4.4 shows measurements of a standard sphere made using a dual/split-beam system (Traynor and Ehrenberg, 1990). For a standard sphere suspended within the acoustic beam, target strength estimates as well as beam pattern estimates obtained using the dual-beam were much more variable than the corresponding split-beam measurements. Traynor and Ehrenberg also present target strength measurements of walleye pollock (*Theragra chalcogramma*) using both the split- and dual-beam systems. The two systems provided similar trends in target strength (Figure 4.5), but the split-beam measurements more closely tracked the expected beam pattern distribution than did the dual-beam measurements (Figure 4.5), due to the effect of noise on the beam pattern measurements.

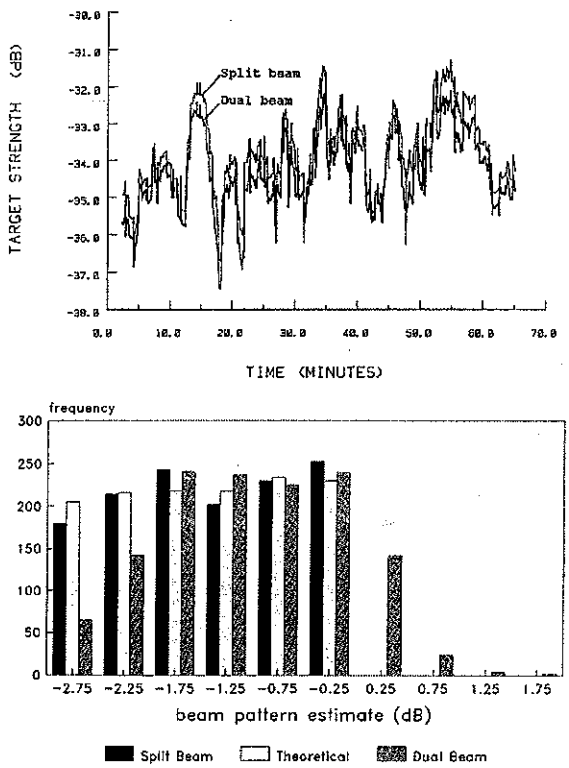

Figure 4.5. Comparison of dual-beam and split-beam target strength measurements of walleye pollock (*Theragra chalcogramma*). The top diagram shows running averages of 49 target strength values. The bottom diagram compares beam pattern distribution collected using the dual beam and split beam systems with theoretical calculations. (From Traynor and Ehrenberg, 1990).

References

Ehrenberg, J. E. 1974. Two applications for a dual-beam transducer in fish assessment systems. Proceedings 1974. International Conference on Engineering in the Ocean Environment 1: 152–155.

Foote, K. G., Knudsen, H. P., Vestnes, G., MacLennan, D. N., and Simmonds, E. J. 1987. Calibration of acoustic instruments for fish density estimation: a practical guide. Cooperative Research Report, International Council for the Exploration of the Sea, 144, 1–69.

MacLennan, D. N., and Simmonds, E. J. 1992. Fisheries Acoustics. Chapman and Hall, London, 325 pp.

Rose, G. A., and Porter, D. R. 1996. Target strength studies on Atlantic cod (*Gadus morhua*) in Newfoundland waters. ICES Journal of Marine Science, 53(2): 259–265.

Traynor, J. J. 1975. Studies on indirect and direct methods of *in situ* fish target strength measurements. In Acoustic surveying of fish populations. Proceedings of the Specialist Meeting held at the Fisheries Laboratory of the Ministry of Agriculture, Fisheries and Food, Lowestoft, 17 December 1975. Birmingham, University of Birmingham, 6 pp.

Traynor, J. J., and Ehrenberg, J. E. 1990. Fish and standard-sphere target strength measurements obtained with a dual-beam and split-beam echo-sounding system. Rapports et Procès-Verbaux des Réunions du Conseil International pour l'Exploration de la Mer, 189: 325–335.

Weimer, R. T., and Ehrenberg, J. E. 1975. Analysis of threshold-induced bias inherent in acoustic scattering cross section estimates of individual fish. Journal of the Fisheries Research Board of Canada, 32(2): 2547–2551.

5 Split beam method

P. Reynisson

5.1 Principle

The split-beam method has been used for direction-sensing applications both in radio and sonar for several decades. The principle is simply illustrated by considering the angle of incidence in θ of a wave arriving at two point-element sensors separated by a distance d as shown in Figure 5.1. For a plane wave passing at an angle θ between the line of elements and the wavefront,

$$\sin\theta = c\Delta t/d, \tag{5.1}$$

where Δt is the time difference between arrivals of identical wave features at each element and c is the propagation speed in the medium. The distance $c\Delta t$ can be expressed in terms of the phase difference δ ($-\pi<\delta<\pi$) and the wavelength λ,

$$c\Delta t = \delta\lambda/2\pi = \delta/k, \tag{5.2}$$

where k is the wave number. Substituting (5.2) into (5.1) and rearranging leads to:

$$\theta = \sin^{-1}(\delta/kd). \tag{5.3}$$

The constant $kd = \delta/\sin\theta$ characterizes this particular geometry of elements for a given wavelength. With the addition of another pair of elements oriented at a non-zero angle with respect to the first pair, a second angle can be determined and the precise direction of the wave can be found.

In fisheries research the split-beam technique has been realized by using a transducer divided into four quadrants (Carlson and Jackson 1980). During transmission all quadrants are driven simultaneously, but under reception each one forms its own beam. The individual outputs are combined to form a full beam and two split-beam sets. A schematic view of a split-beam transducer is shown in Figure 5.2. To determine the angle of a target relative to the acoustic axis in the alongship-plane, the summed signals of the two fore quadrants (F.P.+F.S.) are compared to the summed signals of the "aft" quadrants (A.P.+A.S.). Similarly the angle in the athwartship- plane is determined from the phase difference between the summed port- and starboard quadrants (F.P.+A.P. and F.S.+A.S.).

Let the angles α and β define the target direction relative to the acoustic axis of the transducer in the alongship- and athwartship plane, respectively. The normal spherical coordinates (θ and ϕ) are expressed in terms of α and β by the formulas:

$$\theta = \sin^{-1}\left((\cos^2\alpha + \cos^2\beta)^{1/2}\right) \text{ and}$$
$$\phi = \tan^{-1}(\cos\alpha/\cos\beta)\ . \tag{5.4}$$

For small angles, θ and ϕ can be approximated by:

$$\theta = \sqrt{\alpha^2+\beta^2} \text{ and } \phi = \tan^{-1}(\alpha/\beta)\ . \tag{5.5}$$

If the directivity of the split beam transducer is known in terms of either (α, β) or (θ, ϕ), the effect of the beam pattern on the received echo can be estimated and a direct measure of the target strength obtained. The signal-processing algorithm may be designed to accept only those echoes from targets within a chosen acceptance angle.

In the case of a single target such as a fish, the shape and length of the backscattered pulse is similar to the one transmitted. Some elongation and smoothing of the pulse is to be expected because of the finite bandwidth used in the receiver. The phases of successive cycles should also be stable (coherent) within the pulse if the signal is well above the noise level ratio. By restricting the pulse duration and the phase variation within the pulse to be within certain limits, discrimination against multiple targets at similar range within the pulse volume is achieved to some extent.

5.2 Calibration

Consider a single target with an backscattering cross section σ situated at a distance r from the transducer and in a direction relative to the acoustic axis defined by the spherical angles (θ, ϕ) or alternatively by the angles α and β. Let I_t and I_r be the respective intensities of the transmitted and received backscattered pulse referred to the transducer terminals. The transmitting and receiving responses of the transducer on the acoustic axis are g_{t0} and g_{r0}, respectively, and $b^2(\theta, \phi)$ or $b^2(\alpha, \beta)$, is the two-way directivity function. This is illustrated schematically in Figure 5.3. The received signal is:

$$I_r = I_t g_{t0} g_{r0} \sigma r^{-4} 10^{-2\alpha r/10} b^2(\theta,\phi)\ , \tag{5.6}$$

where the term $r^{-4}\ 10^{-2\alpha r/10}$ accounts for the two-way transmission loss of the signal due to spherical spreading and attenuation, and α is the attenuation coefficient in decibels per meter. Applying a range dependent gain function of the form:

$$g(r) = g_0 r^4 10^{2\alpha r/10}\ , \tag{5.7}$$

and rearranging, the following expression for σ is obtained:

$$\sigma = I_c\left(I_t g_{t0} g_{r0} g_0 b^2(\theta,\phi)\right)^{-1} \text{ or} \tag{5.8}$$
$$\sigma = I_c C_g C_b\ ,$$

where I_c is the calibrated output at the receiver terminal, $C_g = (I_t\ g_{t0}\ g_{r0}\ g_0)^{-1}$ accounts for all constant gain factors involved, and $C_b = (b^2(\theta, \phi))^{-1}$. The calibration of a split-beam echo sounder may therefore be conveniently

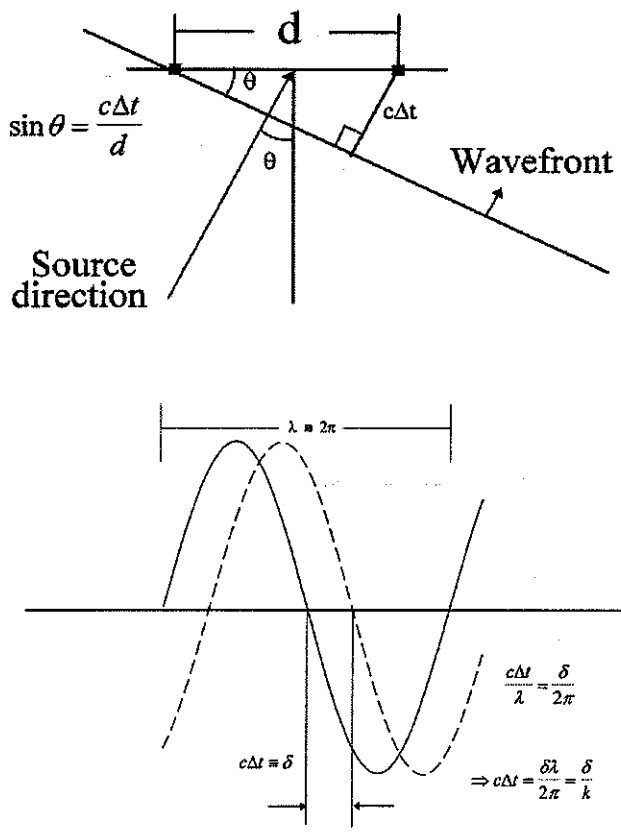

Figure 5.1. An illustration of how the angle of incidence θ of a wave arriving at two point-sensors separated by a distance d is defined. The upper part shows the geometric arrangement of the sensors in a plane normal to the arriving wavefront. The time difference between arrivals of the wavefront is Δt, and c is the sound speed in the medium. The lower part explains how the distance $c\Delta t$ can be expressed in terms of the phase difference δ of the observed signals and the wavelength λ, alternatively the wavenumber k.

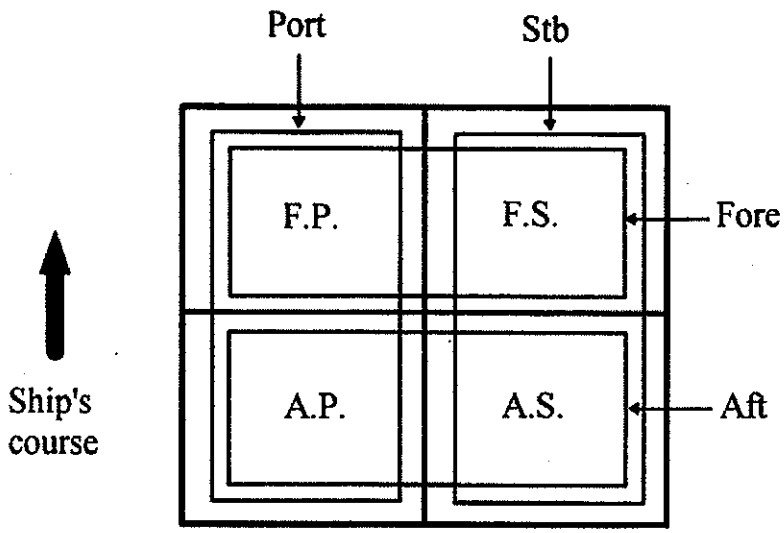

Figure 5.2. A schematic view of a split-beam transducer arranged as four segments whose signals can be accessed independently.

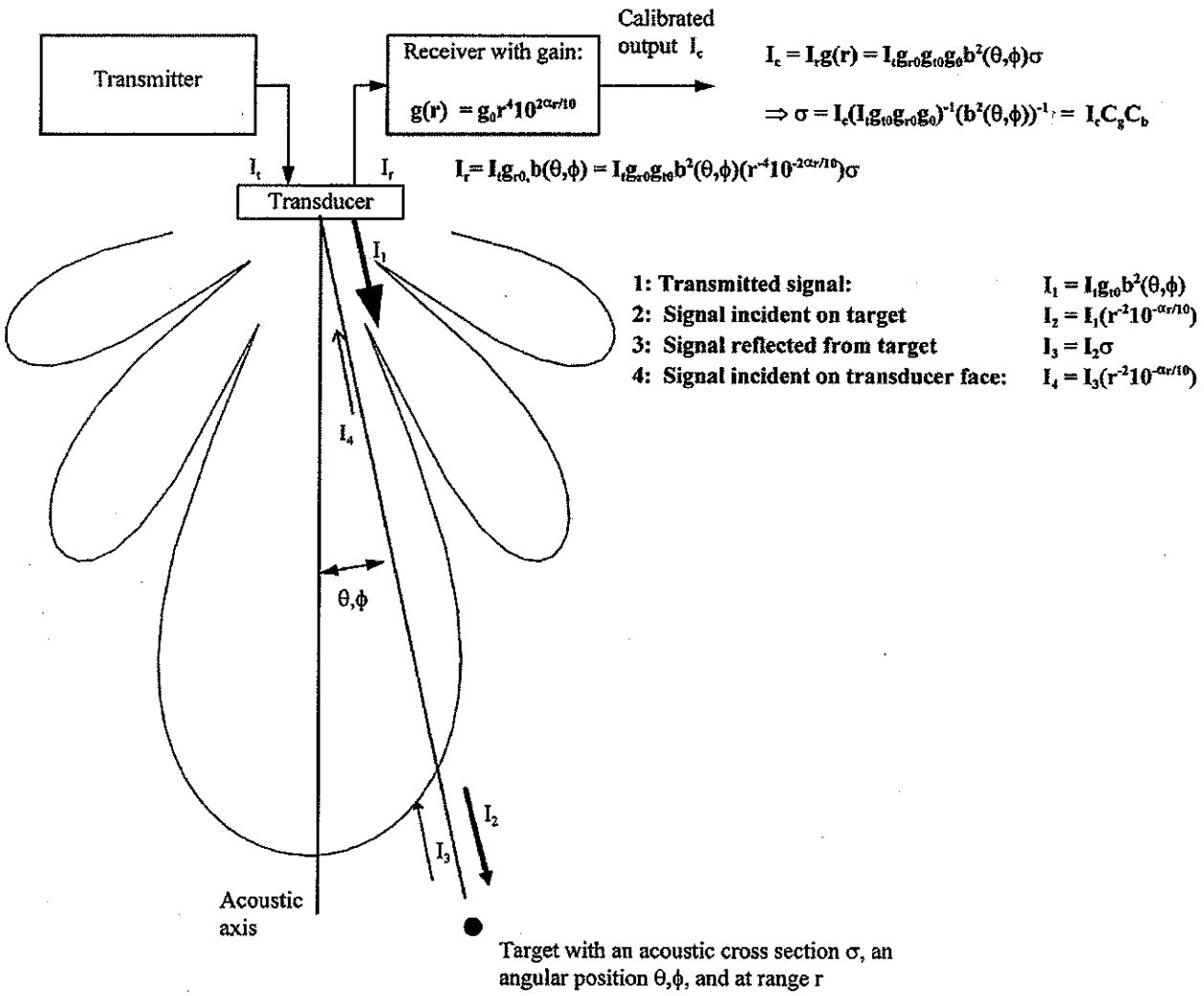

Figure 5.3. Relationship between the acoustic intensities as the sound wave propagates from the echo sounder to a target and back. I_t and I_r are the intensities of the transmitted and received backscattered pulse referred to the transducer terminals. The transmitting and receiving responses of the transducer on the acoustic axis are g_{t0} and g_{r0}, respectively, and b^2 (θ, ϕ) is the two-way directivity function.

separated into two steps: (1) the measurement of the on-axis sensitivity, and (2) the determination of the directivity correction in terms of the direction angles as obtained from the phase information.

5.2.1 On-axis sensitivity

The method for determining the on-axis sensitivity of a split-beam echo sounder is more or less identical to the on-axis calibration of an ordinary single-beam echo-sounder. A calibration sphere with an backscattering cross section σ_0 is suspended below the transducer and centered in the acoustic beam and the maximum amplitude or the pulse energy measured. A detailed explanation of this procedure will be found in Foote *et al.* (1987). If α_0 and β_0 are the direction angles of the acoustic axis, then $b^2(\alpha_0, \beta_0) = 1$ and the expression for σ in Equation (5.8) reduces to:

$$\sigma_0 = I_{c_0} C_g \,, \tag{5.9}$$

where I_{c0} is the measured echo intensity on the acoustic axis.

If the four quadrants of the transducer and the processing circuitry are properly aligned, α_0 and β_0 should be close to or equal to zero, although this is not strictly required. By measuring I_{c0}, one can determine C_g as the scaling factor taking into account all equipment parameters except the directivity pattern of the transducer.

A range-dependent gain function as in Equation (5.7) was assumed to account for the transmission loss of the wave propagating through the medium. In echo sounders this is generally referred to as time-varied gain (TVG). The implemented TVG will in general not compensate for the range dependence exactly, although in modern equipment using digital processing the deviations are small. If it is suspected that these deviations may affect the target strength measurements to a significant degree, the error must be estimated (Ona *et al.*, 1996). This is done by comparing the TVG-function of the equipment to the ideal one, thus determining the error as a function of range. The detailed procedure is outside the scope of this manual, but some measurement methods are given in Foote *et al.* (1987).

5.2.2 Acoustic beam

The purpose of this part of the calibration is to determine the average sensitivity of the active area of the beam and the additional variance of the output signal due to errors in compensation for the target direction. When using the split-beam technique the main concern is not the actual d-irectivity pattern, although a fair knowledge of it is necessary, but the value of the two-way sensitivity b^2 in terms of coordinates (such as θ and ϕ) derived from the measured phase differences. By recording the echo signal from the standard target at a number of representative positions in the active area of the beam, the sensitivity across the beam can be estimated. Two alternatives must be distinguished: (1) the echo signal with directivity correction as implemented in the equipment, and (2) the echo signal without directivity correction.

(1) Suppose that n measurements are made, and $B_i = I_{ci}/I_{c0}$ is the observed sensitivity at the ith position of the target. The mean $\bar{B}$ and the variance V_B of the sensitivity are estimated by weighting each measurement in proportion to the area it represents,

$$\bar{B} = \sum_{i=1}^{n} B_i w_i / \sum_{i=1}^{n} w_i \,, \tag{5.10}$$

and

$$V_B = (n-1)^{-1} \left(\sum_{i=1}^{n} w_i \right)^2 \sum_{i=1}^{n} \left(B_i - \bar{B} \right)^2 w_i^2, \tag{5.11}$$

where w_I is the weighting factor of the it measurement. If $\bar{\sigma}$ and V_s are the mean and variance of a sample of observed cross sections, then $\bar{\sigma}\,\bar{B}$ is an unbiased estimator of the true mean of the backscattering cross-section $\bar{\sigma}$. MacLennan and Simmonds (1992) propose the following expression for obtaining an unbiased estimate of V_σ, the variance of $\bar{\sigma}$:

$$V_\sigma / \bar{\sigma}^2 = \left(1 - V_B / \bar{B}^2\right)^{-1} \left(V_S / \bar{\sigma}^2 - V_B / \bar{B}^2 \right) \tag{5.12}$$

Equation (5.12) holds true under the assumption that the targets are randomly distributed over the active area and that the variations of sensitivity and target strength are not correlated.

(2) The second alternative is to record the echo signal without directivity correction. In this case the transducer's directivity b^2 is measured in terms of α and β. From these measurements a correction factor C_b, applicable for each pair of angles within the active area of the beam is estimated. Ideally $C_b = (b^2(\alpha, \beta)^{-1}$, but in practice C_b will not compensate b^2 exactly throughout the beam. As before the main concern is the estimation of the mean sensitivity $\bar{B}$. Methods for optimizing the correction function will be the subject of Section 5.2. Let I_0 and I_i be the observed echo intensities on the acoustic axis and at some other position in the beam, while $_{CBI}$ and $_{CB} \cong 1$ are the corresponding values of the beam-pattern correction function. Then the sensitivity B_i is calculated by the formula

$$B_i = \frac{C_{b_i} I_i}{C_{b_0} I_0} \,. \tag{5.13}$$

Equation (5.10) and (5.11) can now be applied to estimate the mean sensitivity $\bar{B}$ and its variance V_B as before.

5.3 Detailed example

Detailed measurements of a 120- kHz split-beam echo sounder

On the Icelandic research vessel "Árni Friðriksson", a SIMRAD EK500 split beam echo sounder system (Bodholt *et al,*. 1989) is installed. One of the transceivers has a working frequency of 120 kHz. The transducer is of the type ES120-7, with a 3-dB beamwidth of 7.2 degrees and an equivalent beam angle of -20.6 dB. A polar diagram of the directivity pattern supplied by the manufacturer of this transducer is shown in Figure 5.4.

The on-axis sensitivity of the echo sounder was calibrated in the manner described by Foote *et al.* (1987) and the EK500 manual. The gain of the receiver (C_g) was adjusted so that a correct target strength reading was obtained from the calibration sphere on the acoustic axis. In the EK500 this is equivalent to adjusting the "TS-transducer Gain" in the "Transceiver Menu".

In order to measure the performance of the split-beam operation, the target strength data available on one of the EK500 serial ports (port 1) were logged on a personal computer by a suitable communication programme (Procomm). The split-beam data on this port are termed "echo trace" data and include these quantities: target strength with directivity correction, so-called target strength without directivity correction, angular position of the target, and target depth. The calibration sphere was moved continuously through a cross section of the beam, by keeping the lengths of two of the suspension lines constant while the length of the third line was changed. In this

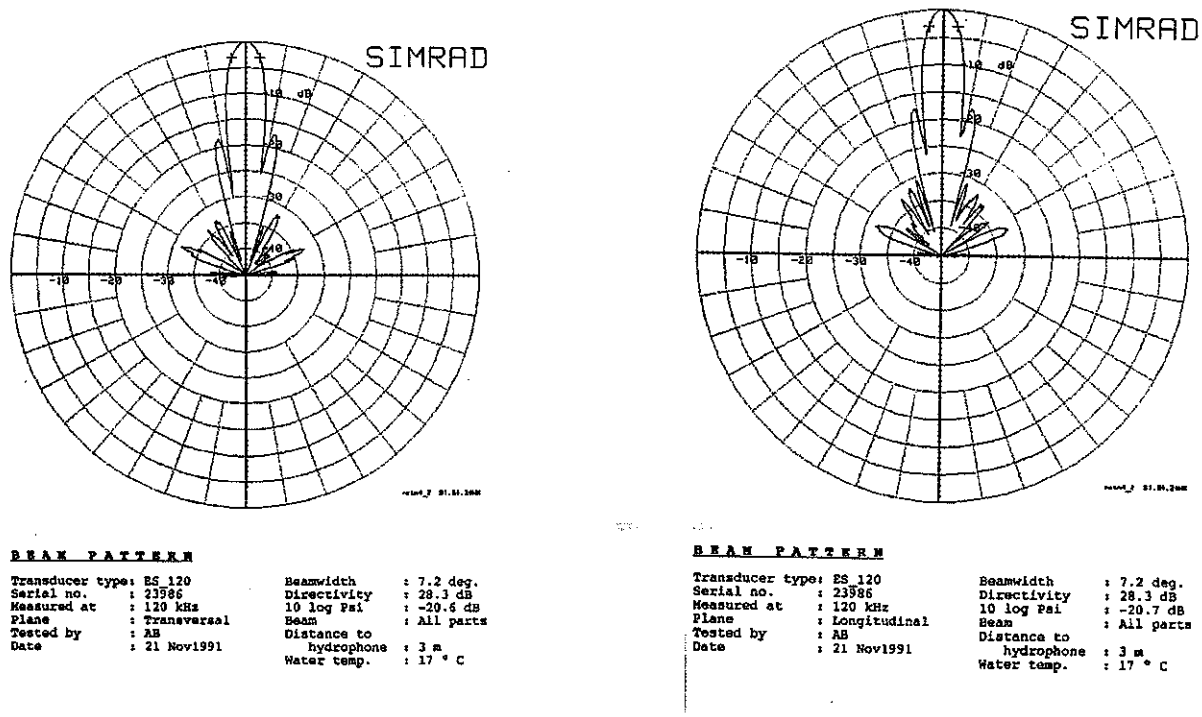

Figure 5.4. A polar diagram of the beam pattern of the 120-kHz split-beam transducer installed in R/V "Árni Friðrikson".

manner calibration data were recorded from three cross sections, all intersecting at the acoustic axis.

The aims of further measurements and analysis were, (a) to determine the values of the parameters for which the EK500 internal beam-compensation is optimal, (b) to determine or test a function C_b appropriate for directivity correction in postprocessing of uncompensated target strength data, and © to estimate the mean sensitivity $\bar{B}$ and the variance V_B in both cases.

(a) Internal directivity correction

The internal directivity correction of the EK500 is based on a function of the form

$$10\log C_{EK500}(\alpha,\beta) = 6\left[\left(\frac{\alpha-\alpha_0}{\frac{1}{2}\Phi}\right)^2 + \left(\frac{\beta-\beta_0}{\frac{1}{2}\Phi}\right)^2 - 0.18\left(\frac{\alpha-\alpha_0}{\frac{1}{2}\Phi}\right)^2\left(\frac{\beta-\beta_0}{\frac{1}{2}\Phi}\right)^2\right], \quad (5.14)$$

where C_{EK500} is equivalent to C_b in equation (5.8), and Φ is the half-power beamwidth of the transducer in question. In the EK500, four parameters can be adjusted in order to optimize the directivity correction. These are the beamwidth Φ, the offset angles α_0 and β_0 and the "angle sensitivity". The "angle sensitivity" is similar to the constant kd in equation (5.3). By substituting $\theta = \delta/kd$ in the expression for C_{EK500} it is obvious that as long as the product $\Phi = kd$ is constant, nearly identical values of the directivity correction function should be obtained.

Preliminary tests had shown that for a beamwidth around 7-7.5°, an angle sensitivity of the order of 25-30 was appropriate. In the following measurements the angle sensitivity was set to 28.0 and $\Phi = 7.5°$. The offset angles were set to zero. A total of 1475 data points were recorded. A mean residual of the internally compensated acoustic cross-section of the calibration sphere was calculated within each 1 dB interval of the two-way beam pattern, in other words for each 1 dB interval of the difference between the so-called uncorrected and corrected target strength ($\Delta TS = TS_U - TS_C$). This is a quick check on how far out into the beam one can expect reasonably correct target strength data. The result is shown in Figure 5.5a. Representing the residual as a function of ΔTS is convenient, since one of the criteria used for accepting split-beam data in the EK500 is that ΔTS should be within a certain value.

A nonlinear iteration algorithm from the statistical software Statistica by StatSoft Inc. was used to optimize C_{EK500} for values within the -9 dB limit of the two-way beam pattern, and resulted in $\Phi = 7.8$, $\alpha_0 = 0.13$, and $\beta_0 = 0.19$, which are valid for $kd = 28.0$. It was decided to use the measured value of Φ, which according to the polar diagram in Figure 5.4 is 7.2°. Keeping the product $\Phi\, kd$ constant requires that $kd = 30.3$. With these values the measurements along the three transects were repeated and a total of 2837 data points were recorded. The residual acoustic cross section as a function of ΔTS is shown in Figure 5.5b, and is obviously an improvement compared to Figure 5.5a.

In later versions of the EK-500 echo sounder software, from V. 4.01 and later versions, the transducer half power angles in alongship and athwartship directions, Φ_α and Φ_β, can be estimated separately, as needed for non-circular transducers, and as suggested as an improvement also for near-circular transducers by Ona (1990). Computer software, the LOBE.EXE, is also delivered by the manufacturer for recording and performing the best-fit iteration of the five calibration parameters of the split beam system. Calibration of gain and beam parameters are then done simultaneously, by non-linear regression, and not independently, as described here.

(b) Beam pattern correction by postprocessing.
In earlier versions of the echo sounder software, significant improvements in calibration, hence also in target strength measurements, could be achieved through post-processing the data. As the raw target strength data, without beam compensation are available on each accepted target data set, the calibration parameters could be better estimated outside the echo sounder, then by using the internal echo sounder beam compensation.

The uncorrected split-beam data were fitted to a generalized three-dimensional model suggested by Ona (1990). Rewritten for C_b the equation is:

$$C_b(\alpha,\beta) = 4\left[\left(\frac{\alpha-\alpha_0}{\frac{1}{2}\Phi_\alpha}\right)^2 + \left(\frac{\beta-\beta_0}{\frac{1}{2}\Phi_\beta}\right)^2\right]^E , \qquad (5.15)$$

Table 5.1 Results from calculations of the mean sensitivity of the 120- kHz split-beam echo sounder installed in R/V "Árni Friðriksson". SD = standard deviation.

	Internal beam correction 1st measurement			Internal beam correction 2nd measurement			Beam correction by postprocessing		
-*N*	B_1	B_N	S.D.	B_1	B_N	S.D.	B_1	B_N	S.D.
-1	1.000	1.000	0.001	0.999	0.999	0.001	1.002	1.002	0.001
-2	1.018	1.009	0.007	1.001	1.000	0.006	1.002	1.002	0.005
-3	1.039	1.019	0.009	0.994	0.998	0.006	0.990	0.998	0.006
-4	1.049	1.027	0.009	0.990	0.996	0.007	0.988	0.996	0.006
-5	1.080	1.037	0.010	0.986	0.994	0.007	0.987	0.994	0.006
-6	1.113	1.050	0.010	0.988	0.993	0.007	0.994	0.994	0.006
-7	1.172	1.067	0.011	1.007	0.995	0.008	1.023	0.998	0.006
-8	1.204	1.089	0.013	1.019	0.998	0.009	1.039	1.003	0.006
-9	1.202	1.097	0.013	0.998	0.998	0.010	1.043	1.008	0.006
-10	1.170	1.105	0.015	0.948	0.993	0.011	1.018	1.009	0.006
-11	1.146	1.108	0.015	0.971	0.991	0.012	1.024	1.010	0.007
-12	1.006	1.100	0.015	0.859	0.980	0.012	0.953	1.005	0.008

where Φ_α is the effective alongship beamwidth measured across the beam between opposite half-power levels, Φ_β is the corresponding beamwidth in the athwartship plane, and E is shape parameter to be empirically estimated.

As before, a nonlinear iteration algorithm was used to estimate the parameters, resulting in Φ_α = 7.56°, α_0 = 0.07°, Φ_β = 7.04°, β_0 = 0.11°, and E = 1.00. The residual acoustic backscattering cross section as a function of ΔTS is shown in Figure 5.5c.

(c) Estimation of B and V_B
In this particular case the cross section of the acoustic beam was divided into contours of equal sensitivity such that the solid angle or areas within the limits of every two adjacent contours were equal. This division was based on the assumption that the directional sensitivity of the transducer in decibels (10 log b^2) and the solid angle ($\Omega = 2\pi(1 - \cos\theta)$) are linearly related. This is a reasonable approximation for the main lobe of ordinary transducers. The area was further divided into segments on the basis of the azimuthal angle (φ) of the transects. The division is shown schematically in Figure 5.6. Let w_{ij} be the weight representing the area bound by segment j and contours *I-1* and *I*. If $\Delta\phi$ is the arc of the segment represented by half-transect j, and N is the number of contours, then:

$$w_j = \frac{\Delta\phi_j}{2\pi} ,$$

$$w_i = \frac{1}{N} \text{ and} \qquad (5.16)$$

$$w_{ij} = w_i w_j .$$

For more randomly distributed data, the beam area could preferably be divided into several equal segments such that the weights are all equal.

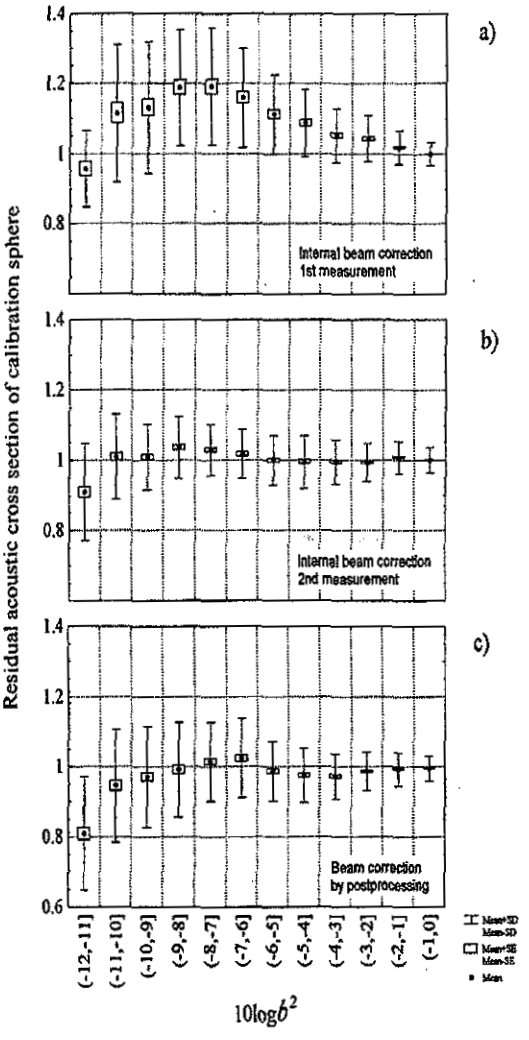

Figure 5.5. The mean residual of the acoustic cross section of the calibration sphere within 1 dB intervals of $\Delta TS = TS_U - TS_C$ or 10 log b^2, where TS_U and TS_C are the observed target strength values of the sphere respectively before and after directivity correction. a) EK500 internal correction, 1st measurements, b) EK500 internal correction, 2nd measurement and c) correction by post-processing.

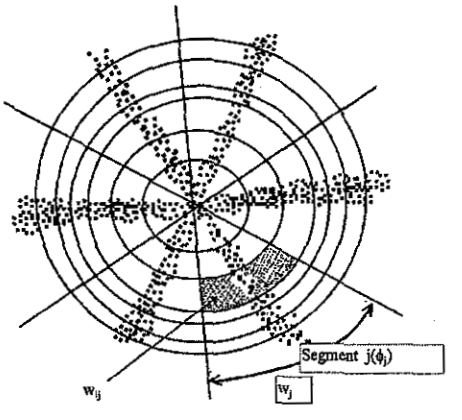

Figure 5.6. Division of the beam cross section into sub-areas. The areas within every two adjacent circular contours are equal. Division into segments is based on the azimuthal angles of the transects. The shaded part shows a sub-area bound by segment *j* and contours *I-1* and *I*, with weight w_{ij} and mean sensitivity $\bar{B}_{ij}$.

For every half-transect j, mean values of sensitivity $(\bar{B}_{ij})$ were calculated within each 1-dB interval of the two-way directivity pattern. Consequently mean values $(\bar{B}_i)$ within each 1-dB interval were calculated according to the formula:

$$\bar{B}_i = \sum_{j=1}^{6} \bar{B}_{ij} w_j \,. \tag{5.17}$$

The values within the innermost contour were treated a little differently. In that case a simple average of all measurements within that area was calculated. In order to comply with the above definition of w_{ij}, the following definition of was used:

$$\bar{B}_{1j} = \bar{B}_1 \text{ for } j = 1, 2, \ldots\ldots, 6.$$

If $(-N)$ is the preferred acceptance limit, then in this particular case the corresponding mean $(\bar{B}_N)$ and variance V_{BN} of the sensitivity are:

$$\bar{B}_N = \frac{1}{N}\sum_{i=1}^{N} \bar{B}_i \quad \text{and} \tag{5.18}$$

$$V_{B_N} = \frac{1}{6(N-1)} \sum_{i=1}^{N} \sum_{j=1}^{6} \left(\bar{B}_{ij} - \bar{B}_N\right)^2 w_{ij}^2 \tag{5.19}$$

for $N > 1$.

In Table 5.1 we give values of $(\bar{B}_N)$ and the standard deviation for acceptance limits $(-N)$, ranging from -1 to -12 dB. It is to be borne in mind that these limits refer to levels of the two-way beam pattern. Drawing the values of $(\bar{B}_i)$ from Table5.1 as a function of $(-N)$ will result in figures very similar to the ones shown in Figures 2(a-c). In Figure 5.7 is an example showing the $(\bar{B}_{ij})$ values for the six half transects in the case of the internal directivity compensation, second measurement. Note that the variations from the nominal value of 1 are clearly seen on the individual transects, but will tend to compensate each other so a smaller effect will be seen in and even less in $\bar{B}_N$.

After introducing separate alongship and athwardship half power beam angles, the Φ_α and Φ_β, the described variations with azimutal angle are significantly reduced (Ona 1990; Ona *et al.*, 1996).

Further, a detailed case study on target strength measurements on oceanic redfish, using the split beam method, are found in Chapter 6.3.

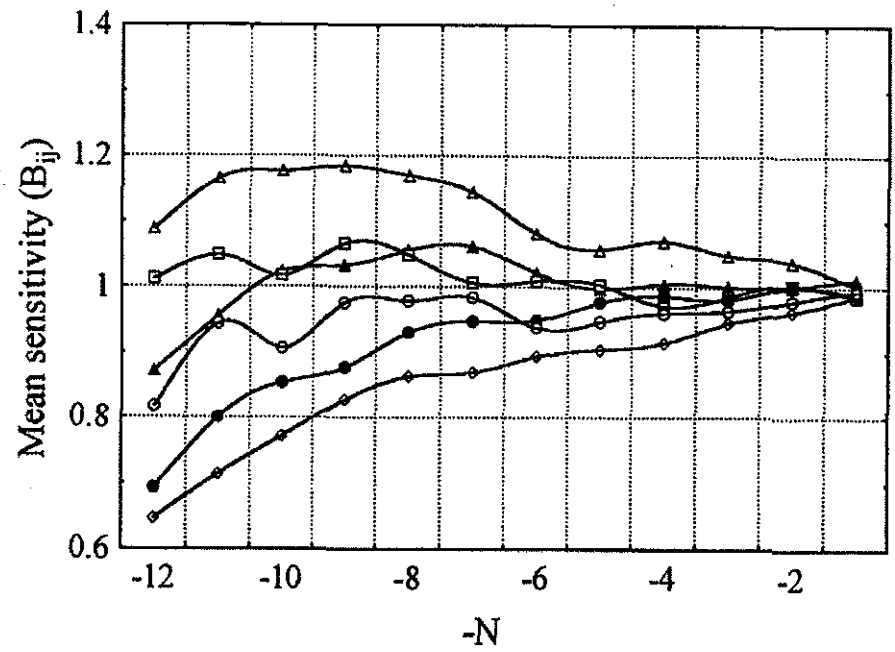

Figure 5.7. Variations in $\bar{B}_{ij}$ values as a function of $(-N)$ (equivalent to ΔTS) on the separate half-transects in the case of the second measurement of the internal beam compensation in EK500.

References

Bodholt, H., Nes, H., and Solli, H. 1989. A new echo sounder system. Int. Conf. Progress in Fisheries Acoustics, Lowestoft. Proceedings of the I.O.A., St. Alban, UK, 11(3): 123–130.

Carlson, T. J., and Jackson, D. R., 1980. "Empirical evaluation of the feasibility of split-beam methods for direct *in-situ* target strength measurements of single fish", Report of the Applied Physics Laboratory, University of Washington, APL-UW8006.

Foote, K. G., Knudsen, H. P., Vestnes, G., MacLennan, D. N., and Simmonds, E.J. 1987. Calibration of acoustic instruments for fish density estimation: a practical guide. Cooperative Research Report, International Council for the Exploration of the Sea, 144, 69 pp.

MacLennan D. N., and Simmonds, J. 1992. Fisheries Acoustics, Chapman & Hall, London.

Ona, E. 1990. Optimal acoustic beam pattern corrections for split beam transducers. ICES CM 1990/B:30, 12 pp.

Ona, E., Zhao, X., Svellingen, I., and Foote, K. G. 1996. Some pitfalls of short-range standard-target calibration. ICES CM 1996/B:40.

6 Single-target recognition

E. Ona and M. Barange

6.1 Maximum resolution densities

6.1.1 The concept of one target per reverberation volume

The primary purpose of the single-target detectors implemented in existing echo sounders is to select isolated targets for TS measurement. In this context, an isolated target is one far enough from its neighbours to avoid any interference of echoes. Physically this means that only one target can occupy the acoustic resolution volume for the measurement to be valid.

The size of the resolution volume is defined here in the implicit limit of high signal-to-noise ratios by the acoustic beam and the transmitted pulse length. The split-beam system will generally accept echoes from an angle larger than the beamwidth of the transducer as usually defined (between -3-dB points). The acceptance angle, for example, might be set to the -12-dB points to maximise the sampled volume. Inside this sampled volume, only one target should appear at a given time:

With a typical 38-kHz transducer, $\theta_{3\ dB} = 7.1°$, but the angle detectors work over about 10° in total, or 5° to each side of the axis in alongship and atwarthship directions. If θ_D is half the total detection angle; the solid angle of the sampled volume is

$$\Omega_D = 2\pi\left(1 - \cos\hat{\theta}_D\right), \tag{6.1}$$

hence $\Omega_D = 0.02391$ steradians for $\theta_D = 5°$. The detection volume can then be defined as:

$$V_D = \frac{c\tau}{2} r^2 \Omega_D , \tag{6.2}$$

where c is the sound speed and τ is the pulse duration. Using the echo integrator in combination with the split-beam system, the volume density of targets may be measured as:

$$\rho_V = \frac{s_A}{<\sigma>\Delta z} \tag{6.3}$$

where

$$s_A = 4\pi(1852)^2 \int_{z_1}^{z_2} s_v dz . \tag{6.4}$$

Here s_A is the area backscattering coefficient over the depth interval $\Delta z = z_2 - z_1$, derived from the volume backscattering coefficient and normalized to 1 square nautical mile (Knudsen 1990), also developed in Section 2, $<\sigma>$ is the mean acoustic cross section of the fish, and the so-called average target strength is defined as in equation (2.7):

$$<TS> = 10\log\frac{<\sigma>}{4\pi} . \tag{6.5}$$

From equations (6.2) and (6.5), if N is the number of fish in the detection volume,

$$\frac{N}{V_D} = \frac{s_A}{<\sigma>\Delta z(1852)^2} , \tag{6.6}$$

$$N = \frac{s_A(c\tau/2)r^2\Omega_D}{4\pi\, 10^{TS/10}\Delta z(1852)^2} . \tag{6.7}$$

Thus, if the aim is 1 fish per detection volume, the relation between area backscattering coefficient, range and TS is given by equation (6.7) in which $N = 1$. This is the nominal upper limit of density for correct operation of the single-fish detector. This is called N_{max} since the fish cannot be expected to be uniformly distributed in a grid-like pattern.

A more realistic approach is to assume that the fish in a layer (at least in layers where it is possible to extract TS data) are randomly distributed in space. If this is the case, we can use Poisson statistics. If N now denotes the mean number of fish in the sampled volume and $N = 1$, it can be shown that about 42% of all detections will be of multiple targets if the fish are randomly distributed in space.

It is desirable to work with a much lower probability for multiple targets, for example, p = 10%. In this case, the corresponding mean density is $N = 0.2$. Table 6.1 shows the maximum average density corresponding to various limits on the probability of encountering multiple targets.

It is therefore possible to ensure that the target strength data are negligibly affected by multiple targets by sampling only when the value of density, or integrated energy s_A, is below some limit. For example, if the chance of having more than one fish in the detection volume should be less than 1/10, then the limit is p ($N > 1$) = 0.1, and the graph in Figure 6.1 can be used to find the corresponding s_A for a particular average target strength and depth. The relation between target strength and size of the fish is roughly established for several species, at least with the precision needed for this purpose. Therefore, TS in decibels and σ in square meters may be related to the average fish length L in centimeters, using the following formula as being representative of swimbladder-bearing fish:

$$<TS> = 20\log L - 70 , \tag{6.8}$$

or:

$$<\sigma> = aL^b = 1.25\ 10^{-6}\ L^2 . \tag{6.9}$$

Writing $N = N_1$ as the selected upper limit of density, then substituting equation (6.8) in equation (6.7), the following expression for the maximum acceptable s_A in units of [m^2/n.mi^2] is derived:

$$s_A = \frac{4.287 L^2 \Delta z N_1}{\left(\frac{c\tau}{2}\right) r^2 \Omega_D} . \qquad (6.10)$$

Table 6.1 Mean number of fish per sampled volume (N) giving a probability p of multiple targets assuming a random (Poisson) distribution of fish.

p	N
0.01	0.02
0.02	0.04
0.05	0.10
0.10	0.21
0.20	0.43
0.30	0.68
0.40	0.95
0.50	1.26
0.60	1.62
0.70	2.06
0.80	2.66
0.90	3.61

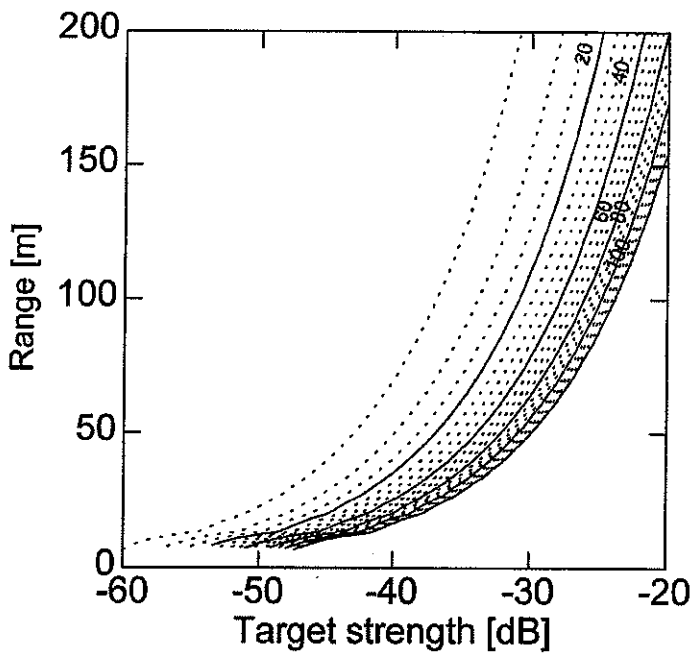

Figure 6.1. Chart of s_A values (in $m^2/n.mi.^2$) in a 1 m wide layer corresponding to a mean of 0.1 fish per sampled volume which, for Poisson-distributed targets, implies a 5% chance of multiple-target detections, as a function of TS and depth of layer.

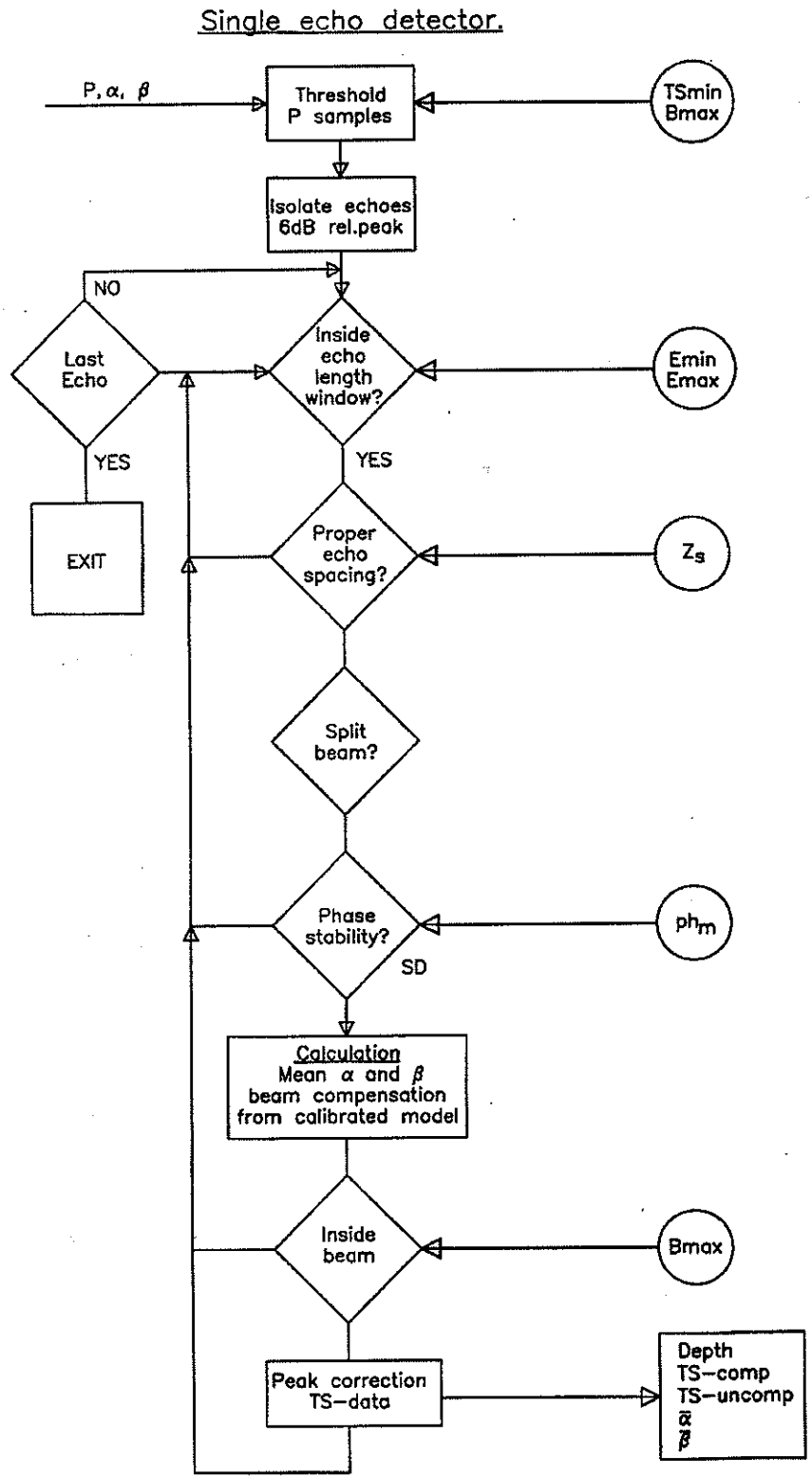

Figure 6.2. Flow diagram, single fish detector of a typical split beam system.

For example, with $p = 0.1$ and $N_1 = 0.2$, typical parameters for a 38-kHz system are: $L = 30$ cm, $\Delta z = 50$ m, $R = 100$ m, $(c\tau/2) = 0.75$ m and $\Omega_D = 0.02391$ (for 10° total detection angle). Substituting in equation (6.10) gives $s_A = 215$ m^2/n.mi.^{2} as the maximum which should be sampled to give reasonably unbiased TS estimates.

6.1.2 Single-fish detection

The objective of the single-target detection algorithm is to select the echoes from isolated targets in each transmission for subsequent target-strength analysis. Signals rejected by such an algorithm include echoes from fish schools, the bottom, overlapping echoes from targets at similar range, noise, and interference. All single-fish detectors, simple or complex, should work well in ideal situations where the individual targets are well spaced. However, in general the target distribution is not ideal, and it is essential to apply filtering to separate echoes originating from isolated fish from all other echo sources.

As the accuracy of the subsequent target strength estimate is totally dependent on the filters used in the detection process, which may all accept false candidates or reject valid signals, this is treated in a separate part of the report. In order to understand the measured results, it is necessary to know how the filters work and what their strengths and weaknesses are. The filtering criteria described here are equally valid for the dual-beam, split-beam and single-beam methods, but the implementation might be system dependent.

Filters may fail to reject unwanted data, and it must be stressed that the user should optimize the filtering process in such a way that the consequent bias in the TS measurement is as low as possible.

The filters may be preset in the echo sounder or signal processor, or accessible to operator control, either during sampling or in later examination of the data by post processing.

6.1.3 Typical single-echo detector

The following algorithm is essentially the one implemented in the Simrad EK500 echo sounder system. In each transmission, the data available to the single-target detector algorithm are the raw, digitized, TVG-corrected and calibrated echo amplitudes, together with the relative phase angles in the alongship and athwarthship directions (ref. Chapter 5). The amplitude digitizer works on the detected signal, while the phase measurements are made on the original, analog signal (Figure 6.2). The echo-amplitude and phase angles are sampled at a rate sufficiently high to give a good reproduction of the analog signal.

Step 1 Following each transmission (Figure 6.2), echoes below a threshold chosen by the operator are removed from the data matrix (Figure 6.3). The threshold corresponds to the condition that a small target TS_{min} subject to the maximum directivity compensation B_{max} will just be detected.

Step 2 On each of the remaining echoes, the duration is measured at the -6 dB level relative to the peak amplitude. Echoes are rejected if they do not satisfy the pulse duration window with limits E_{min} and E_{max}, i.e., echoes from schools, the bottom, most overlapping fish echoes, and noise.

Step 3 Reject echoes which are too close in vertical range at the -6 dB level according to a fixed or operator-controlled limit. This is done in order to further discriminate against overlapping echoes.

These three steps are basically the same for the single-target detectors used with single-beam, dual-beam or split-beam echo sounders. In the split-beam system, the phase differences between paired quadrants are used to locate the target relative to the transducer axis. The stability of the phase angle as measured between successive samples throughout the pulse can also be used in the filtering process.

Step 4 Some of the echoes accepted as single targets by the pulse-duration filter may originate from two or more targets at nearly the same range, but horizontally distinct within the pulse volume. Such target pairs are likely to show instability in the phase angles measured over the pulse, and so they might be rejected by using a filter based on the phase-angle stability index. The efficiency of this filter in practice has recently been questioned, and it will therefore be discussed later in this chapter in Section 6.2.2.

Step 5 After the filtering process, the mean phase angles and α and β are computed for each remaining echo to determine the target position within the acoustic beam, hence the directivity compensation to be applied to the echo amplitude. The directivity compensation is now calculated, using the parameters from an earlier sphere calibration (see Section 5.2).

Step 6 Refining the TS-data. Since TS is computed from the maximum pulse amplitude as sampled by the digitizer, a reconstruction of the actual peak level by using a pulse-shape model improves the stability of the peak measurement, especially for short pulse duration. As seen in Figure 6.4, the target echo will be randomly positioned relative to the digitizing steps, so the observed peak level of the constant pulse will be slightly variable. A simple curve-fitting procedure may be used to estimate the precise position and amplitude of the peak.

This refining process greatly reduces unwanted ping-to-ping jitter in the measured target strength, and is used both during the sphere calibration (on the sphere echo) and in the field (on the fish echo). Since the target strength measurement is always referred to the result of a sphere calibration, no bias is likely to be introduced by the refining process. Increasing the digitizing frequency by a large factor would yield the same result, but the additional computation would greatly reduce the speed of real-time signal processing.

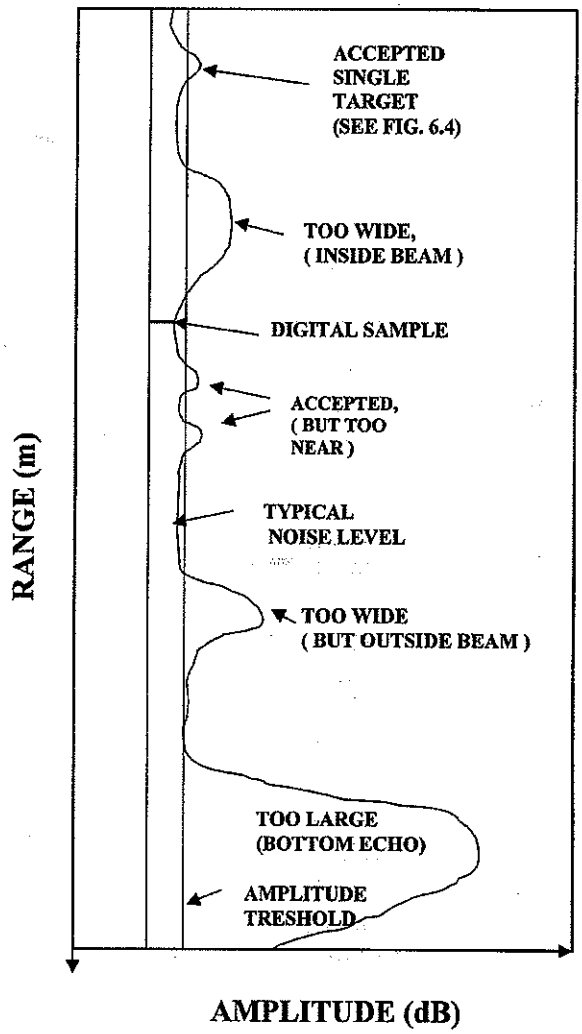

Figure 6.3. Schematic diagram of an echo signal.

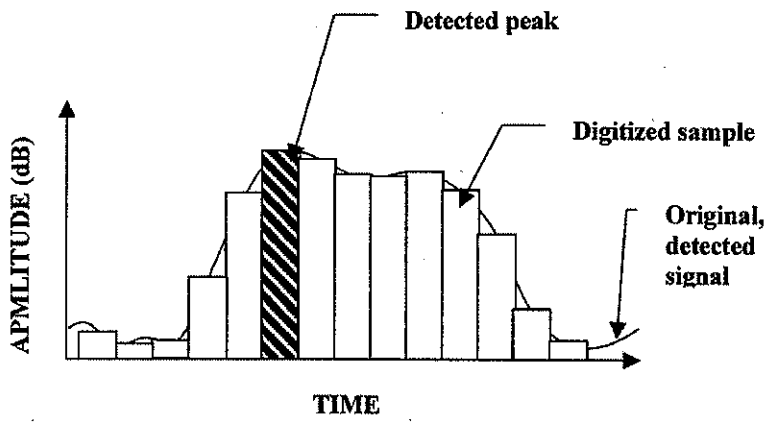

Figure 6.4. Location of the amplitude samples on the echo envelope for a short pulse duration relative to the sampling period. The target sample value is generally less than the true peak value, and the bias varies with precise position of the pulse.

Step 7 Data output. The output from the single target detector typically consists of depth, TS_C, TS_U, α, β, and time, where TS_C is the TS with compensation for the beam pattern, and TS_U is the so-called uncompensated TS.

If improved directivity correction models become available, the data can easily be reanalysed with the new models through postprocessing.

As described above, the signal processing in the split-beam system involves five different filters, all of which may be adjusted by the operator. Although there may be factory-preset nominal setting for all the variables, these are often selected as the best for certain ideal situations. Extensive tests with different parameter values are needed to fully understand the filtering process. Such exercises are strongly recommended by the study group.

Improved filtering techniques may be developed in the years to come, but there are disadvantages to be considered as well as benefits. In particular; there is a higher risk of biasing the target strength when filtering of the primary echo signal is more complex.

6.2 Performance of single-target detectors at high target densities

6.2.1 Theoretical biases when two targets contribute to the echo

When two scatterers are closely spaced in range (say within 1 wavelength), the received echo will appear to originate from a single target at a location which depends on the phase difference between the received echoes (Nes 1994). According to Foote (1996), the combined echo p is given by

$$p = b_1\sigma_1^{1/2} + b_2\sigma_2^{1/2} \exp(i\chi) , \qquad (6.11)$$

where b_i is the beam directivity factor for the ith target, σ_i is its backscattering cross section, and χ is the relative phase. In the particular case where $b_1\sigma_1^{1/2}$ is very similar to $b_2\sigma_2^{1/2}$, and χ is close to π, the phase of the combined signal becomes unstable, and the compound echo can appear to originate from a position outside the transducer's defined beamwidth. For very different values of $b_1\sigma_1^{1/2}$ and $b_2\sigma_2^{1/2}$, however, the echo appears to originate from a position within the beamwidth (Foote 1996). Current single-target detectors, based on echo duration and/or phase-stability algorithms, would thus accept the overlapping echoes as a single echo and apply a compensation factor related to the apparent position in the transducer beam.

The potential bias in the estimates of mean TS arising from this problem was studied by simulation (Foote 1996). Two targets were positioned at ranges within 1/2 wavelength of each other, with an equal probability of occurrence within the -6dB level of the transducer beam (~4.7°). Two cases were considered: the illustrative one of fixed target strengths and the more realistic situation where the target strengths are drawn from the same normal distribution. Apparent target bearings were computed according to the principles adopted in split-beam systems. In the case of constant target strengths, the strongest effect was observed when targets were of equal strength, resulting in a mean TS approximately 2.0 dB higher than that expected for individual targets. For a 10 dB difference in TS , the mean TS indicated by the combined echo was distorted by only 0.12 dB. Intermediate differences in TS resulted in biases lying between these extreme values.

Distributions of apparent TS for the case where the individual target strengths were normally distributed are shown in Figure 6.5. While the biases were qualitatively similar to those occurring in the case of fixed TS values, their magnitude increased, due to the log-normal character of the backscattering cross-sections. The mean target strengths of the apparent distributions were between 2.04 dB (for narrow distributions, SD = 0.1 dB) and 9.4 dB (for wide distributions, SD = 5 dB) higher than the true value for the actual targets.

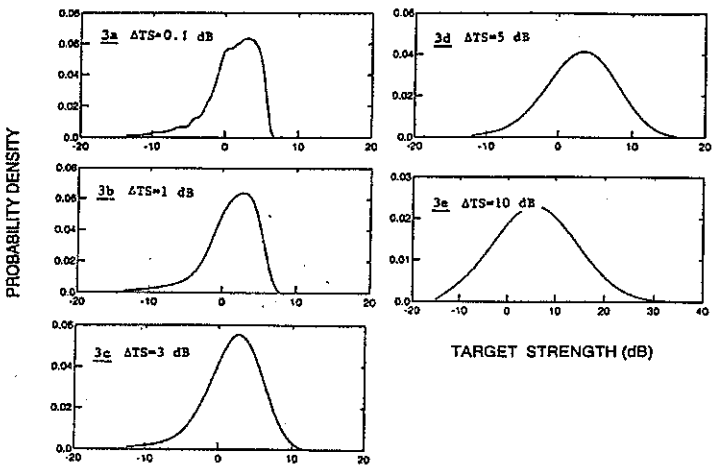

Figure 6.5. Probability density function of the apparent single-target T due to coincident echoes from two targets in the main transducer beam, with target strengths independently drawn from the same normal distribution (0, ΔTS) (modified from Foote 1994).

6.2.2 Performance and biases generated by incomplete discrimination of overlapping echoes

The magnitude of the bias reported above, however, applies exclusively to the case where all accepted echoes are formed by the combination of two scatterers at very similar ranges. In reality, it would be more reasonable to expect a random positioning of the two targets within the sampled volume. Under these circumstances, single target detection algorithms are expected to reject some, if not most of the multiple-scatterer echoes, at least for split-beam systems (Bodholt and Solli 1992). To investigate the effectiveness and potential biases of single-target detectors, the rejection mechanism of the different algorithms must be understood. The performance of five single target detection algorithms utilising phase, amplitude and echo duration information as rejection criteria was simulated by Soule *et al.* (1996). Pairs of targets were generated with random positions in a 3-dimensional sampling volume, and independent log-normally-distributed individual back-scattering cross sections. The amplitude and phase of the resultant multiple echo at each receiving element was computed and applied to each of the detectors. The performance of each detector was evaluated according to two criteria:

(i) the frequency with which it rejected the echo (effectiveness) and
(ii) the potential for biases in the rejection/acceptance of multiple echoes (selectivity).

The five detectors are:

(1) Average phase deviation: Echoes are rejected if the absolute average phase deviation, taken within -6dB of the peak, exceeds a pre-set limit. This algorithm had previously been found by Soule *et al.* (1995) to be somewhat ineffective and selective in tank-test experiments.
(2) Standard phase deviation: The data are treated as above, but echoes are rejected if the standard phase deviation exceeds a pre-set limit.
(3) Phase comparison: Echoes are accepted if the phase difference between adjacent elements in each pair are approximately equal. Comparisons are made between the fore/aft and the port/starboard pair.
(4) Echo duration: This algorithm rejects targets if the number of samples occurring within -6 dB of the peak exceeds a pre-set limit. A fixed minimum of 7 samples (0.8 times the pulse length) is specified. This algorithm is widely used, and is implemented in most commercial split- and dual-beam systems. Its effectiveness was studied by Ona and Røttingen (1986) for the Simrad ES400 echo-sounder.
(5) Amplitude deviation: This method is based on the differences between the resultant amplitudes in each receiving element. As with the phase comparison method, it can only be applied to systems where signals from individual elements are accessible.

The performance of each of the five methods is summarized in Figure 6.6. Each datum represents the rejection rate for 5000 random independent target pairs, as a function of the selected rejection limits. Of the phase methods investigated, the standard-phase-deviation method performed most effectively. However, even with tighter rejection limits (e.g. SD < 0.3°, equivalent to a phase jitter of 2.3 steps), more than 45% of multiple echoes would be accepted as singles. This percentage increases to nearly 80% in the case of the average phase deviation algorithm. Excessive tightening of these limits is not recommended, as the selection bias against weak targets will then increase (Soule *et al.*, 1995).

The performance of the echo-duration method was limited by the need to have the normalized duration limit sufficiently large to ensure that single targets are accepted. The maximum theoretical rejection rate is therefore only 33%. The limitations of this algorithm have been highlighted by Ona and Røttingen (1986), who observed that it causes unrealistically high TS estimates to be obtained at high fish densities.

The performance of the amplitude-deviation algorithm depends on the signal-to-noise ratio. For a target strength of -45 dB and typical noise levels observed in the field, Soule *et al.* (1986) estimate that a rejection performance close to 80% could be achieved, making this algorithm potentially the most effective of the five tested.

Soule *et al.* (1995) also raised the issue of the potential bias occurring in the acceptance of multiple echoes. From their experimental tank results, the authors report that the average-phase-deviation algorithm preferentially rejects weak echoes, and when accepting multiple echoes it is biased towards those which are in phase. This finding was developed in their subsequent simulation study (Soule *et al.*, 1996), which indicated that in fact, all three phase-based algorithms preferentially accept overlapping echoes when they happen to interfere constructively (namely when they are separated by multiples of half a wavelength, Figure 6.7). Since in these cases the resultant amplitude is enhanced, this effect aggravates the positive bias due to the acceptance of multiple echoes. A similar effect was evident in the case of the echo-duration algorithm. The amplitude-deviation method, on the other hand, accepted both in-phase and out-of-phase echoes equally (Figure 6.7), with a resultant smaller bias.

Finally, several authors have recommended the use of amplitude thresholds to isolate specific components of the scattering populations. This procedure is risky, however, as demonstrated by Wiener and Ehrenberg (1975), and should be used with great care. They observed that the threshold procedure overestimated TS and distorted the TS frequency distribution, due to discrimination against smaller fish. In some cases, and when conducted with care, like by Reynisson (1993), thresholding procedure may be well justified. The effect of the thresholding should then be investigated.

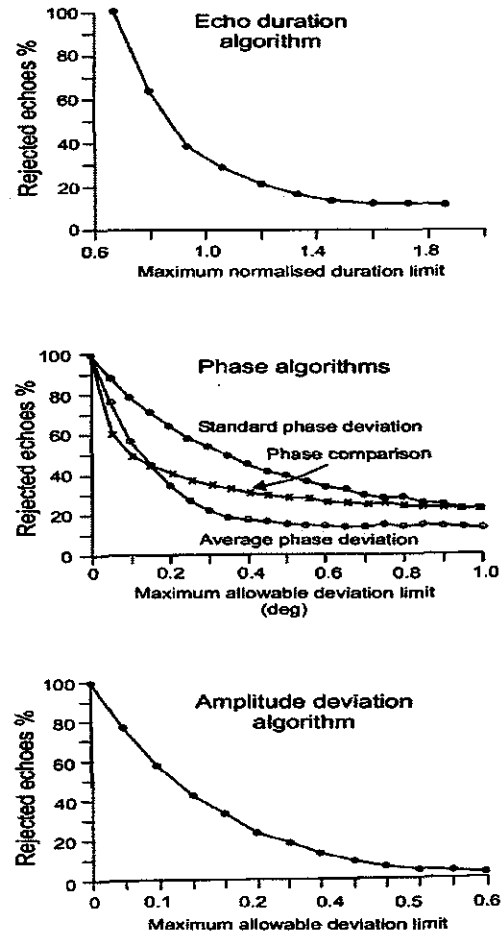

Figure 6.6. Multiple target rejection rate as a function of the detection limit for the five investigated algorithms. Each datum represents the average rejection rate for 5000 randomly selected target pairs (from Soule *et al.*, 1996).

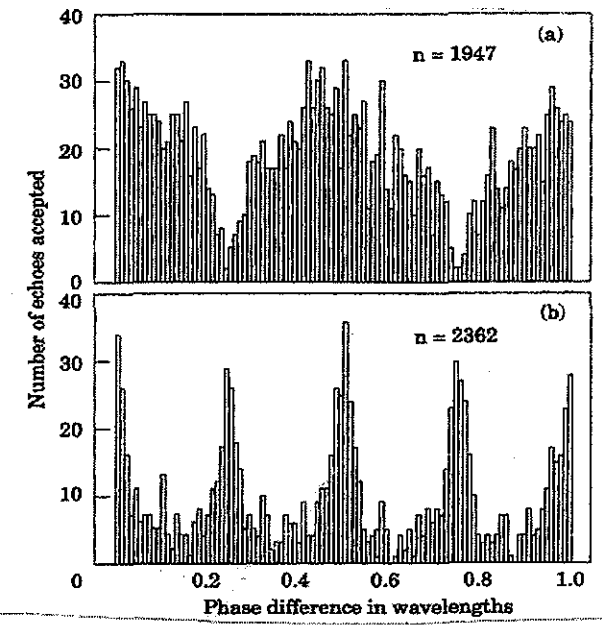

Figure 6.7. Number of accepted overlapping echoes versus the phase difference between targets expressed as a fraction of a wavelength, for the standard phase and amplitude deviation algorithms (from Soule *et al.*, 1996).

The conclusion from these studies is that single-target detectors are not fail-safe, and will tend to generate biases in target strength estimates when densities exceed one target per reverberation volume. All the biases discussed would tend towards overestimating target strength, and it is therefore not surprising that unexpectedly high TS values have been obtained (Ona and Røttingen 1986, Nainggolan *et al.*, 1993, Reynisson 1993, see references in Soule *et al.*, 1995), especially for highly aggregated pelagic species. The amplitude deviation algorithm appears to offer a marked improvement in performance (Soule *et al.*, 1996), particularly at higher signal-to-noise ratios. With the introduction of noise-averaging and faster sampling rates, this performance may be extended to weaker targets. Cases of ambiguity could also be resolved by employing more than one frequency simultaneously (Foote 1996) or by two or several receiving transducers properly positioned.

6.2.3 Empirical solutions to limit TS overestimates due to multiple echo acceptance

Until technological advances improve the quality of *in situ* TS measurements, users are compelled to analyze their data empirically to detect the presence of overlapping echoes. For example, conditions for precise TS measurement of walleye pollock, *Theragra chalcogramma*, were studied by Sawada *et al.* (1993). For their purposes two indices were introduced:

(1) The number of fish in the nominal sampled volume (N_v):

$$N_v = \frac{1}{2} c\tau \Psi r^2 n \ , \tag{6.12}$$

where r is the target range, n the volume density of fish (estimated using echo integration data and a TS/fish length relationship), and Ψ is the equivalent beam angle as defined by Urick (1975):

$$\Psi = \frac{(\theta_a \theta_b)^2}{1445} \ , \tag{6.13}$$

where θ_a and θ_b are the athwartships and alongships half-power angles of the transducer.

(2) The percentage of multiple echoes: According to Sawada *et al.* (1993), if the single-target detection method is effective, the number of discriminated single echoes (N_E) is proportional to a cutoff solid angle (Ω),

$$N_E = n_s \frac{1}{3}(r_2^3 - r_1^3)\Omega P \ , \tag{6.14}$$

where n_s is the density of single echoes and P the number of pings sampled. The percentage of multiple echoes, M, is then defined as:

$$M = \frac{n - n_s}{n} 100 \ . \tag{6.15}$$

The results, summarized in Figure 6.8, indicate a strong empirical relationship between the number of fish in the reverberation volume (N_v) and the estimated target strength. The TS estimates are also shown to become strongly biased when the frequency of overlapping echoes increases above 70%. The value of M is not entirely reliable, as it depends on the successful rejection of all multiple targets by the signal processor.

Sawada *et al.* (1993) concluded that an empirical value of 0.04 fish per sampled volume is effective as a limit above which *in situ* target strength measurements would be unreliable. It is important to note that this value is much lower than the nominal limit of one target per sampled volume suggested earlier, and probably reflects the fact that the fish density was averaged over too-large distances compared to the scale of local patchiness. It probably indicates that, should the mean density exceed this threshold, fish densities are likely to exceed one target per sampled volume at some stage during the integration period. The authors also compare the empirical bias generated by dual- and split-beam systems, and conclude that the addition of a phase-deviation algorithm in the split-beam system, although reducing the magnitude of the bias, makes little difference in the overall trend.

In a similar study, using a split-beam system, Barange *et al.* (1996) observed that, in the case of the South African pilchard, *Sardinops sagax*, TS overestimation also occurs at densities below 1 target per sampled volume (Figure 6.9).

Case study

Páll Reynisson

Oceanic redfish

Split-beam data on oceanic redfish have been collected onboard the Icelandic research vessel Bjarni Sæmundsson during acoustic surveys in the Irminger Sea since 1991 (Reynisson 1992, Reynisson and Sigurðsson 1996).

The conditions for in situ target strength measurements on oceanic redfish in the area have proven to be excellent during the summer. The fish is rather uniformly distributed over the area and single-fish echoes are dominant, allowing more or less continuous monitoring of target strength. The fish is of a rather uniform size (mean length ≈37 cm) and little mixing with other species is observed during daylight hours at depths 50-350 m. The echogram in Figure 6.10 shows a typical day-time situation.

The acoustic instruments used are an EK500 echo sounder and a BI500 postprocessing system (Bodholt *et al.*, 1989, Foote *et al.*, 1991). Typical settings of the equipment are given in Table 6.2.

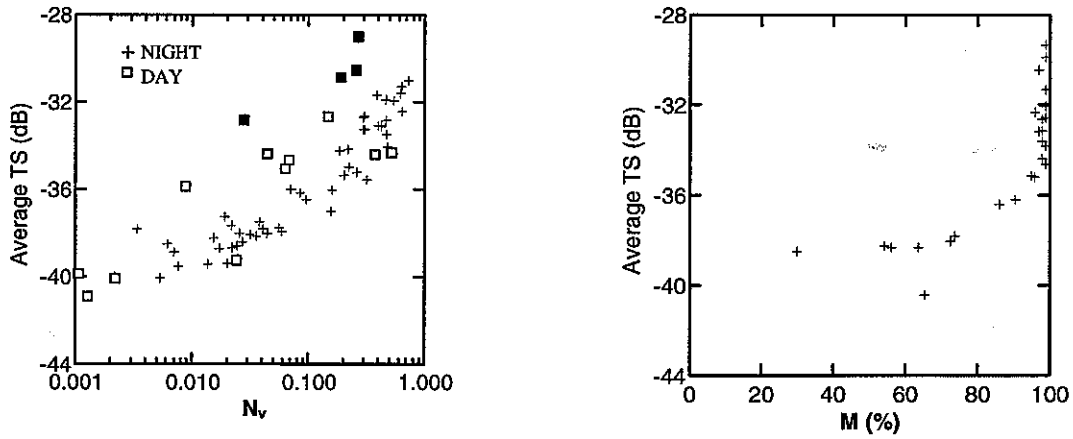

Figure 6.8. Relationship between the fish density per reverberation volume (N_v), the frequency of multiple target echoes (M) and the mean estimate of target strength, in a layer between 72 and 88 m depth (modified from Sawada *et al.*, 1993).

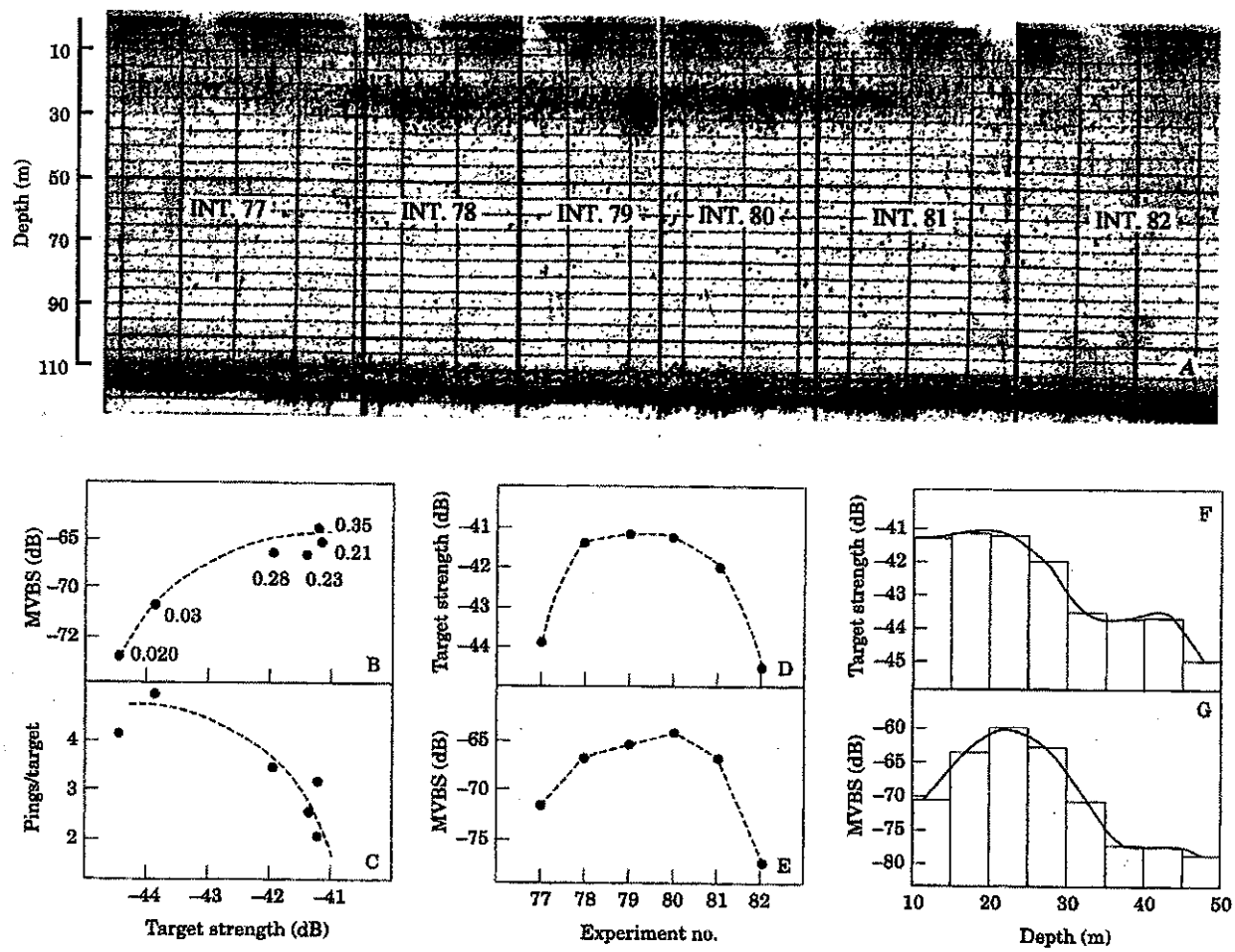

Figure 6.9. Echogram of a pilchard aggregation at night, showing relationships between mean estimated target strength, mean volume backscattering strength, and the ratio between the number of pings sampled and the number of single targets detected in six resets sampled across the aggregation (modified from Barange *et al.* 1996).

Table 6.2 Settings of acoustic instruments on R/V "Bjarni Sæmundsson". Note that in rev. 3.01 of the EK500 software, the average phase deviation is used (refer Section 6.2.2).

Echo sounder/integrator	Simrad EK500 (rev. 3.01)/BI500
Frequency	38 kHz
Transmitter power	2000 W
Absorbtion coefficient	10 dB/km
Pulselength	1.0 ms
Bandwidth	3.8 kHz
Transmission rate	1.5 s per ping
Transducer type	ES38-B, hull-mounted
2-way beam angle	-20.6 dB
TS-threshold in split-beam operation	-60 dB
Pulselength criteria in split-beam operation	0.7 and 1.4 of nominal pulselength
Maximum gain compensation	-6.0 dB (one-way beam pattern)
Maximum Phase deviation	2.0 deg
Sound velocity	1475 m/s

According to Reynisson (1992) the mean target strength of 37 cm oceanic redfish in the depth interval 100-200 m is about -40 dB. Applying Equations 6.1-6.7, the quality of the split-beam data may be checked to some extent. Using the highest s_A-values in Figure 6.10 within each 50 m depth interval over 1 nm sailed, a target strength of -40 dB and a detection angle of 10.2 deg, the average number of fish in the detection volume ($N = \rho \cdot V_D$) was estimated. The results are shown in Table 6.3. The probability (p) of receiving multiple echoes is estimated from Table 6.1. Accordingly p should be less than 5 %, even at 300-350 m depth.

Examination of the split-beam data revealed that this may not be the case. Averaging σ within 50 m depth intervals and limiting the detection angle (θ) over the range 1.1-5.1 deg, showed that $<\sigma>$ is dependent on θ, and increasingly so as the depth increases. This could indicate that the averaging distance is to large compared to the scale of local patchiness.

A more detailed analysis of a data set extending over the daylight hours (06-22 GMT) was carried out. The fish density was averaged over 0.1 nm distance and 25 m depth intervals. The results were similar, that is on the average $p<0.05$ at all depths. In Figure 6.11, several s_A-values within each 25 m depth interval are shown: 1) the mean SA, 2) the limit below which 90 % of the values were observed, 3) the largest values observed and 4) the limit below which there is less than 10 % probability of multiple targets. The last case is obtained by solving Eq. 6.7 in terms of s_A with N=0.21. According to this result the presence of multiple targets should be negligible at all depths of interest.

The mean backscattering cross section, $<\sigma>$ was calculated for each 25 m depth interval from 100 to 350 m depth. Averaging of $<\sigma>$ was carried out for several values of the maximum detection angle (θ = 1.3, 2.6 and 5.1 deg). In Figure 6.12, $<\sigma>$ is related to depth with θ as parameter. Evidently $<\sigma>$ is to some degree influenced by the choice of θ, but of more concern is the sudden increase below 275 m. A comparison of the target strength distributions obtained from depth 150-200m and 250-300m (Figure 6.13) shows that at the lower depth interval the smaller echoes are missing, but at the higher end larger echoes are present. This might be due to larger fish, but the biological sampling did not confirm this. The most likely explanation is that noise is affecting the single-target detector, thus excluding the weaker echoes, and that multiple target detection are affecting the higher end.

In an acoustic situation where single targets are dominant, as in Figure 6.10, one might expect that the average density of fish as estimated by integration (ρ_{SA}) is comparable to the average number of detected single-fish echoes divided by the sampling volume and the number of pings (ρ_{TS}). It is of special interest to investigate how well these numbers compare as the depth increases.

The ρ_{SA} and ρ_{TS} may be defined as follows:

$$\rho_{SA} = \frac{s_A}{\langle\sigma\rangle \cdot \Delta z \cdot (1852)^2} \qquad (6.16)$$

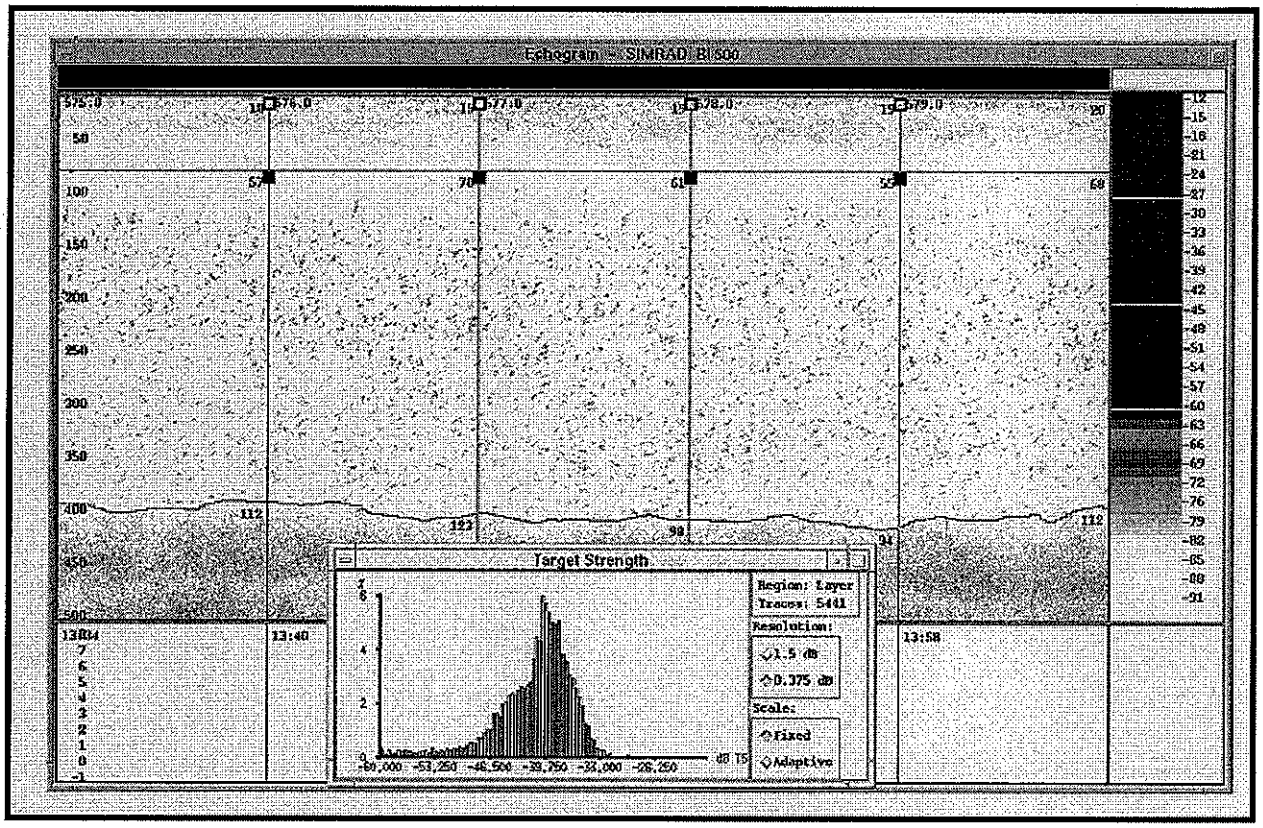

Figure 6.10. Typical 20logR-echogram of oceanic redfish during daylight hours. Pure redfish registrations are observed from 100 m down to about 350 m. Below 350-400 m, a rather dense scattering layer of smaller organism is observed. Integrator values in 50 m depth intervals from 100-350 m are shown for each 1 nm sailed.

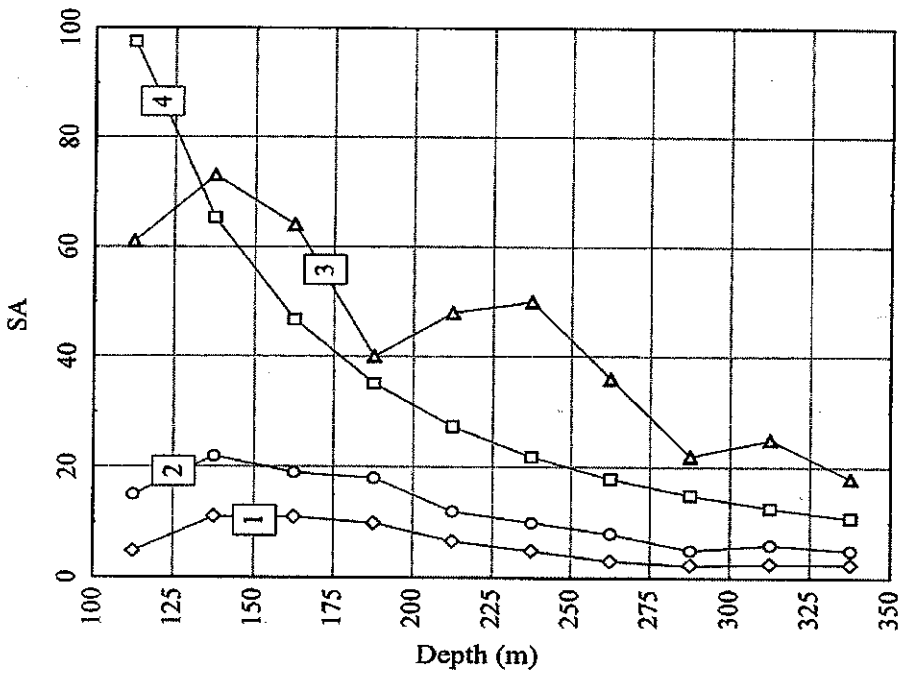

Figure 6.11. SA-values pertinent to split-beam data on oceanic redfish. 1) mean values, 2) the limit below which 90 % of the SA-values were observed, 3) the largest values observed and 4) the limit below which there is less than 10 % probability of multiple targets, s_A(N=0.21).

which is comparable to Eq. (6.3) and:

$$\rho_{TS} = \frac{(N_{ST})}{\Delta z \cdot V_D \cdot (N_{ST})} \qquad (6.17)$$

where (N_{ST}) is the number of detected single-targets and (N_P) the number of transmissions or pings. Assuming that all the fish can be resolved by the equipment and that the single-target detector is 100 % efficient, the ratio ρ_{TS}/ρ_{SA} should be equal to unity.

Calculation of ρ_{TS}/ρ_{SA} for 25 m depth interval from 100-350 m depth was carried out, using <σ> from Figure 6.12 and with θ=1.3, 2.6 and 5.1 degrees. The results are shown in Figure 6.14. In all cases the ratio is fairly constant above the 250 m depth, although below unity. This indicates that the single-target detector is rejecting some echoes which are included in the integration process. Of course small deviations of θ from the true angle, or uncertainty in ι will affect the results. At 275 m a sudden decrease is noted, indicating that a bias is present below that depth.

For θ = 1.3 and 2.6 deg, ρ_{TS}/ρ_{SA} is closer to unity as compared to θ = 5.1, indicating that relatively fewer echoes are rejected for smaller angles, most likely due to higher signal-to-noise ratio in the inner parts of the beam. The main results and some relevant data from the calculations described above are summed up in Table 6.4.

The conclusion is that the split-beam data of oceanic redfish are reliable down to about 250-275 m depth and that redfish with similar target strength inhabit depths from 250-350 m as well. Biological sampling has established that oceanic redfish is the main scatterer down to about 350 m, at least during daylight hours. Regarding the target strength, experimental verification with conventional hull-mounted transducers will be difficult, although new developments in single echo detectors may improve the quality of future data. The best solution would be to lower the transducer closer to the targets (refer chapter 8.1 on deep-water observations).

6.3 Concluding remarks

The authors recommend that TS data collected from fish scattering layers be analysed as a function of the estimated number of fish per sampled volume, and that data be rejected from areas where there is a high probability of overlapping echoes (Figure 6.9). They also suggest that the ratio of the number of pings to the number of identified single targets (detection rate) be used to analyse empirically the quality of *in situ* target strength data.

The case study presented clearly that a critical approach should be applied to TS data collected *in situ*, at least until technological advances have improved the performance of single-target detectors.

Table 6.3 Average number of fish per m^3 (ρ) and per sampled volume (N) at different depths, using s_A-values shown in Figure 6.10, TS =- 40 dB and detection angle (θ) 10.2°. Probability (p) of multiple targets is obtained from Table 6.1. For comparison the s_A-values are given for which p = 0.1.

Depth interval (m)	s_A (p = 0.1) (m^2/nm^2)	s_A (Fig. 6.10) (m^2/nm^2)	$\rho \cdot 10^6$ (fish/m^2)	V_D (m^3)	$N = \rho V_D$	p
100-150	158	13	60.3	287	0.017	<0.02
150-200	81	11	51.0	562	0.029	<0.02
200-250	49	12	55.7	929	0.052	<0.05
250-300	33	8	37.1	1387	0.052	<0.05
300-350	23	8	37.1	1938	0.072	<0.05

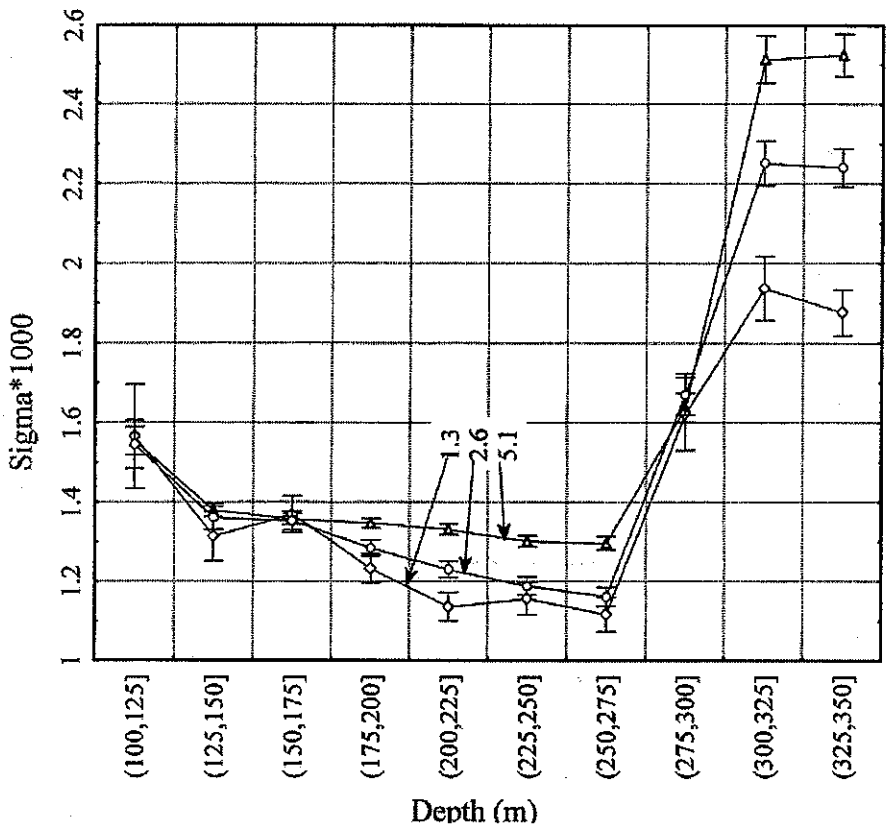

Figure 6.12. Mean acoustic cross section <σ>, obtained within 25 m depth intervals for different limits on the beam acceptance angle (θ=1.3, 2.6 and 5.1 deg). The standard error of <σ> is indicated.

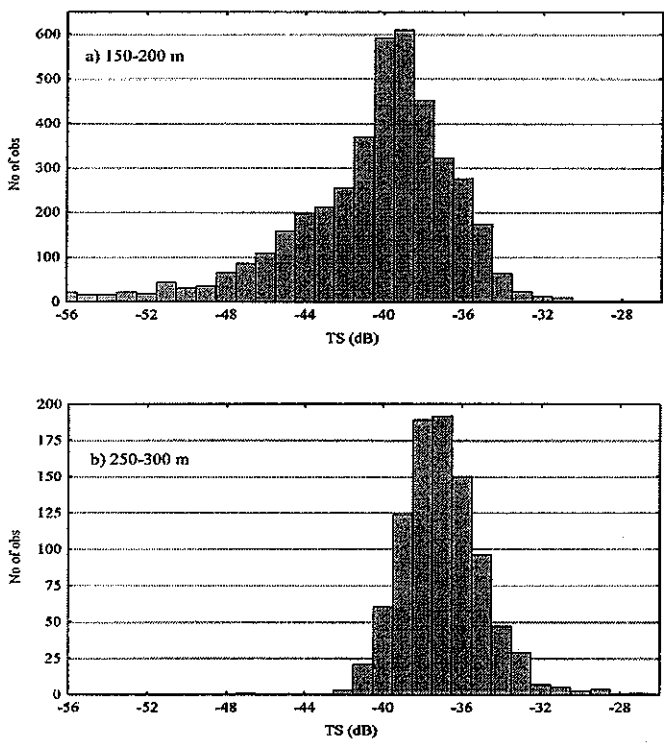

Figure 6.13. Target strength distributions of oceanic redfish obtained two depth intervals: a) 150-200 m and b) 250-300 m.

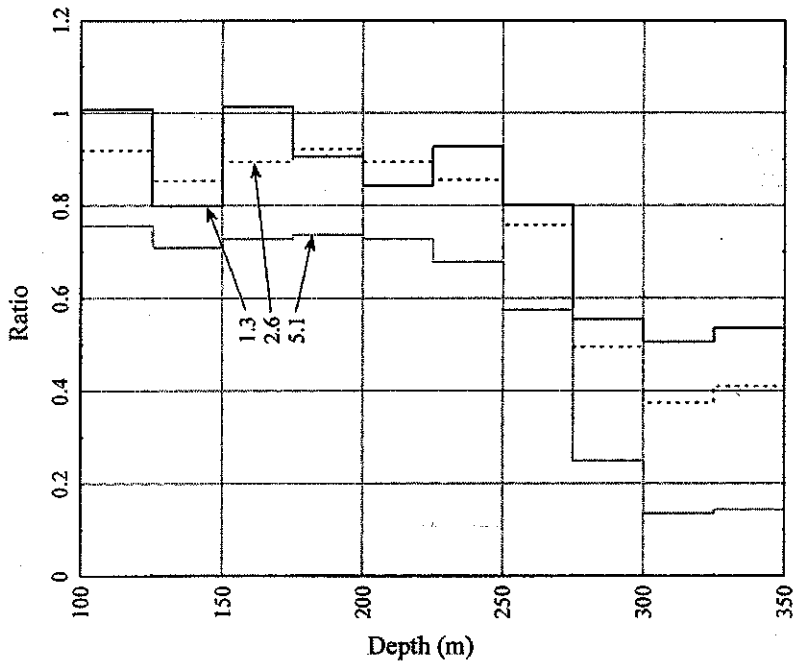

Figure 6.14. The ratio of average fish density estimated by Equations 6.15 and 6.16 in 25 m depth intervals for different limits on the beam acceptance angle (θ=1.3, 2.6 and 5.1 deg).

Table 6.4 Average fish density. The upper half of the table shows ρ_{TS} ,and the lower half ρ_{SA} calculated according to Equations 6.15 and 6.16 respectively, for three different limits of the detection angle (θ=1.3, 2.6 and 5.1 deg). The number of pings is 7200.

	No of single targets			Sampling volume V_D (m^3)			$\rho_{TS} \cdot 10^6$ (fish/m^3)		
Depth range (m)	θ=1.3	θ=2.6	θ=5.1	θ=1.3	θ=2.6	θ=5.1	θ=1.3	θ=2.6	θ=5.1
100-125	98	362	1139	15.1	60.4	232.2	36.1	33.3	27.2
125-150	318	1312	4127	22.5	90.2	346.8	78.4	80.8	66.1
150-175	498	1780	5554	31.5	126.0	484.4	87.8	78.5	63.7
175-200	593	2318	6782	41.9	167.7	644.9	78.6	76.8	58.4
200-225	554	2172	6278	53.9	215.4	828.4	57.2	56.0	42.1
225-250	554	1987	5533	67.3	269.1	1034.8	45.8	41.0	29.7
250-275	376	1368	3581	82.2	328.7	1264.1	25.4	23.1	15.7
275-300	163	564	1121	98.6	394.3	1516.3	9.2	8.0	4.1
300-325	161	412	510	116.5	465.8	1791.5	7.7	4.9	1.6
325-350	201	516	619	135.9	543.4	2089.6	8.2	5.3	1.6

Table 6.4 continued.

Depth range (m)	Mean s_A	$\langle\sigma\rangle \cdot 10^3$ (m^2)			$\rho_{SA} \cdot 10^6$ (fish/m^3)			ρ_{TS}/ρ_{SA}		
		$\theta = 1.3$	$\theta = 2.6$	$\theta = 5.1$	$\theta = 1.3$	$\theta = 2.6$	$\theta = 5.1$	$\theta = 1.3$	$\theta = 2.6$	$\theta = 5.1$
100-125	4.8	1.56	1.54	1.55	35.8	36.2	36.0	1.01	0.92	0.76
125-150	11.0	1.31	1.36	1.38	98.1	94.7	93.4	0.80	0.85	0.71
150-175	10.2	1.37	1.35	1.36	86.7	87.7	87.5	1.01	0.89	0.73
175-200	9.2	1.23	1.28	1.35	86.7	83.2	79.3	0.91	0.92	0.74
200-225	6.6	1.14	1.23	1.33	67.8	62.6	57.9	0.84	0.89	0.73
225-250	4.9	1.16	1.19	1.30	49.3	47.9	43.8	0.93	0.86	0.68
250-275	3.0	1.12	1.16	1.30	31.7	30.5	27.4	0.80	0.76	0.58
275-300	2.3	1.62	1.67	1.64	16.5	16.0	16.4	0.56	0.50	0.25
300-325	2.5	1.94	2.25	2.51	15.2	13.1	11.7	0.51	0.38	0.13
325-350	2.5	1.88	2.24	2.52	15.4	12.9	11.4	0.53	0.41	0.14

References

Barange, M., Hampton, I., and Soule, M. A. 1996. Empirical determination of *in situ* target strengths of three loosely-aggregated pelagic fish species. ICES Journal of Marine Science, 53: 225–232.

Bodholt, H., and Solli, H. 1992. Application of the split-beam technique for *in-situ* target strength measurements. World Fisheries Congress, Athens, 1992, 20 pp.

Bodholt, H., Nes, H., and Solli, H. 1989. A new echo sounder system. Proceedings of the IOA 11(3), pp 123–130.

Foote, K. G., Knudsen, H. P., Korneliussen, R. J., Nordbö, P. E., and Röang, K. 1991. Post-processing system for echo sounder data. The Journal of the Acoustical Society of America, Vol. 90, pp 37–47.

Foote, K. G. 1994. Coincidence echo statistics. ICES CM 1994/B:40, 10 pp.

Foote, K. G. 1996. Coincidence echo statistics. Journal of the Acoustical Society of America, 99: 266–271.

Knudsen, H. P. 1990. The Bergen Echo Integrator: an introduction. Journal du Conseil International pour l' Exploration de la Mer, 47: 167–174.

Nainggolan, C., Hamada, E., and Sato, K. 1993. A new method for fish abundance estimation using split-beam echosounder. Journal of the Tokyo University of Fisheries, 80: 83–92.

Nes, H. 1994. Split beam dual target detection properties. ICES CM 1994/:27, 6 pp.

Ona, E., and Røttingen, I. 1986. Experiences using the ES400, split-beam echo sounder, with special reference to the single-target recognition criteria. ICES CM 1986/B:38, 8 pp.

Reynisson, P. 1992. Target strength measurements of oceanic redfish in the Irminger Sea. ICES CM 1992/B:8.

Reynisson, P. 1993. *In situ* target strength measurements of Icelandic summer spawning herring in the period 1985-1992. ICES CM 1993/B:40, 15pp.

Reynisson, P., and Sigurdsson, T. 1996. Diurnal variation in acoustic intensity and target strength measurements of oceanic redfish (*Sebastes mentella*) in the Irminger Sea. ICES CM 1996/G:25

Sawada, K., Furusawa, M., and Williamson, N. J. 1993. Conditions for the precise measurement of fish target strength *in situ*. Journal of the Marine Acoustics Society of Japan, 20: 15–79.

Soule, M. A., Barange, M., and Hampton, I. 1995. Evidence of bias in estimates of target strength obtained with a split-beam echo-sounder. ICES Journal of Marine Science, 52: in press.

Soule, M., Hampton, I., and Barange, M. 1996. Potential improvements to current methods of recognising single targets with a split-beam echo-sounder. ICES Journal of Marine Science, 52: 237–243.

Weimer, R. T. and Ehrenberg, J. E. 1975. Analysis of threshold-induced bias inherent in acoustic scattering cross-section estimates of individual fish. Journal of the Fisheries Research Board Canada, 32: 2547–2551.

7 Biological sampling

I. Everson and D. Miller

7.1 Introduction

The essential aim of biological sampling is to obtain samples that are representative of the targets under consideration. Sampling in support of *in situ* target strength studies should be aimed closely at those targets from which acoustic information is being collected. Other components of the population and contamination of the sample should be avoided if at all possible. Thus if the acoustic measurements are being made on spawning concentrations, it is pointless for the biological sampling to include immature fish. Similarly, when sampling in a two-layer situation, where the TS data were collected only from the lower layer, it is quite possible that incidental catches from the upper layer may contaminate the trawl sample. The ideal study location would only contain a single species with a narrow unimodal size distribution. The overall programme of target strength studies and the associated sampling should, however, be aimed at providing information on all life history stages of the species relevant to the population being surveyed.

It is important to recognise that TS estimation requires precise sampling only of the stock component that contributes to the TS measurements, whereas acoustic abundance surveys require sampling which is aimed at providing information on the entire target population.

7.2 Recommended biological measurements

Target strength is known to vary with a variety of characteristics of the species under consideration. These characteristics may, for convenience, be considered under three headings: those intrinsic to the animal, essentially a result of size, anatomy, and physiology; those extrinsic to the animal arising from behavioural characteristics; and those controlled by environmental features which affect the behaviour of the targets.

Intrinsic factors: These may cover features of size, shape and composition, all of which may vary with time. Some examples are:

(1) Length and weight which must of course be clearly defined (e.g. total or fork length; live or gutted weight). The length/weight relationship and derived indices such as the condition factor should also be determined.
(2) Gas-filled buoyancy mechanisms such as swimbladders, which may be open to the oesophagous (physostomes) or closed (physoclists), provide a major contribution to fish target strength (Foote 1980a, 1987). Some fish maintain buoyancy by concentrations of oil, lipids or waxes but these mechanisms have much less effect on target strength (Kloser *et al.*, 1996).
(3) Biochemical composition (which might include lipid or oil content, liver index, water content), size and distribution of hard structures (endo or exoskeleton) can all affect TS, not necessarily by their own scattering, but mainly through how they affect the buoyancy and the swimbladder size (Ona 1990).
(4) Maturity stage and stomach fullness (Ona 1990).

The relevance of each of these features to some species that are commonly surveyed acoustically is indicated in Table 7.1.

Extrinsic factors: These fall under the general heading of behaviour. Specific topics of importance are:

(1) Orientation of the fish, especially tilting relative to the horizontal plane is the greatest potential source of variation in acoustic target strength. The degree of variation with the tilt angle depends on the size of the target fish, the shape of the swimbladder and the acoustic frequency in use.
(2) Many aspects of behaviour such as feeding, degree of aggregation, diurnal migration and avoidance of vessels can affect orientation as mentioned above (Olsen *et al.*, 1983a, b).
(3) Some species of fish may move vertically at such a rate as to be unable to compensate the swimbladder volume and the target strength will vary during and for some time after such vertical movement (Blaxter and Tytler 1978, Ona 1984, 1990).

Environmental factors: Several environmental factors may affect the target strength because of consequential changes in fish behaviour. Some examples are: temperature, salinity, current speed, light level, season and depth. Wherever possible these should be reported with the results of target strength experiments.

7.3 Sampling methods and associated errors

A variety of sampling techniques are available, each of which is liable to introduce bias. The following is a brief description of some of these techniques, with comments on their effectiveness.

7.3.1 Net sampling

The ideal sampling net should provide a catch composition the same as the fish population on which the target strength measurements are being made. In practice, two sources of bias need to be borne in mind when using nets: changes in capture efficiency due to avoidance or herding, and selectivity in catch due to escapes through the netting meshes.

(i) Fish reactions to the gear are characterised by attraction (herding) or repulsion. The following points need to be considered:

(1) Do the fish respond to the presence of the vessel?
(2) How do the fish react to the presence of sweep wires? Are all sizes affected equally?
(3) How do the fish react to the presence of the headrope and footrope? Do they dive? Do all sizes react in a similar manner?
(4) When in the net do they all 'fall back' into the codend or are larger fish able to swim out? This factor depends on the towing speed and, possibly, on the visual and acoustic stimuli generated by the fishing vessel and the gear.

(ii) Mesh selection operates by retaining only those fish that are unable or unwilling to pass through the meshes of the net. An ideal sampling trawl would have a constant capture efficiency over the size range of the fish whose target strength is being measured. Mesh selection can be an active process, with fish struggling to get through the meshes, or a passive process with the net acting more or less as a filter. The following questions need to be considered:

(1) Does mesh selection operate in the same way for fish in all parts of the net? It is pointless having a fine mesh liner in the codend when all the small fish escape through the larger meshes of the main part of the net.
(2) How is mesh selection affected by the rigging and towing speed of the net?
(3) Mesh selection will certainly be important if we have to sample fish over a large size range. Because of this constraint, each target strength experiment should preferably be made on fish which are similar to one another and unimodally distributed within a small range of sizes.

7.3.2 Direct observations

Two commonly applied methods of direct observation are underwater television and stereophotography. Television provides effectively continuous observations, so that changes in behaviour can be investigated, whilst stereophotography provides a series of snapshots from which precise geometrical information can be extracted. Care should be taken in the use of both of these methods to ensure that the presence of cameras has minimal effect on the fish. Specific points to bear in mind are to avoid bright reflective components on the equipment, and the need for careful control of lighting.

Television is a valuable tool in assessing the behaviour of fish in their undisturbed state as well as in observing their reaction to nets. Important applications are studies of schooling behaviour and, in particular, the tilt angle distribution. Ideally, only ambient lighting should be used whenever possible. There is some evidence that strobe lighting invokes a much smaller fright response in the fish than continuous direct light.

Stereophotography can be used to provide snapshots of the orientation, packing density and size of the fish. The resolution required of stereophotographs means that it is normally essential to use some form of artificial illumination. This might be a synchronised flashlight, but care is needed to ensure that the fish have 'recovered' from the previous flash before further photographs are taken. In static experiments, this may require several minutes, but when the photographic rig is being towed, the only requirement will be for the rig to have moved away from the area of influence of the previous flash exposure.

7.4 Case study for Atlantic herring

Acoustic surveys of the herring (*Clupea harengus* L.) have been extensively conducted in the North Sea over the last three decades. Considerable research has gone into finding a representative TS - length relationship and the study of factors which may modulate this.

The TS - length relationship for herring is generally supposed to take the form TS = 20 log (L) - *b*, giving TS in dB for the total length L in cm. The factor *b* is assumed to be independent of L but it may change with frequency.

Edwards *et al.* (1984) have reported results from experiments using caged aggregations of fish, giving *b* values between 71.3 and 76 dB at 38 kHz. *In situ* experiments, either indirect or using split-beam echosounders, have resulted in b values of 71.9 dB (Foote 1987), 73.2 dB (Haldorsson & Reynisson 1983), and 69.9 dB (Rudstam *et al.*, 1988). The latter two studies used the indirect method in Iceland and the Baltic, respectively. The value of b currently recommended by the Herring Survey Planning Group of ICES is 71.2 dB.

Herring is a physostome, with open swimbladder, and, it is believed, without a gas secretion gland (Blaxter & Batty 1987). Many physiological and behavioural factors are believed to influence the observed TS of herring. In general, all these factors will affect the size or aspect of the swimbladder, and hence the TS, as noted below. Relevant measurements should be made to quantify the effect.

7.4.1 Physiological factors

Fat content

As the primary role of the swimbladder is buoyancy, it follows that a fish with a higher percentage of fat will tend to have a smaller swimbladder, and hence a lower TS (Ona 1990). Reynisson (1993) predicted a reduction of 0.2 dB per 1% increase in fat content. The fat content should be measured as a percentage of the total weight. Simple instruments are available to measure this, see for example Kent (1990). As most pelagic schooling species exhibit similar seasonal changes in fat content as herring throughout the year (Stoddard 1967, Iles and Wood 1965), similar effects on TS are expected on these.

The condition factor, defined as 100 times the weight divided by the length cubed, has also been suggested as a

determinant of the target strength. It may be assumed that fish with a low condition factor, i.e. lighter for a given length, will have a less inflated swimbladder, hence a lower TS. This effect has not been quantified. Fish weight as well as the length should therefore be included in the measurements.

Maturity and feeding state

As the gonads develop, they will tend to compress the swimbladder and thus may reduce the TS (Ona 1990). A full stomach may also have the same effect. Ona (1990) has suggested that this may cause between 2 and 5 dB reduction in the mean TS. The recommended measurements in this case are the gonad maturity stage on the standard scale I - VIII (Landry & McOuinn 1988), and the percentage stomach fullness.

Water depth (Pressure)

As the herring has no gas secretion gland, it is unable to inflate the swimbladder while below the surface (Blaxter and Batty 1984). Experimental work has shown that the swimbladder volume and hence TS decreases with depth (Edwards & Armstrong 1984, Olsen 1987, Olsen & Ahlquist 1989). Some *in situ* measurements have confirmed these observations (Huse & Ona 1994, Haldorsson and Reynisson 1983, Ona 1984), but other studies have shown no depth dependence (Reynisson 1993). The effect of depth is complicated by the observation that gas diffuses out of the swimbladder which can be refilled only when the fish rises to the surface. The TS at depth would therefore be expected to reduce steadily with time (Blaxter and Batty 1984). This has been confirmed by cage studies (Edwards and Armstrong 1984). One further complication is that a reduced swimbladder volume will give less buoyancy. The swimming behaviour of the fish may then change, with the body tilted more upward, reducing the aspect of the swimbladder in the acoustic beam. It is recommended that the depth of the fish be recorded and, if known, the elapsed time since the fish could re-inflate the swimbladder at the surface. This latter measure is probably only feasible for captive fish in cages.

7.4.2 Fish behaviour

The main behavioural factor affecting the herring TS is believed to be the tilt angle (Foote 1980b, MacLennan *et al.* 1990). This is the angle between the head-to-tail bodyline and the horizontal plane. The tilting behaviour can change for a number of reasons, for example, between day and night, associated with the tendency of fish to swim more slowly in the dark. This occurs because the balance of gravity and dynamic forces makes the fish assume a head-up position while swimming slowly (Huse and Ona 1994). Tilt angles may also vary as a consequence of avoidance reactions to the survey vessel (Haldorsson and Reynisson 1983), and in response to other changes as discussed above, since a less buoyant fish might adopt a more head-up position to maintain depth.

It is not possible to determine the tilt angle from echo measurements alone. The effect of body size and tilt on the indicated TS cannot be separated acoustically. Other means of observing the orientation of the fish are required. In the case of experiments with caged fish, the use of TV-cameras or stereophotography is recommended. Such methods have shown that fish in a school or aggregation can adopt a wide range of tilt angles. Thus the tilt should be described as a statistical distribution; however, this will reduce the variation of the average TS applicable to the ensemble (MacLennan *et al.*, 1989; Huse and Ona 1994). It is much more difficult to measure the tilt angles of wild fish, and further development of instrumentation for that purpose would be useful.

The vertical migration of fish is also likely to alter the TS. It is well known that wintering herring in Norwegian fjords migrate between 50 and 200 m depth or more in a diurnal cycle, resulting in a substantial change of swimbladder volume between night and day (Huse and Ona 1994). It is therefore desirable to record any vertical movement by the observed fish, especially close approaches to the surface when reinflation of the swimbladder might occur (see above).

7.4.3 Additional measurements

A number of other parameters are known to affect the behaviour and distribution of herring, although they have not so far been studied in the context of TS variation. These include the water salinity (Grainger 1979, Maravelias and Reid 1995); the temperature (Grainger 1979, Reid *et al.*, 1993, Maravelias and Reid in press); the light level (Kirk 1983); and the type of seabed topography and substrate (Reid 1994). Information on all these factors should be included in the data collection protocol.

7.4.4 Fish capture

The problems of collecting representative samples by fishing are well documented (Wardle 1983). In the context of herring, there are three methods commonly used to catch samples; purse seine, pelagic trawl and demersal trawl. Each method has different advantages and drawbacks. The purse seine is capable of capturing an entire school, but it is time consuming to operate and only allows one school to be caught in each shot. The gear may also fail to intercept the target school on a regular basis. Pelagic nets cover more area in less time, and probably achieve a higher hit rate, but they tend to capture parts of different schools (possibly with different size, age, and species composition). It is also more than likely that dissimilar sizes of herring will have a different vulnerability to capture, and so the trawl catch may well be unrepresentative of the true size distribution. Demersal trawls can also capture herring which are often found close to the seabed. The question arises, however, as to whether there are differences between the size distributions of herring caught by demersal and pelagic gears, and which is more representative of the population at large.

The development of underwater scanning laser imaging techniques could solve many of the above mentioned

problems. Such systems can provide high quality TV pictures at ranges up to 50 m. It should be emphasised that no trials have yet taken place to establish the suitability of laser techniques for TS experiments, and fishing would still be required to determine biological parameters such as length, weight, condition factor and maturity state of the target fish.

7.5 Concluding comments

There are many behavioural, physiological and environmental factors which can cause substantial changes in the TS of fish or other acoustic targets. Research has demonstrated causal links in a few cases, but present knowledge is not sufficient to provide a complete deterministic model for predicting the target strength and its variation under given conditions.

References

Blaxter, J. H. S., and Batty, R. S. 1984. The herring swim bladder: Loss and gain of gas. Journal of the Marine Biological Association of the United Kingdom, 64(23): 441–459.

Blaxter, J. H. S., and Tytler, P. 1978. Physiology and function of the swimbladder. Advances in Comparative Physiology and Biochemistry, 7: 311–367.

Edwards, J. I., Armstrong, F., Magurran, A ., and Pitcher, T. J. 1984. Herring, mackerel and sprat target strength experiments with behavioural observations. ICES CM 1984/B:34.

Edwards, J. I., and Armstrong, F. 1984. Target strength experiments on caged fish. Scottish Fisheries Bulletin, 48: 12–20.

Foote, K. G. 1980a. Importance of the swimbladder in acoustic scattering by fish: a comparison of gadoid and mackerel target strengths. Journal of the Acoustical Society of America, 67: 2084–2089.

Foote, K. G. 1980b. Effect of fish behaviour on echo energy: the need for measurements of orientation distributions. Journal du Conseil International pour l' Exploration de la Mer, 39: 193–20.

Foote, K. G. 1987. Fish target strengths for use in echo integrator surveys. Journal of the Acoustical Society of America, 82: 981–987.

Grainger, R. J. R. 1979. Herring abundance off the west of Ireland in relation to oceanographic variation. Journal du Conseil International pour l' Exploration de la Mer, 38(2): 180–188.

Haldorsson, O., and Reynisson, P. 1983. Target strength measurement of herring and capelin *in situ* at Iceland. FAO Fisheries Report, 300: 78–84.

Huse, I., and Ona, E. 1994. Experiments on measuring average TS for herring within dense concentrations. Presented at ICES FAST Working Group, Montpellier, 27 April 1994.

Iles, T. D., and Wood, R. J. 1965. The fat/water relationship in North Sea herring (*Clupea harengus*) and its possible significance. Journal of the Marine Biological Association of the United Kingdom, 45: 353–366.

Kent, M. 1990. Hand held instrument for fat/water determination in whole fish. Food Control 1990(Jan): 47–53.

Kirk, J. T. O. 1983. Light and photosynthesis in aquatic ecosystems. Cambridge, Cambridge University Press.

Koslow, J. A., Kloser, R., and Stanley, C. A. 1995. Avoidance of a camera system by a deepwater fish - the orange roughy (*Haplostethus atlanticus*). Deep-Sea Research, (Part 1, Oceanographic Research Papers), 42(2):233–244.

Kloser, J. R., Williams, A., and Koslow, J. A. (in prep). The acoustic target strength of a deepwater fish, orange roughy (*Haplostethus atlanicus*), based on modelling and *in situ* measurements on schools and tethered fish.

Kloser, J. R., Koslow, J. A., and Williams, A. 1996. Acoustic Biomass Assessment of a Spawning Aggregation of orange roughy (*Haplostethus atlanicus*) off Southeastern Australia from 1990–93. Australian Journal of Marine and Freshwater Research, 47: 1015–1024.

Kristensen, A., and Dalen, J. 1986. Acoustic estimation of the distribution and abundance of zooplankton. Journal of the Acoustical Society of America, 80: 601–611.

Landry, J., and McQuinn, I. H. 1988. Guide to the microscopic and macroscopic identification of the sexual maturity stages of the Atlantic herring (*Clupea harengus harengus* L.). Canadian Technical Report of Fisheries and Aquatic Sciences/Rapport Technique Canadien des Sciences Halieutiques et Aquatiques, 1655: 71 pp.

MacLennan, D. N., Magurran, A. E., Pitcher, T. J., and Hollingworth, C. E. 1990. Behavioural determinants of fish target strength. Rapports et Procès-Verbaux des Réunions du Conseil International pour l'Exploration de la Mer, 189: 245–23.

MacLennan, D. N., Hollingworth, C. E., and Armstrong, F. 1989. Target strength and the tilt angle distribution of caged fish. Proceedings of the Institute of Acoustics, 11(3): 11–20.

Maravelias, C., and Reid, D. G. 1995. Relationship between herring (*Clupea harengus*) distribution and sea surface salinity and temperature in the northern North Sea. Scientia Marina (Barcelona), 59(3–4).

Miller, D. G. M., and Hampton, I. 1989. Biology and ecology of the antarctic krill (*Euphausia superba* Dana): a review. Biological Investigations of Marine Antarctic Systems and Stocks (BIOMASS) Volume 9, 166 pp.

Olsen, K. 1987. Vertical migration in fish, a source of ambiguity in fisheries acoustics. ICES CM 1987/B:29, 8 pp.

Olsen, K., and Ahlquist , I. 1989. Target strength of fish at various depths, observed experimentally. ICES CM 1989/B:53, 8 pp.

Olsen, K., Angell, J., Pettersen, F., and Løvik, A. 1983a. Observed fish reactions to a surveying vessel with special reference herring, cod, capelin and polar cod. FAO Fisheries Report, 300: 131–138.

Olsen, K., Angell, J., and Løvik, A. 1983b. Quantitative estimations of the influence of fish behavior on acoustically determined fish abundance. FAO Fish. Rep., 300: 139–149.

Ona, E. 1990. Physiological factors causing natural variations in acoustic target strength of fish. Journal of the Marine Biological Association of the United Kingdom, 70: 107–127.

Ona, E. 1984. *In situ* observation of swimbladder compression in herring. ICES CM 1984/B:18.

Reid, D. G., Williams, D., Gambang, A., and Simmonds, J. 1993. Distribution of North Sea herring and their relationship to the environment. ICES CM 1993/H:23.

Reid, D. G. 1994. Relationships between herring school distribution and seabed substrate derived from ROXANN. Presented at ICES FAST Working Group, Montpellier, 27 April 1994.

Reynisson, P. 1993. *In situ* target strength measurements of Icelandic summer spawning herring in the period 1985–1992. ICES CM 1993/B:40, 15 pp.

Rudstam, L. G., Lindem, T., and Hansson, S. 1988. Density and target strength of herring and sprat: a comparison between two methods of analyzing single beam sonar data. Fisheries Research (Amsterdam), 6(4): 305–315.

Stoddard, J. H. 1967. Studies of the condition (fatness) of herring. Canadian Technical Report of Fisheries and Aquatic Sciences/Rapport Technique Canadien des Sciences Halieutiques et Aquatiques, 5, 17 pp.

Wardle, C. S. 1983. Fish reaction to towed gears. In: MacDonald, A. and Preide, I. G. (Eds.). Marine Biology at Sea. Academic Press, London.

8 Special techniques

R. Kloser and J. Dalen

8.1 Deep-water observations/towed systems

8.1.1 Need for deep-water *in situ* TS measurements

The knowledge of marine resources and community structure generally reduces with increasing depth due to inadequate observation systems and also to some extent the lack of commercial fishing. Interest in deep-water 400 - 1500 m has increased substantially over the past decade both from commercial fishing operators and researchers.

The commercial fishing of deep-water stocks extends down to 1200 m for species such as orange roughy (*Hoplostethus atlanticus*) currently found in Australian, New Zealand and North Atlantic waters. To manage this resource acoustic echo integration techniques are currently used in Australian waters. Research into the deep-scattering layers to assess its biomass, community structure and role in the trophic pathways to deep-water fisheries is also of continual interest. Conventional sampling such as nets can yield a highly biased assessment of marine pelagic communities. The chief causes are escapement by larger, more motile animals; extrusion through the meshes of smaller forms; and destruction of more fragile organisms, such as gelatinous creatures. The acoustic *in situ* TS method using split- or dual-beam technologies provide a potential tool to sample the composition of these deep-water marine communities.

8.1.2 Obtaining *in situ* TS measurements

Obtaining unbiased echo integration and associated *in situ* target strength measurements of fish at these depths requires a deeply deployable transducer (Dalen *et al.*, 1995, Kloser 1996). A deeply deployed transducer can be lowered close to the targets, so that a single fish can be detected in the pulse volume irrespective of depth from the vessel. This ability to reduce the range to the target significantly decreases the sampling volume and increases the signal-to-noise ratio of detected targets. If there is no avoidance reaction of targets close to the transducer and the density of targets within one pulse resolution volume is less than one, a major source of multiple target bias can be removed from the *in situ* data, (as discussed in chapter 6 on single target recognition criteria).

Several deployment procedures can be employed to obtain the *in situ* measurements. These can be divided into three categories:

1. With vessel stationary, lower the transducer vertically into the scattering layer of interest.
2. Tow the transducer at a constant height above or through a layer.
3. Perform oblique tows through large vertical and horizontal layers.

8.1.3 Hardware considerations

To deploy a transducer using either split- or dual-beam technologies with stationary or towed vehicle requires associated electronics to overcome cable attenuation and ensure matching. When the cable length reaches more than 1/8 th of the acoustic wavelength in the cable (calculated as the speed of light $3 \cdot 10^8$ m/s times a cable correction coefficient, which is usually 0.6-0.7, and divided by the acoustic frequency) the cable needs to be treated as a transmission line. For example at 38 kHz and 120 kHz the length of line required to reach 1/8th of the wavelength is approximately 600 m and 200 m, respectfully. To avoid these transmission line problems, and associated cable attenuation and noise, the transmitter and receiver should be placed as close to the transducer as practical. These and other design problems associated with deep-water towed and vertically lowered systems are:

(1) need to reduce drag on the towed vehicle and cable to achieve greater depths with shorter cable lengths,
(2) towed body design needs be stable and fly horizontally over a wide speed range,
(3) place transmitter and receivers in the towed vehicle to overcome cable attenuation, matching problems (transmission line), and electrical noise,
(3) systems must be robust to withstand open ocean treatment,
(4) monitoring information is required on the towed bodies depth/pitch/ roll and internal voltages,
(5) deep-water transducers, preferably oil filled, do not change their characteristics with depth are required,
(6) the transducers should be flush-mounted to reduce air bubble adhesion on the internal window face and the transducer face.

8.1.4 Some present systems

Currently there are several deep-water split/dual-beam systems that can be deployed at various depths. One such split-beam system, described by Kloser (1995), can be deployed to depths up to 1000 m for obtaining target strength measurements. The transmitter and preamplifiers are housed in the towed body which is connected to the vessel by 3000 m of electromechanical cable. Another more technologically advanced system that can be deployed to depths up to 500 m is described in Dalen *et al.* (1995). It is based on the Simrad EK500 echo sounder, where the transmitter and receiving circuitry, including the digitizer, is placed inside the towed vehicle. The digital signals are then sent to the vessel via an optical cable, greatly reducing the susceptibility of the system to noise.

8.1.5 Calibration of deep-water systems

The use of split-beam transducers greatly simplifies the routine calibration of deep-water transducers. Suspending a sphere for and aft under a transducer and lowering it through the water column can be a simple task even in open-ocean conditions. Results from such calibrations give some interesting results for an air-backed transducer that has a rubber matching face (Kloser 1995 symp.). The calibration profile with depth, Figure 8.1, shows that the transducer is depth sensitive and that there is a marked hysteresis between down- and up-casts. These results highlight the need to calibrate transducers at their operating depth and to be cautious when using transducers that have an air-backed design. Results from a deep-water calibration to 500 m of an oil-backed transducer with an epoxy matching face (Ona, unpubl. data) do not show the same depth sensitivity or hysteresis.

8.1.6 Results from deep-water *in situ* measurements

Some interesting results deploying these deep-water towed vehicles have been obtained.

Avoidance problems

Avoidance of deep-water fish such as orange roughy to the towed bodies is experienced at depths to 800 m. Figure 8.2 shows the towed body being deployed at a depth of 700 m at 2-3 knots over an aggregation of orange roughy and lowered gradually towards the aggregation. The aggregation disperses away from the lowered transducer at vertical distances up to 150 m (Koslow *et al.*, 1995). The avoidance reaction of the fish ensures that the criteria for target detection of one fish within the pulse resolution volume is not attained and hence no *in situ* measurements can be obtained.

Increased sampling of smaller targets at depths of 200 - 400 m

Dalen *et al.* (1995), compare two target strength distributions from a hull-mounted and towed transducer over the same depth layer Figure 8.3. The upper one is from the hull-mounted transducer and the lower one is from the towed transducer. The instrument settings were equal for both systems. Because of the improved spatial resolution of the towed system, it detects more smaller targets than does the hull-mounted transducer.

Oblique towing through a deep scattering layer 0-1000 m

The deep-towed transducer described by Kloser (1995) was used to study nekton from 0-1000 m (Koslow *et al.*, 1995). The transducer was lowered to 900 m depth and slowly brought to the surface, so the water column was evenly sampled. The results show different nekton communities through the depth layers. Because of the even sampling of depth layers, an empirical correction of bias due to lower-target-strength nekton can be achieved. Bias in the TS data grouped in 5-dB steps is shown in Figure 8.4 for three TS groups at -70, -55 and -40 dB. Due to the conical spread of the acoustic beam, the number of detections should increase with distance from the transducer. Bias was considered present when the number of detections peaked or declined with increasing distance.

8.2 Measuring Target Strengths for Zoo-plankton and Micronekton

D. V. Holliday

8.2.1 Background

In comparison to fisheries acoustics, the use of underwater sound to study zooplankton and micronekton is a relatively new application of acoustical technology. Acoustical methods for determining target strengths for zooplankton and micronekton appear to be evolving with slightly different emphases than is the case in estimation of the target strengths of fish. In fisheries work, a great deal of emphasis is on *in situ*, single-frequency measurements. The development of general, validated mathematical descriptions (models) for target strength prediction is the focus of more intensive, active, current research in zooplankton acoustics than has traditionally been the case with fish target strength research. Additionally, wideband and multiple frequency issues have received a great deal of attention in zooplankton target strength modelling and measurement.

8.2.2 Dependence of target strength on size

In attempting to assess populations of zooplankton and micronekton, it was recognized at an early stage that it was necessary to operate acoustical instrumentation at frequencies that would make the wavelength of the sound in water comparable to the size of the animals one wished to study (McNaught, 1968; McNaught, 1969). For animals with dimensions of millimeters or less, this means using hundreds of kilohertz or even higher frequencies. Anderson (1950) was one of the first investigators to recognize that one's choice of acoustical frequency was important in determining the amount of scattering observed when examining zooplankton with sound. For small zooplankters, e.g., most copepods and their early life stages, the level of scattering observed depends, to first order, on the ratio of the size of the animal to the wavelength of the sound used to ensonify it. For both small zooplankton and centimeter-sized micronekton, target strength varies in a non-monotonic manner with the ensonifying frequency and the dimensions of the target organism for that frequency regime where the acoustic wavelength is greater than the maximum organism dimension.

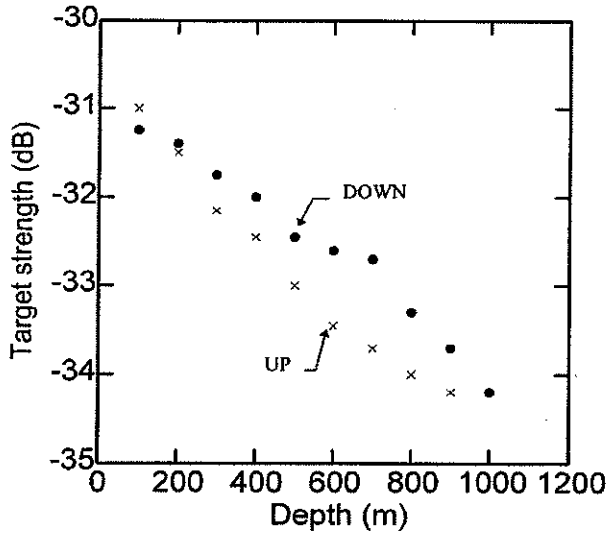

Figure 8.1. Plot of calibration profile for down and up casts for the deep water transducer. Showing mean TS for the -33.6 dB copper sphere at each 100 m interval.

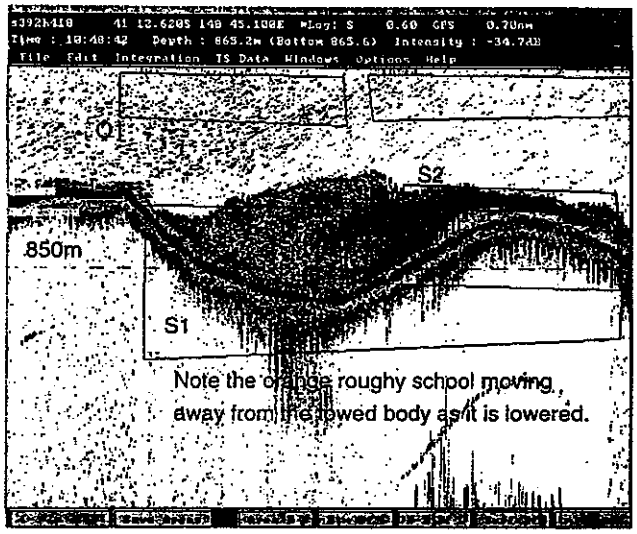

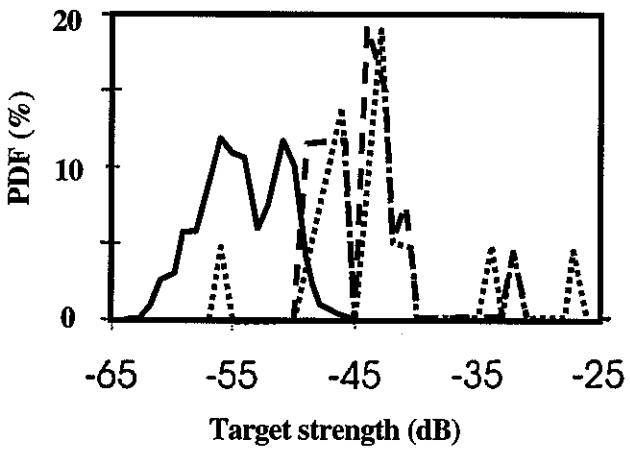

Figure 8.2. An example of deep water target strength data obtained by towing a deep water transducer at 750 m depth. Note that close to the transducer in region 01, a large number of targets, 793, are resolved. In the school region, however, region S1, only 26 targets are accepted. Due to school density, most of these are likely to arrive from multiple targets in the pulse resolution volume.

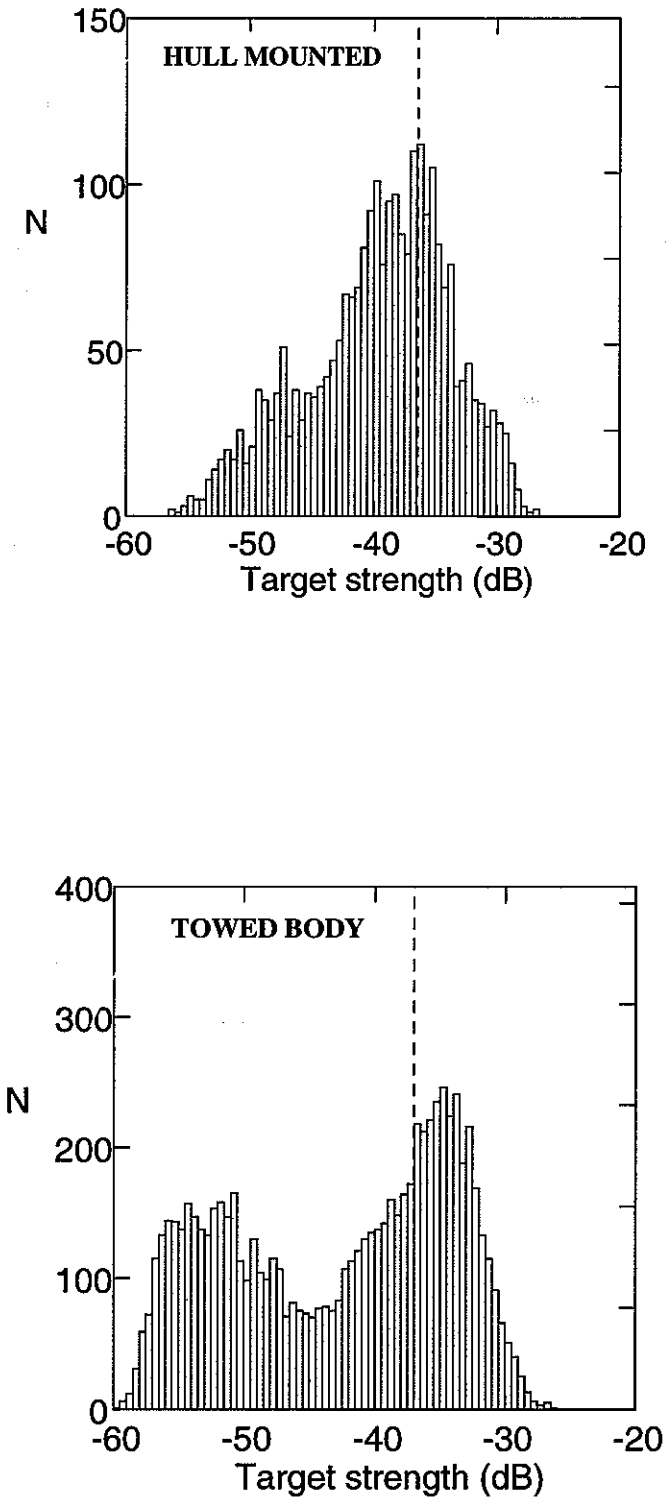

Figure 8.3. Target strength distribution from the same depth layer (200-250 m). Upper diagram is from the hull mounted 38 kHz transducer, while the lower is recorded from a similar transducer in a towed body at 150 m depth. Note the higher number of small targets resolved, or accepted bu the towed body, and also the absent upper tail of the target strength distribution.

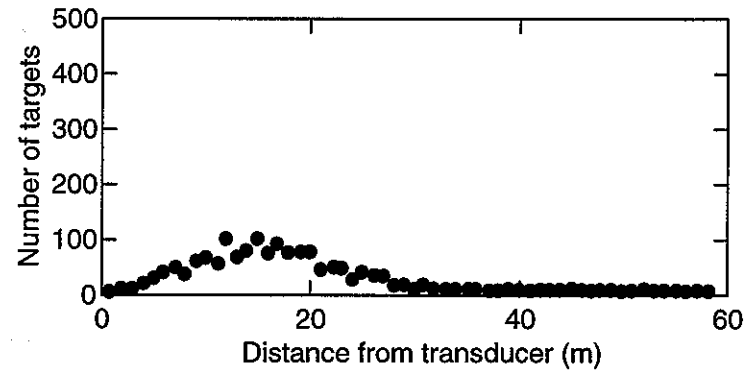

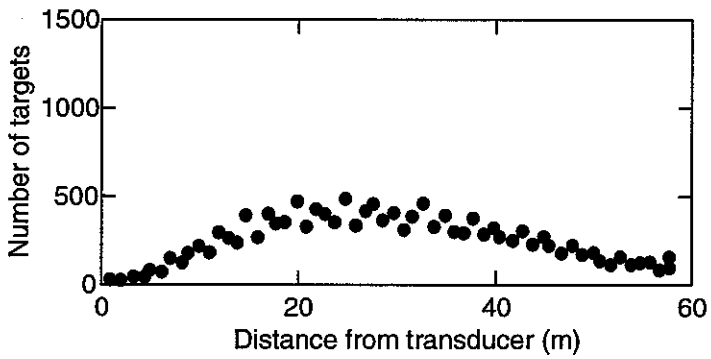

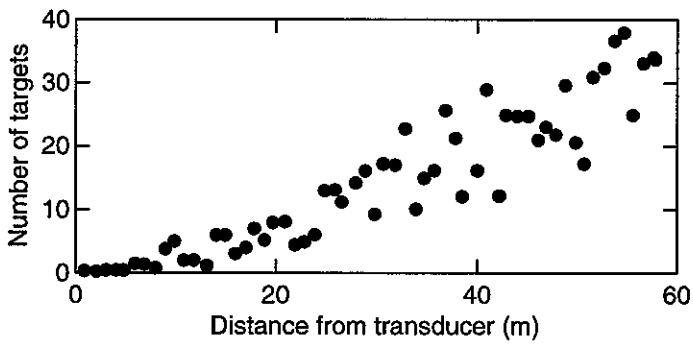

Figure 8.4. The number of acoustic targets detected in relation to distance (0-60 m) from the transducer of target strength classes: TS=-70 dB, -55 dB and -44 DB (number of targets are summed over 5 dB steps (e.g. -67.5 to -72.5 for the -70 dB class). The regression lines are fitted to the initial portion of the data, at shorter range, before the plateau-effect.

8.2.3 Dependence of target strength on organism shape

To some degree for all zooplankton, but to a larger degree for micronekton, e.g., euphausiids, shape becomes an increasingly important factor, influencing both the spatial and spectral position of scattering maxima and minima, which are the result of constructive and destructive interferences of all of the modes of vibration stimulated by the ensonifying waveform. While these complexities of the scattering often offer challenges in the interpretation of acoustical data, they also are the source of information about the target organism, quantitatively embedding such information as shape and animal size into the echo waveform (e.g., Stanton, 1986).

8.2.4 Dependence of target strength on physical properties of the tissue

In addition to a complex dependence on size and frequency, the level of sound scattering also depends on the contrasts of the density and compressibility of the material of the plankter in relation to the surrounding water. In many cases, these dependances are smaller effects in relation to the variability that occurs due to size and its relation to the frequency employed. There are a few notable exceptions, however, e.g., the pneumatophores of some siphonophores. Most species of plankton do not contain included gas, thus direct analogies with scattering from fish with gas - filled swimbladders are rarely appropriate. Some species of zooplankters have significant skeletal structure or shells, e.g., shelled pteropods (Hunkins, 1965; Hansen and Dunbar, 1970). When such scatterers are present, the effects of the density and compressibility contrasts become important, with the dependence of scattering level on density and compressibility approaching that of the dependence due to size and frequency (Stanton *et al.*, 1994).

8.2.5 Target strength estimation: modelling

The maturity of a scientific discipline is often reflected in the robustness of a method for making quantitative predictions. Target strength is a basic, critical term in equations that relate acoustical backscattering to the numerical density, size and other biophysical parameters that one can extract about populations and assemblages in marine ecosystems. It is not surprising, considering the importance of the target strength in relating volume backscattering measurements to plankton biomass and *in situ* target strengths to organism size, that a few investigators continue to pursue relatively low-level, but long-term investigations into developing and validating models that will predict an animal's acoustical reflectivity from a knowledge of biophysical parameters. Achieving the ability to predict the target strength from the size, species and shape over a range of acoustical frequencies is essential if we are to accomplish the inverse, i.e., estimate the numerical density, size, shape and species based on acoustical measurements.

A useful predictive capability for zooplankton target strength, with its attendant strong multiparameter dependances, is difficult to achieve by applying traditional methods of measuring scattering responses over the full ranges of all the important parameters (e.g., size, shape, orientation, acoustical frequency, waveform), varying each independently, and applying multi parameter regression methods to establish a "model" with universal (or even wide) applicability. There are both technical and cost factors that preclude making this approach to modeling a useful one for the general case (all species, all life stages, all sizes, etc.)

In attempting to achieve predictive modeling capabilities for zooplankton target strengths, most researchers have attempted to model the sound scattering process by applying the basic principles of scattering and mathematical physics (for an example of this approach, see Stanton *et al.*, 1993). When a mathematical model is constructed from first principles and measurable descriptors of the organisms, it must then be tested against direct measurements for a limited number of cases or ranges of the key variables. Validation, or testing, of these mathematical models is then essential. These validations, usually made by direct measurement on individuals, are used to define the useful range of the parameters included in models (e.g., size, shape and acoustical frequency) and to assess the accuracy of models.

Validated mathematical models for the scattering from zooplankton and micro nekton are invaluable in designing acoustical systems to study the animals in an ecosystem. They are also exceptionally useful in determining the accuracy of surveys or investigations conducted with available acoustical systems, which might not be optimal but are the only viable option for an investigator. For example, the complexities of scattering from zooplankton, in particular, the non-monotonic behavior of scattering with size at a particular frequency, have limited the usefulness of single-frequency measurements on multispecies, multisize assemblages of zooplankton. However, since the availability of single-frequency acoustical systems far exceeds that for multiple-frequency systems, there has been good reason to consider the dependence of target strength on size, acoustical frequency and such biophysical characteristics as shape and the density and compressibility contrasts. Knowing the implications of variations in these parameters for scattering from zooplankton allows one to make estimates of errors in the estimation of biomass and size of the organisms one studies with these systems.

Finally, access to a validated model for zooplankton and micro nekton target strengths is a necessary condition to maximizing the information one can extract from wideband or multifrequency acoustical measurements. Such methods can be used to extract zooplankton numerical density by size and depth (e.g., Holliday, 1977; Greenlaw and Johnson, 1983). Additional information is embedded in echoes that result from these wideband measurement systems, and if acoustical classification, leading to remote species identification, is to become a future reality,

accurate, validated mathematical models for zooplankton target strengths will undoubtedly be an essential element of the successful method.

8.2.6 Target strength estimation: measurement and model validation: comparison of acoustical and conventional samples from the open sea

Historically, biological oceanographers and acousticians have made comparisons of the results of acoustical scattering measurements and the results of conventional sampling with nets and pumps. This is a challenging, labor intensive and often frustrating exercise for at least four reasons.

The first reason is that none of the sampling methods, conventional and acoustical, are perfect. While the speed of sound and the remote sampling available with echo ranging acoustics are an advantage in limiting avoidance, there are limits on the performance of acoustical systems at both ends of the size spectrum. At small sizes, medium absorption of the high frequencies needed to obtain reasonable scattering levels limits performance. At large sizes, the numbers of animals that occur in a given acoustical sample volume on each ping or sequence of pings often limits performance. If either method were perfect, or even universally acceptable, there would be no call for the other! Thus it is not surprising that there are always questions regarding whether both methods are examining the same organisms.

Secondly, all conventional direct capture methods have well documented limitations. Nets clog, and metering the exact volume of water filtered is not trivial. Zooplankters and micro nekton are relatively good swimmers over short distances and are often adept at avoiding capture in nets and by pumps. Small animals can pass through or be extruded through the mesh.

Sorting, identifying, counting and measuring animals collected in nets and pumps is well known to be a tedious, time-consuming and costly process. This is essential however if collections from conventional samplers are to be used in estimating target strengths for zooplankton or micro nekton. Few budgets and few investigators are willing to take the time and care necessary to obtain the quality and quantity of data from net or pump samples to make this method practicable. Questions also arise regarding the effects of preservation, e.g., shrinkage. This can be critical in view of the strong power law dependence of scattering on animal size.

Finally, patchiness in spatial distribution creates a serious challenge for the comparison approach. Regardless of cause, whether behavioral, biological or physically driven, marine animals are patchy on any scale one wishes to examine. Thus, even when taking exceptional care to sample the same animals with nets or pumps and acoustical systems, it is difficult to do so. For example, one can not examine the volume precisely at the end of a plankton pump hose acoustically without including scattering, often on a sidelobe of the transducer, from the end of the hose. In one attempt at validation of a technique by such a comparison, Costello *et al.* (1989) found that attempts to validate an acoustical inverse procedure was limited by the fact that the acoustics and the pump samples collected at the same time were better matched than two pump samples collected one minute apart from a slowly drifting ship.

Even with the attendant problems with the methodology, the comparison technique has been widely used to evaluate a variety of target strength models. Over a period of several years and numerous cruises, Pieper and Holliday (1984) determined that the target strengths estimated by using the truncated-fluid-sphere model for small zooplankton were better than those estimated with either the full-fluid-sphere or the high-pass models. This conclusion resulted from comparing measured scattering levels to those computed from size - numerical density data in samples collected with a high-volume pump system. Several models were evaluated at several acoustical frequencies, and the model resulting in the closest agreement was considered the "best" of the set.

8.2.7 Measurements with animals in cages

In theory, one can measure the scattering from a group of animals, and assuming that the density is not so great that the process of echo formation is non-linear (multiple scattering, shadowing), then one can estimate the target strength of an individual by dividing by the number of animals in the measurement volume. This is the principle underlying several measurements reported in the literature, including those done in cages. The best experiment would be one in which all of the animals were of the same size. This is rarely the case when one obtains the sample from a natural population, though often the variability in size is sufficiently small that one can proceed to derive a useful answer. Care must be taken in assessing the results of such measurements because when one is operating in the Rayleigh scattering region, as is often the case when working with small animals (i.e., copepods or krill), the dependence of scattering may be as strong as a sixth - power dependence on size. Even greater variability could result due to small differences in animal size if the size and acoustical frequency chosen for the measurement were to fall in one of the interference nulls in the target strength spectrum. In the absence of *a priori* information, one must assume that small variations in size can make big differences in the scattering.

As is also the case with making target strength measurements on caged, live fish, the "tilt angle" or aspect of ensonification and reflection, the relative positions of the scatterers and the motions of the animals within the scattering volume and during the time duration of the pulse are all potential sources of variability in the measurements. At the higher frequencies often used in zooplankton acoustics, scattering from the cage itself can be non-negligible. Scattering arriving at the same time as the echo from the target animal, but via the sidelobes of the

acoustical system (transmit or receive), as well as bi-static scattering from cage and supporting structure can also lead to errors. Bubbles often adhere to the mesh in nets and to supporting structure as well. Scattering and resonance ringing of these bubbles can add unwanted signals during the range gate used in the measurement. Bubbles can also cause anomalous attenuation of the ensonifying and echo signals.

It must also be remembered that if an echo is measured from a set of randomly positioned scatterers, the echo is itself a random variable. Thus, one must average over an ensemble of sufficient size to achieve a valid estimate of whatever parameter one is trying to extract, whether it be peak target strength, average or rms target strength or the spectrum level of the echo energy at a particular frequency. On the other hand, examination of the statistics of echo ensembles and comparison with the results expected for volume scattering can help validate a data set for estimation of a mean target strength.

A recent example of an experiment in which estimates were made for krill target strengths using caged animals can be found in Foote *et al.* (1990).

8.2.8 Measurements on individual animals in tanks

The geometry of the target strength measurement system varies among different investigators. One popular arrangement is an upward-looking beam, above which a tethered animal is placed. This arrangement has the advantage that one can easily manipulate the location of the animal, centering it over the transducer. There is also an advantage in that an echo from the water surface can also be observed, providing a "standard" reference echo. This surface echo also can be used in a self - reciprocity calibration for the measurement system. This method works especially well in the laboratory, but on shipboard or in a windy outdoor environment, care must be taken to assure that waves on the tank surface do not cause focusing or defocusing of the surface reflection. Such an effect as well as non-normal orientations of the surface to the acoustical beam may introduce errors during a self-reciprocity calibration.

In designing a target strength measurement facility, it is important to consider the size and shape of the tank. The physical dimensions, along with the placement of supporting structures in the tank, if any, will determine the range of frequencies over which valid measurements can be made. One must have a geometry that allows one to find a location for the transducer and target organism which is free of multipath arrivals from all boundaries, including the surface. The acoustical reflectivity of small zooplankton and even large micro nekton can be several orders of magnitude less that the scattering from a steel or fiberglass wall or support, even when received on a sidelobe of the transducer. Anechoic coatings can help, but at higher frequencies, the echo reduction obtained with common wall treatments is not sufficient to allow one to ignore the basic tank dimensions and geometry.

It is also necessary that the distances between the transducer and the target organism place the transducer in the far field of both the measurement transducer and the target organism. Typical guidelines are that the far-field begins at a distance of twice the square of the maximum dimension of the animal (or transducer) divided by the wavelength of the sound. A second distance criteria would indicate that the distance to the target from the transducer be at least ten wavelengths. Neither of these criteria is absolute, since the far-field to near-field boundary is a transition zone rather than discrete boundary. The greater the distance, the lesser the errors incurred by not having an infinite separation (or a point target and source). Bobber (1970) discusses this error budget subject in some detail.

When working at frequencies with wavelengths smaller than the dimensions of the animals, target aspect becomes an important source of variability in acoustical backscattering. The animal becomes a spatially distributed radiator of sound, there are interferences of sound waves scattered from the animal's different parts, and in an analogy with the pattern radiated by a transducer, the animal exhibits directivity in its scattered sound field. The associated beam pattern for the animal can be extremely complex and will depend on the precise curvature of the animal. If the animal moves during the measurement, changing the relative position of its body parts with respect to the measurement transducer, as is often the case, the backscattered acoustical energy varies as well.

In the late 1970s and early 1980s measurements of target strength for zooplankton and micro nekton were made on dead, preserved or freshly thawed individual animals (Greenlaw, 1982). These measurements were valuable in the development of methodology for making target strength measurements on single animals, but the values obtained were significantly lower (6 to 12 dB) than were required to explain volume scattering from aggregations of animals *in situ*. The reasons for the low target strength estimates are thought to reside in a rapid change of the animal's modulus of compressibility at death. Major changes occur within minutes of death. Thus, it is critical that measurements of target strength be made on live, healthy zooplankters and micro nekton, even though this can be extremely difficult.

An important part of the methodology developed for measuring target strengths of zooplankton and micro nekton involves tethering the animals to control the aspect and allow the animal to be centered in the acoustic beam. Tethering the animals also has the considerable benefit that they do not swim immediately to the most distant corner of the measurement tank, though this usual behavior can be considerably slowed or modified with an anesthetic. Tethering the animals under test must be done carefully, lest the tether itself become a significant part of the measured target strength. Tether materials have included human hair for larger micro nekton such as euphausiids and single fibers dissected out of a silk medical suture for

attachment to small plankton and even small planktonic eggs. Acceptable methods of attachment of the tether to the animal vary, with small knots in fine human hair (e.g., from a young child) being acceptable for larger organisms. Very small quantities (a thin film) of cyanoacrylate adhesive have been successfully used to attach both hair and silk to animals. Investigators usually measure the target strength of the knot or the fiber and (if used) the adhesive to assure that the reflectivity of the tether is substantially less than that of the intended target.

Finally, considerable care must be taken so that bubbles of air not adhere to the animal during the target strength measurements. Bubbles, even microscopic ones, are often captured under some part of the carapace if the animal is exposed to air or if gas is coming out of solution as a result of changes in ambient temperature. These bubbles are usually better scatterers, even at micron sizes, than many of the zooplankton and micro nekton one wishes to measure. One defense against this potential source of error is to keep the container and the measurement tank at temperatures that are comparable to the water from which the animals were collected. One effective technique is to use a fine steel probe (e.g., a needle) to move only the part of the animal to which the tether is to be attached, for example, an antenna, out of a drop of water which covers the whole animal. Once the attachment is accomplished, one can reintroduce the animal and the drop covering it into the test tank without exposing it to air. This reduces the chances that bubbles will adhere to the animal's body.

8.2.9 Acoustical methodology

While single-frequency methods can sometimes be useful for examining zooplankton and micro nekton populations, the assumptions needed to do single-frequency quantitative work are quite restrictive, and most investigators now consider it important to know the reflectivity (target strength) of zooplankton and micro nekton as a function of frequency, even if the field work is to be done at a single frequency. The range of frequencies of interest depends on the size of the animals one is interested in measuring. The most important part of the spectral response curve, if it is to be used for estimation of animal size, is the transition from Rayleigh scattering to geometric scattering. If k is the wavenumber at frequency f, and a is a measure of the animal size, then the transition is usually in the vicinity of ka = 1. For small copepods, the range of frequencies is nominally from 100 kHz to as much as 10 MHz. For larger animals, such as polar species of krill, the range of frequencies needed may be from as low as 10 kHz to several hundred kHz.

For reasons that are embedded in the physics of acoustical transduction, when working over several octaves of frequency, it is usually necessary to use several transducers to achieve sufficient source level and to have adequate receiving sensitivity to make high-quality estimates of target strength for relatively weak zooplankton scatterers (e.g., with target strength in the range from -120 dB to - 60 dB). Several approaches have been used to define the frequency dependence of zooplankton target strength.

One approach is to transmit short pulses sequentially at several discrete frequencies. This is probably the most common method. In this method short pulses are transmitted at discrete center frequencies. It is important to use pulses that have sufficient bandwidth to achieve sufficient range resolution to discriminate against multipath reflections from tank walls and supporting structure, but it is also important to realize that pulse length and signal bandwidths are linked for continuous wave (CW) signals. If the pulse is too short, then the measurement is not at a "single" frequency. The resulting target strength is the convolution of the pulse spectrum and the target frequency response. It is important to use a pulse that is long enough to stimulate the "fine structure" or variations with frequency in the target response to steady state. This requires that the number of cycles at a particular frequency be several times greater than the "Q" for any resonances or anti-resonances in the target response.

Another method used for measuring target strength involves stimulating each of a series of transducers with an impulse. The spectrum of an impulse is wideband and essentially transmits all of the frequencies that are within the passband of the transducer (usually about 20 to 30% of the center frequency, more for special transducer designs). These frequencies are transmitted simultaneously, therefore the echo that is formed at each frequency is from the same animal in the same orientation at the same time. The echoes are usually digitized and stored. Post-data-collection spectral analysis is then used to separate the echo energy by frequency, and the data are normalized by the spectrum of transmitted signal, resulting in an estimate of the target strength over the effective two - way bandwidth (combined transmit and receive response) of the transducer. If one transducer does not cover the entire band of interest, then the operation is repeated with other transducers and the curves are merged until the spectral reflectivity has been defined. The reader is cautioned that the same rules hold in this method as in all of the other methods regarding the random nature of any particular single echo from a set of randomly spaced scatterers. In this case, the randomness is due to changes in orientation of the animal and to relative change in the location of the scattering highlights on the animal. An ensemble average will be needed to obtain convergence to a good estimate of the power spectrum of the echoes. It should also be noted that the spectral density of the incident signal (energy per unit bandwidth) is often significantly lower for impulse methods compared to discrete-frequency-measurement techniques. There is a trade - off necessary in determining whether it is more important to ensonify the animal at a high level at different times at several frequencies or whether the changes in animal orientation between measurements at different frequencies justify attempting to use lower levels at each frequency in the transmitted signal.

The spectral response of a flat air - water interface does not vary with frequency. It is a "perfect" reflector acoustically, i.e., there is negligible loss for our purposes. Thus, the surface reflection is often used to estimate the necessary transducer characteristics, e.g., spectral response, source level, transmit and receive beam patterns and receiving sensitivities that are required for estimating the target strength of the animals measured by this method. This kind of system calibration is called a self-reciprocity calibration and is described in Bobber (1970).

A third variation on multifrequency target strength methods involves use of signals with specially designed temporal and spectral characteristics. Properly executed, this method can allow one to generate more energy per unit bandwidth that the impulse technique discussed above and simultaneously shorten the time between ensonifying the animals at different frequencies. There are a variety of signals available for this use, including a variety of psuedo-random codes (PRN) and frequency-modulated (FM) codes. The differences involve sidelobe structure in the autocorrelation functions of the temporal signal waveform and the spectrum actually transmitted into the water. One of the simpler codes to generate is the linear-frequency modulated (LFM) code. This code has been successfully used by Stanton's group for measuring the target strengths of a variety of micro nekton (Chu, *et al.*, 1992). This work has been in support of the development and validation of some quite sophisticated mathematical models for scattering from micro nekton.

Regardless of the code chosen for the measurement, one must allow a sufficient range gate in the receiver to include the "ringing" of all of the excited modes of the target. If one is using a very short pulse length for the measurements, which is normally the case in order to exclude multipath reflections from the tank walls via the side lobes of the transducer, then one must also recognize that the pulse must be sufficiently long to allow the actual target response at each frequency to reach a steady state. If this is not the case, then the measured target strength will be a convolution of the target strength of the animal and the spectrum of the pulse. The answer may be correct for that particular pulse, but will be in error if a different pulse is used. Similarly, for the case of the LFM codes, where the frequency of the signal is swept across a frequency band during the time of the duration of the pulse, the dwell time at any one frequency must be sufficient to fully excite the resonant modes in the target's physical structure.

8.2.10 Summary

There has been progress during the last decade in both modeling and in validation of models of scattering from zooplankton and micro nekton, however, the number of investigators is small and their efforts are not fully dedicated to examining the issues that remain in understanding target strengths for small zooplankton and micro nekton. While the results to date and current models are sufficient to allow one to work the inverse problem in many interesting cases, instrumentation for collecting volume scattering data are improving at a rate that will soon demand better, more accurate and more detailed models of target strengths of individual zooplankton and micro nekton. Validation of these models is tedious and labor intensive and will require both new, innovative methods and increased automation.

Crustaceans are an important part of most marine and fresh-water ecosystems. One specific area that merits serious investigation includes the effects of the stage of the molt for these animals on their reflectivity. Soft-bodied animals such as chaetognaths and salps have only begun to be modeled and examined quantitatively. Shelled animals, such as pteropods, can, when present, dominate scattering at a particular depth or through the water column.

While our ignorance of the details of the target strength spectrum for all species, genera, shapes, sizes and life stages of plankton will probably never be completely eliminated, there are likely useful generalizations that can be made based on animal morphology and physiology. Insofar as the state of zooplankton acoustics is currently dependent on direct samples for identification, the approximations we must make now do not necessarily have to lead to serious errors if we find that the scattering is dominated by a life form for which we do not yet have a model.

Finally, multiple wideband acoustical sensors operating over several decades of frequency are becoming more common for studding zooplankton and micro nekton. The wideband characteristic of these instruments allows one to gain additional information about the animals being observed. An important part of that information is embedded in the structural detail of the animal's morphology. Wideband systems can presently resolve parts of small zooplankton, e.g., antenna, feeding parts, swimming appendages, attached egg masses, etc. In acoustics, the signals in the echo that result from scattering from the internal and external details of a target are termed "highlights". The echo is no longer a simple, steady state replica of the transmitted signal. When the bandwidth of a system reaches the point at which these details are temporally resolved (in the classical Rayleigh sense), the classical definition of target strength breaks down.

Further, ping-to-ping observations and Doppler analyses of the echoes from individual animals can clearly reveal motion in the various body parts, e.g., the swimming appendages. These motions also can impart information that is potentially valuable for classification and eventual remote identification. Once again, however, the classical, steady state, single-frequency definition of target strength is inadequate as a descriptor when the target's motion (i.e., frequency modulation or Doppler) is added as a target descriptor. While it is clear that advancing technology has limited the applicability of the classical definition of target strength, the capability to achieve such resolution is still relatively new, and much discussion, field experience, analysis and data interpretation are necessary before a new, more general, useful definition can be proposed and hope to gain universal acceptance.

References

Anderson, V. C. 1950. Sound scattering from a fluid sphere. Journal of the Acoustical Society of America, 22: 426–431.

Bobber, R. J. 1970. Underwater electroacoustic measurements, Naval Research Laboratory, Underwater Sound Reference Division, US Govt. Printing Office Catalog No. D 210.2; UN 2/2.

Chu, D. 1992. Frequency dependence of sound backscattering from live individual zooplankton, ICES Journal of Marine Science 49: 97–106.

Costello, J. H., Pieper, R. E., and Holliday, D. V. 1989. Comparison of acoustic and pump sampling techniques for the analysis of zooplankton distributions, Journal of Plankton Research 11: 703– 709.

Dalen, J., Bodholt, H., and Sogn, K. T. 1995. Deep-water towed vehicle with optical fiber in tow-cable. International Symposium on Fisheries and Plankton Acoustics, Aberdeen, 12–16 June 1995. (Poster).

Foote, K. G., Everson, I., Watkins, J. L., and Bone, D. G. 1990. Target strengths of Antarctic krill (*Euphausia superba*) at 38 and 120 kHz, Journal of the Acoustical Society of America, 87: 16 –24.

Greenlaw, C. F. 1977. Backscattering spectra of preserved zooplankton populations. Journal of the Acoustical Society of America, 62: 44–52.

Greenlaw, C. F. 1979. Acoustical estimation of zooplankton populations, Limnology and Oceanography 24: 226–242.

Greenlaw, C. F. 1982. Physical and acoustical properties of zooplankton. Journal of the Acoustical Society of America, 72: 1707–1710.

Greenlaw, C. F., and R. K. Johnson. 1983. Multiple frequency acoustical estimation. Biological Oceanography 2: 227–252.

Hansen, W. J., and M. J. Dunbar. 1970. Biological causes of scattering layers in the Arctic Ocean, in Proceedings of an International Conference on Biological Sound Scattering in the Ocean, MC Report 005, Maury Center for Ocean Science, Washington, DC, pp. 508– 526.

Holliday, D. V. 1977. Extracting bio-physical information from acoustic signatures of marine organisms, pp. 619– 624, in Oceanic Sound Scattering Prediction, N. R. Andersen and B.J. Zahuranec, eds., Plenum Press, NY, 859 pp.

Hunkins, K. 1965. The seasonal variation in the sound - scattering layer observed at Fletcher's Ice Island (T-3) with a 12 - kc /s echo sounder. Deep Sea Res. 12: 879– 881.

Kloser, R. J. 1996. Improving precision of acoustic surveys on benthopelagic fish by the use of a deeply-towed transducer. ICES Journal of Marine Science 53(2): 407–414.

Koslow, J. A., Kloser, R. J., and Stanley, C. 1995. Avoidance of a camera system by a deepwater fish, the orange roughy (*Hoplostethus atlanticus*). Deep-Sea Research (Part I, Oceanographic Research Papers), 42(2): 233–244.

Koslow, J. A., Kloser, R. J., and Williams, A. 1997. Pelagic biomass and community structure over the mid-continental slope off southeastern Australia based upon acoustic and midwater trawl sampling. Marine Ecology Progress Series, 146(1-3): 21–35.

McNaught, D. C. 1968. Acoustical determination of zooplankton distributions, Proc. 11th Conf. Great Lakes Res. 1968. International Association for Great Lakes Research, pp. 76–84.

McNaught, D. C. 1969. Developments in plankton sampling, Proc. 12th Conf. Great Lakes Res. 1969. International Association for Great Lakes Research, pp. 61–68.

Pieper, R. K. and D. V. Holliday. 1984. Acoustic measurements of zooplankton distributions in the sea, Journal du Conseil International pour l'Exploration de la Mer 41: 226–238.

Stanton, T. K. 1986. Simple Approximate Formulas for Backscattering of Sound by Spherical and Elongated Objects, Journal of the Acoustical Society of America, 86: 1499–1510.

Stanton, T. K., Wiebe, P. H., Chu, D. Benfield, M. C., Scanlon, L., Martin, L., and Eastwood, R. L. 1994. On acoustic estimates of zooplankton biomass, ICES Journal of Marine Science, 51: 505–512.

Stanton, T. K., Chu, D., Wiebe, P. H., and Clay, C. S. 1993. Average echoes form randomly oriented random-length finite cylinders: Zooplankton models, Journal of the Acoustical Society of America, 94: 3454–3462.